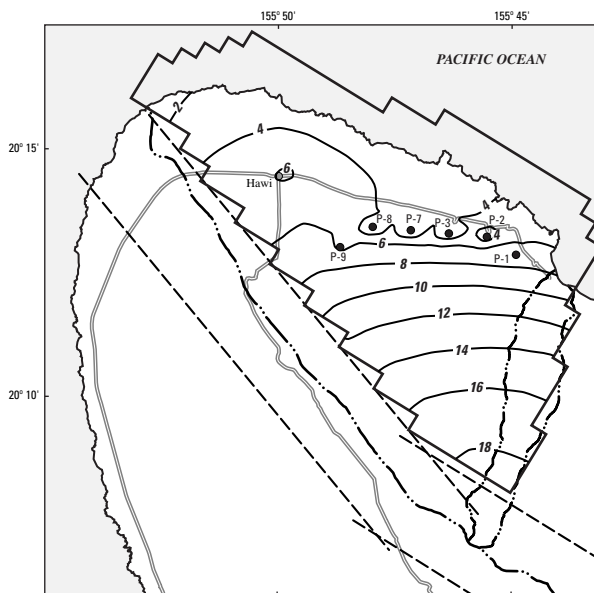
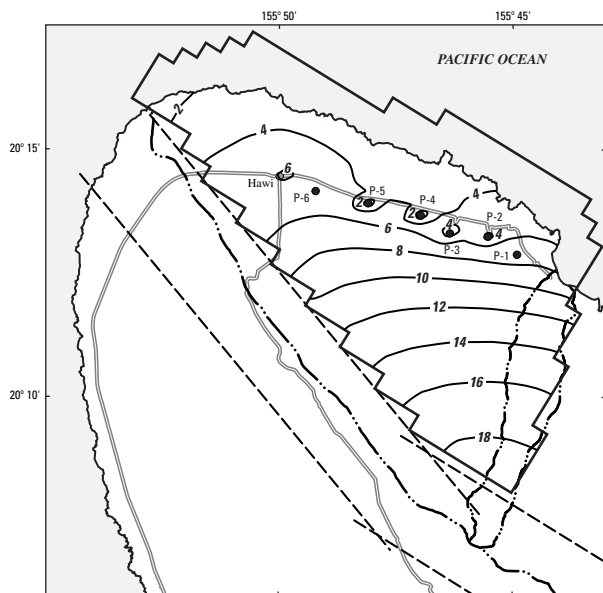
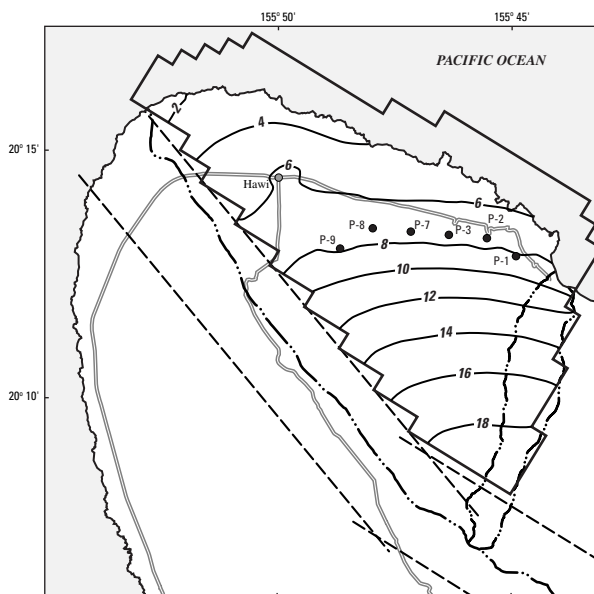
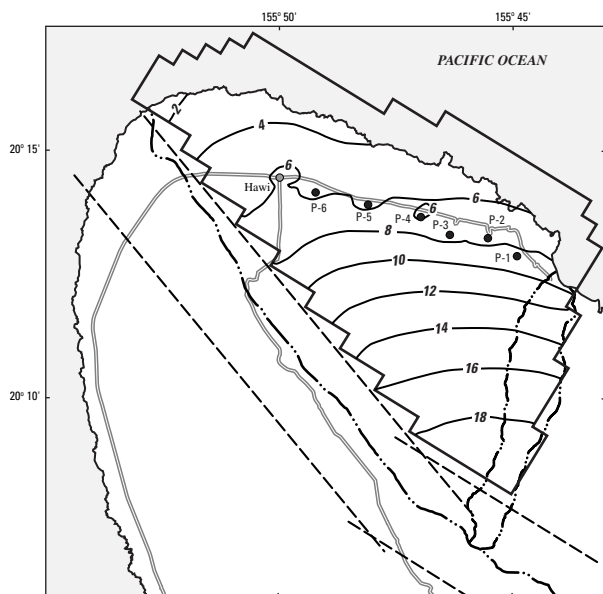


Reassessment of Ground-Water Recharge and Simulated Ground-Water Availability for the Hawi Area of North Kohala, Hawaii

U.S. Department of the Interior

U.S. Geological Survey

Water-Resources Investigations Report 02-4006



Reassessment of Ground-Water Recharge and Simulated Ground-Water Availability for the Hawi Area of North Kohala, Hawaii

By Delwyn S. Oki

U.S. GEOLOGICAL SURVEY

Water-Resources Investigations Report 02-4006

Honolulu, Hawaii
2002

U.S. DEPARTMENT OF THE INTERIOR
GALE A. NORTON, Secretary



U.S. GEOLOGICAL SURVEY
Charles G. Groat, Director

The use of firm, trade, and brand names in this report is for identification purposes only and does not constitute endorsement by the U.S. Geological Survey.

For additional information write to:

District Chief
U.S. Geological Survey
677 Ala Moana Blvd., Suite 415
Honolulu, HI 96813

Copies of this report can be purchased
from:

U.S. Geological Survey
Branch of Information Services
Box 25286
Denver, CO 80225-0286

CONTENTS

Abstract	1
Introduction	1
Purpose and Scope	3
Description of Study Area	3
Hydrogeologic Setting	6
Kohala Volcano	6
Hydraulic Conductivity of the Rocks	8
Soils	8
Ground Water	8
Dike-Impounded System	9
Freshwater-Lens System	10
Perched System	10
Ground-Water Levels	10
Ground-Water Withdrawals	13
Water Budget	17
Daily Water-Budget Method	17
Rainfall	19
Irrigation	22
Fog Drip	22
Runoff	24
Potential Evapotranspiration	24
Soil-Moisture Storage Capacity	28
Recharge	29
Recharge Uncertainty	33
Numerical Ground-Water Flow Models	35
Model Construction	35
Model Mesh	39
Boundary Conditions	39
Model Zones	39
Recharge	40
Withdrawals	40
Estimation of Hydraulic Characteristics	40
Model 1, Low Recharge	40
Model 2, Intermediate Recharge	40
Model 3, High Recharge	47
Effects of Proposed Withdrawals	47
Model 1	50
Scenario 1.— 10 Mgal/d Withdrawal, Distribution 1	50
Scenario 2.— 10 Mgal/d Withdrawal, Distribution 2	52
Scenario 3.— 15 Mgal/d Withdrawal, Distribution 1	53
Scenario 4.— 15 Mgal/d Withdrawal, Distribution 2	53
Model 2	54
Scenario 5.— 15 Mgal/d Withdrawal, Distribution 1	54
Scenario 6.— 15 Mgal/d Withdrawal, Distribution 2	54
Scenario 7.— 20 Mgal/d Withdrawal, Distribution 1	54
Scenario 8.— 20 Mgal/d Withdrawal, Distribution 2	54

Model 3.	56
Scenario 9.— 15 Mgal/d Withdrawal, Distribution 1.	56
Scenario 10.— 15 Mgal/d Withdrawal, Distribution 2.	56
Scenario 11.— 20 Mgal/d Withdrawal, Distribution 1.	56
Scenario 12.— 20 Mgal/d Withdrawal, Distribution 2.	56
Ground-Water Availability.	58
Model Limitations	59
Summary and Conclusions.	59
References Cited	61

FIGURES

1–4. Maps showing:	
1. Hawi study area, north Kohala, Hawaii	2
2. Land cover in the Hawi area, north Kohala, Hawaii	4
3. Average annual rainfall, north Kohala, Hawaii	5
4. Surficial geology of north Kohala, Hawaii	7
5. Schematic cross section showing generalized directions of ground-water flow in the dike-impounded and freshwater-lens systems of the Hawi area, north Kohala, Hawaii	9
6. Map showing selected wells, shafts, and tunnels in the Hawi area, north Kohala, Hawaii	11
7. Graph of chloride-concentration profiles from wells D (7445-01) and I (7549-03) in the Hawi area, north Kohala, Hawaii, March 1990	12
8. Map showing average 1990’s water levels measured in wells and shafts in the Hawi area, north Kohala, Hawaii	14
9–11. Graphs of:	
9. Water levels measured under nonpumped conditions in selected wells in the Hawi area, north Kohala, Hawaii	15
10. Ground-water withdrawal during 1940–99 from wells and shafts in the Hawi area, north Kohala, Hawaii	16
11. Annual rainfall measured at selected rain gages in the Hawi area, north Kohala, Hawaii	20
12. Map showing Thiessen polygons around selected rain gages with daily rainfall data in the Hawi area, north Kohala, Hawaii	21
13. Graph of measured and simulated daily rainfall at rain gage 175.1, north Kohala, Hawaii, in terms of (A) number of dry (or wet) days in a month, (B) standard deviation, (C) skewness coefficient, and (D) maximum daily rainfall.	23
14–15. Maps showing:	
14. Runoff zones in the Hawi study area, north Kohala, Hawaii	25
15. Average annual pan evaporation, north Kohala, Hawaii	27
16. Graph of ratios of monthly mean pan evaporation to annual pan evaporation at selected sites in the Hawi area, north Kohala, Hawaii	28
17. Map showing estimated soil-moisture storage capacity in the Hawi area, north Kohala, Hawaii	30
18. Graph of variations in estimated annual recharge and cumulative average annual recharge with number of years of recharge simulation for the Hawi area, north Kohala, Hawaii.	31

19–26.	Maps showing:	
19.	Estimated average annual ground-water recharge (intermediate estimate of 37.5 million gallons per day) in the Hawi area, north Kohala, Hawaii, computed with a water budget . . .	32
20.	Estimated average annual ground-water recharge (low estimate of 19.9 million gallons per day) in the Hawi area, north Kohala, Hawaii, computed with a water budget	36
21.	Estimated average annual ground-water recharge (high estimate of 55.4 million gallons per day) in the Hawi area, north Kohala, Hawaii, computed with a water budget	37
22.	Leakance zones used in the numerical ground-water flow model for the Hawi area, north Kohala, Hawaii	38
23.	Hydraulic-conductivity zones used in the numerical ground-water flow model for the Hawi area, north Kohala, Hawaii	41
24.	Low estimate of average annual ground-water recharge (19.9 million gallons per day from infiltration of rainfall, fog drip, and irrigation) used in the numerical ground-water flow model (model 1) for the Hawi area, north Kohala, Hawaii	42
25.	Intermediate estimate of average annual ground-water recharge (37.5 million gallons per day from infiltration of rainfall, fog drip, and irrigation) used in the numerical ground-water flow model (model 2) for the Hawi area, north Kohala, Hawaii	43
26.	High estimate of average annual ground-water recharge (55.4 million gallons per day from infiltration of rainfall, fog drip, and irrigation) used in the numerical ground-water flow model (model 3) for the Hawi area, north Kohala, Hawaii	44
27.	Graph of measured and model-calculated water levels for 1990's pumping conditions and three estimated recharge distributions, Hawi area, north Kohala, Hawaii	45
28–33.	Maps showing:	
28.	Measured and model-calculated water levels in the Hawi area, north Kohala, Hawaii, using the low recharge estimate (19.9 million gallons per day from infiltration of rainfall, fog drip, and irrigation)	46
29.	Measured and model-calculated water levels in the Hawi area, north Kohala, Hawaii, using the intermediate recharge estimate (37.5 million gallons per day from infiltration of rainfall, fog drip, and irrigation)	48
30.	Measured and model-calculated water levels in the Hawi area, north Kohala, Hawaii, using the high recharge estimate (55.4 million gallons per day from infiltration of rainfall, fog drip, and irrigation)	49
31.	Model-calculated water levels in the Hawi area, north Kohala, Hawaii, with 19.9 million gallons per day recharge from infiltration of rainfall, fog drip, and irrigation and different withdrawal rates and distributions	51
32.	Model-calculated water levels in the Hawi area, north Kohala, Hawaii, with 37.5 million gallons per day recharge from infiltration of rainfall, fog drip, and irrigation and different withdrawal rates and distributions	55
33.	Model-calculated water levels in the Hawi area, north Kohala, Hawaii, with 55.4 million gallons per day recharge from infiltration of rainfall, fog drip, and irrigation and different withdrawal rates and distributions	57

TABLES

1. Periods of record used to develop monthly fragment sets for selected rain gages in the Hawi area, north Kohala, Hawaii	22
2. Estimated fog-drip to rainfall ratios for the Hawi area, north Kohala, Hawaii	24
3. Estimated runoff-to-rainfall ratios in the Hawi area, north Kohala, Hawaii	26
4. Estimated available water-capacity values for soils in the Hawi area, north Kohala, Hawaii	29
5. Sensitivity of the water-budget estimate of average annual recharge to potential evapotranspiration, available water capacity, root depth, runoff, fog drip, and irrigation in the Hawi area, north Kohala, Hawaii	34
6. Steady-state ground-water budget (1990's withdrawal conditions) for the numerical ground-water flow models, Hawi area, north Kohala, Hawaii	47
7. Recharge and withdrawal (scenarios 1 to 12) for the numerical ground-water flow models, Hawi area, north Kohala, Hawaii	50
8. Model-calculated water levels for scenarios 1 to 12 at proposed sites of withdrawal, Hawi area, north Kohala, Hawaii	52
9. Steady-state ground-water budget (scenarios 1 to 12) for the numerical ground-water flow models, Hawi area, north Kohala, Hawaii	53

Reassessment of Ground-Water Recharge and Simulated Ground-Water Availability for the Hawi Area of North Kohala, Hawaii

By Delwyn S. Oki

Abstract

An estimate of ground-water availability in the Hawi area of north Kohala, Hawaii, is needed to determine whether ground-water resources are adequate to meet future demand within the area and other areas to the south. For the Hawi area, estimated average annual recharge from infiltration of rainfall, fog drip, and irrigation is 37.5 million gallons per day from a daily water budget. Low and high annual recharge estimates for the Hawi area that incorporate estimated uncertainty are 19.9 and 55.4 million gallons per day, respectively. The recharge estimates from this study are lower than the recharge of 68.4 million gallons per day previously estimated from a monthly water budget.

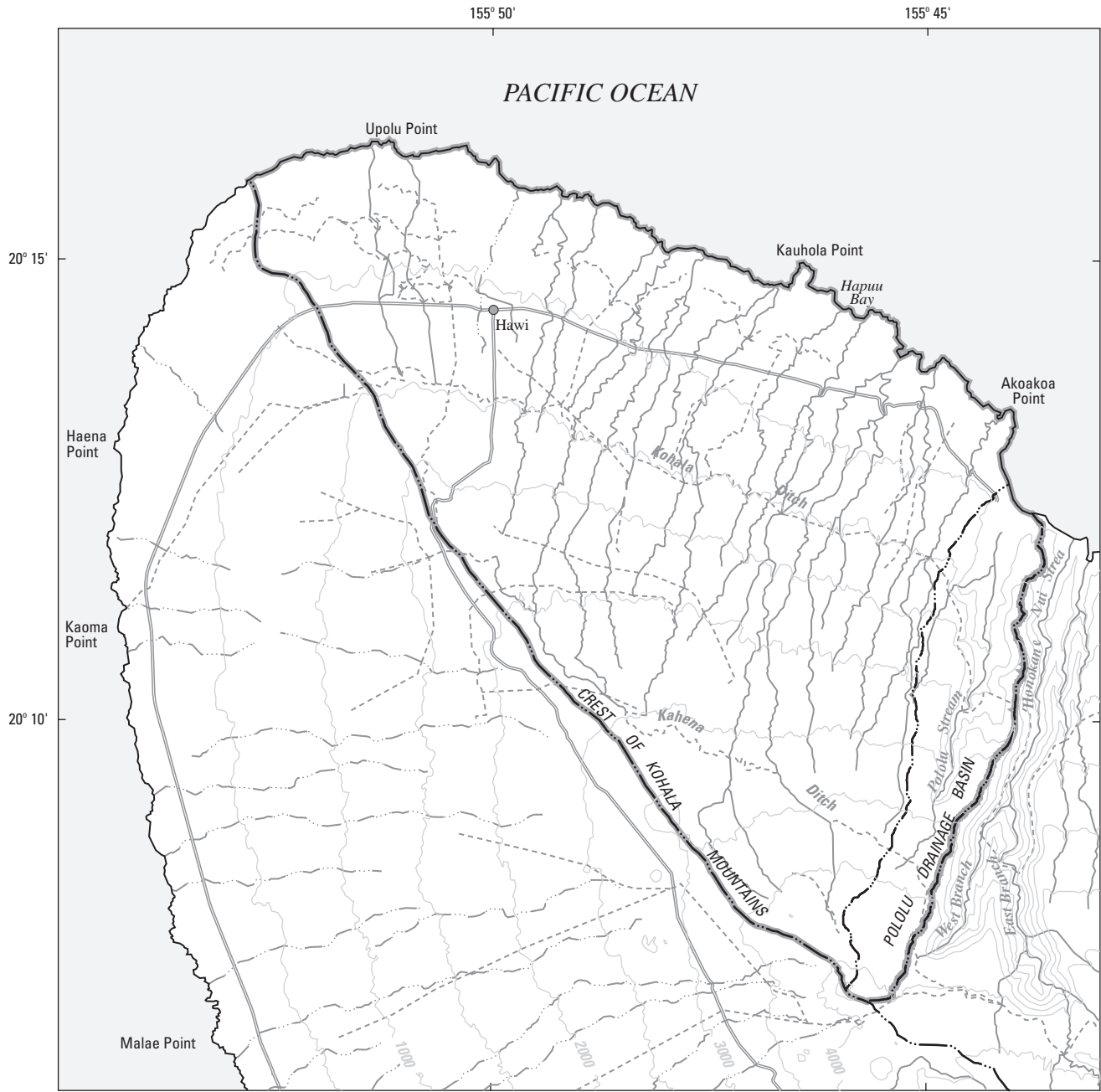
Three ground-water models, using the low, intermediate, and high recharge estimates (19.9, 37.5, and 55.4 million gallons per day, respectively), were developed for the Hawi area to simulate ground-water levels and discharges for the 1990's. To assess potential ground-water availability, the numerical ground-water flow models were used to simulate the response of the freshwater-lens system to withdrawals at rates in excess of the average 1990's withdrawal rates. Because of uncertainty in the recharge estimate, estimates of ground-water availability also are uncertain. Results from numerical simulations indicate that for appropriate well sites, depths, and withdrawal rates (1) for the low recharge estimate (19.9 million gallons per day) it may be possible to develop an additional 10 million gallons per day of fresh ground water from the Hawi area and maintain a

freshwater-lens thickness of 160 feet near the withdrawal sites, (2) for the intermediate recharge estimate (37.5 million gallons per day) it may be possible to develop an additional 15 million gallons per day of fresh ground water from the Hawi area and maintain a freshwater-lens thickness of 190 feet near the withdrawal sites, and (3) for the high recharge estimate (55.4 million gallons per day) it may be possible to develop at least an additional 20 million gallons per day of fresh ground water from the Hawi area and maintain a freshwater-lens thickness of 200 feet near the withdrawal sites. Other well-field configurations than the ones considered potentially could be used to develop more fresh ground water than indicated by the scenarios tested in this study. Depth, spacing, and withdrawal rates of individual wells are important considerations in determining ground-water availability.

The regional models developed for this study cannot predict whether local saltwater intrusion problems may occur at individual withdrawal sites. Results of this study underscore the importance of collecting new information to better constrain the recharge estimates.

INTRODUCTION

Because ground-water availability along the dry western coast of the island of Hawaii is limited, future development in the area may require imported water from other areas. One source of additional ground water that is being considered is the Hawi area of north Kohala (fig. 1) (Underwood and others, 1995). An estimate of ground-water availability in the Hawi area of north Kohala is needed to determine whether ground-



Base modified from U.S. Geological Survey digital data, 1:24,000, 1983, Albers equal area projection, standard parallels 19°08'30" and 20°02'30", central meridian 155°26'30"



EXPLANATION

-  STUDY AREA BOUNDARY
-  DRAINAGE DIVIDE
-  DITCH

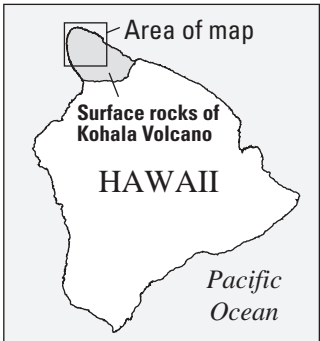


Figure 1. Hawi study area, north Kohala, Hawaii.

water resources in this area are adequate to meet future demand within the area and for export to other areas to the south.

Underwood and others (1995) developed a numerical ground-water flow model of the Hawi area and made an assessment of ground-water availability using recharge estimated from a monthly water budget (Shade, 1995). The uncertainty of ground-water model predictions strongly reflects the accuracy of the estimated recharge to the ground-water system. Overestimates of recharge may result in unrealistically high ground-water availability estimates, whereas underestimates of recharge may result in unrealistically low ground-water availability estimates. Inaccurate ground-water recharge estimates can have a significant effect on the planned use and protection of the ground-water resources.

In Hawaii, ground-water recharge is commonly estimated with annual or monthly water budgets. Because monthly water budgets account for seasonal variability in rainfall and evapotranspiration, monthly water budgets generally provide more accurate recharge estimates than annual water budgets. Similarly, because daily water budgets account for daily variations in rainfall and evapotranspiration, daily water budgets generally provide more accurate recharge estimates than monthly water budgets. For this study, (1) ground-water recharge in the Hawi area was estimated using a daily water budget and compared to recharge previously estimated using a monthly water budget (Shade, 1995), and (2) ground-water availability was estimated and compared to a previous estimate of ground-water availability (Underwood and others, 1995).

Purpose and Scope

The purpose of this report is to describe the (1) calculation of a daily water budget to estimate average annual ground-water recharge for 1990's land-use conditions in the Hawi area of the island of Hawaii, (2) uncertainty in the recharge estimate, and (3) results from numerical ground-water flow models that simulate the hydrologic effects of additional ground-water withdrawals at rates between 10 and 20 million gallons per day (Mgal/d) above average 1990's rates. No new data were collected as part of this study; only existing information was used to compute the water budget. An existing numerical ground-water flow model (Underwood

and others, 1995) formed the basis for models used in this study to simulate the effects of additional withdrawals.

Description of Study Area

The Hawi study area is located on the windward (northeastern) side of the crest of the Kohala Mountains. The Kohala Mountains are formed by the Kohala Volcano, the oldest and northernmost of five volcanoes forming the island of Hawaii. The study area covers about 55 square miles and is bounded on the southwest by the crest of the Kohala Mountains, on the east by the eastern drainage divide of Pololu Stream, and on the north by the coast (fig. 1). Within the study area, the land-surface altitude ranges from sea level at the coast to about 4,000 ft near the headwater of Pololu Stream. In general, the land surface is moderately dissected. The dominant land cover is pasture, with smaller areas used for agriculture, commonly orchards, and rural and urban development (fig. 2). The upland area is covered in places with native forest vegetation (Jacobi, 1989). From the early 1900's to the early 1970's, sugarcane was grown over much of the area that is currently in pasture.

Mean annual rainfall in the Hawi area ranges from less than 40 in. near the coast at Upolu Point to between 120 and 160 in. inland, near the headwater of Pololu Stream (fig. 3). The rainfall distribution is controlled primarily by topography and wind direction. Persistent northeasterly winds, known locally as tradewinds, are forced up the slopes of the Kohala Mountains. The warm, moisture-laden air is orographically lifted and cooled, which frequently results in cloud formation and rainfall. Because the air commonly loses moisture as it flows over the Kohala Mountains, the area on the southwestern, leeward side of the mountain crest is drier, with less than 10 in. of annual rainfall in some coastal areas south of the Hawi study area.

Fog water that is intercepted by vegetation and subsequently drips to the ground is referred to as fog drip. Fog drip can exceed rainfall during some periods and contribute to recharge. For example, over a 100-day period at an altitude of 3,800 ft on the Kohala Mountains, Juvik and Nullet (1995) measured 23.9 in. of canopy throughfall (which includes fog drip), but only 13.2 in. of rainfall. Therefore, it can be inferred that about

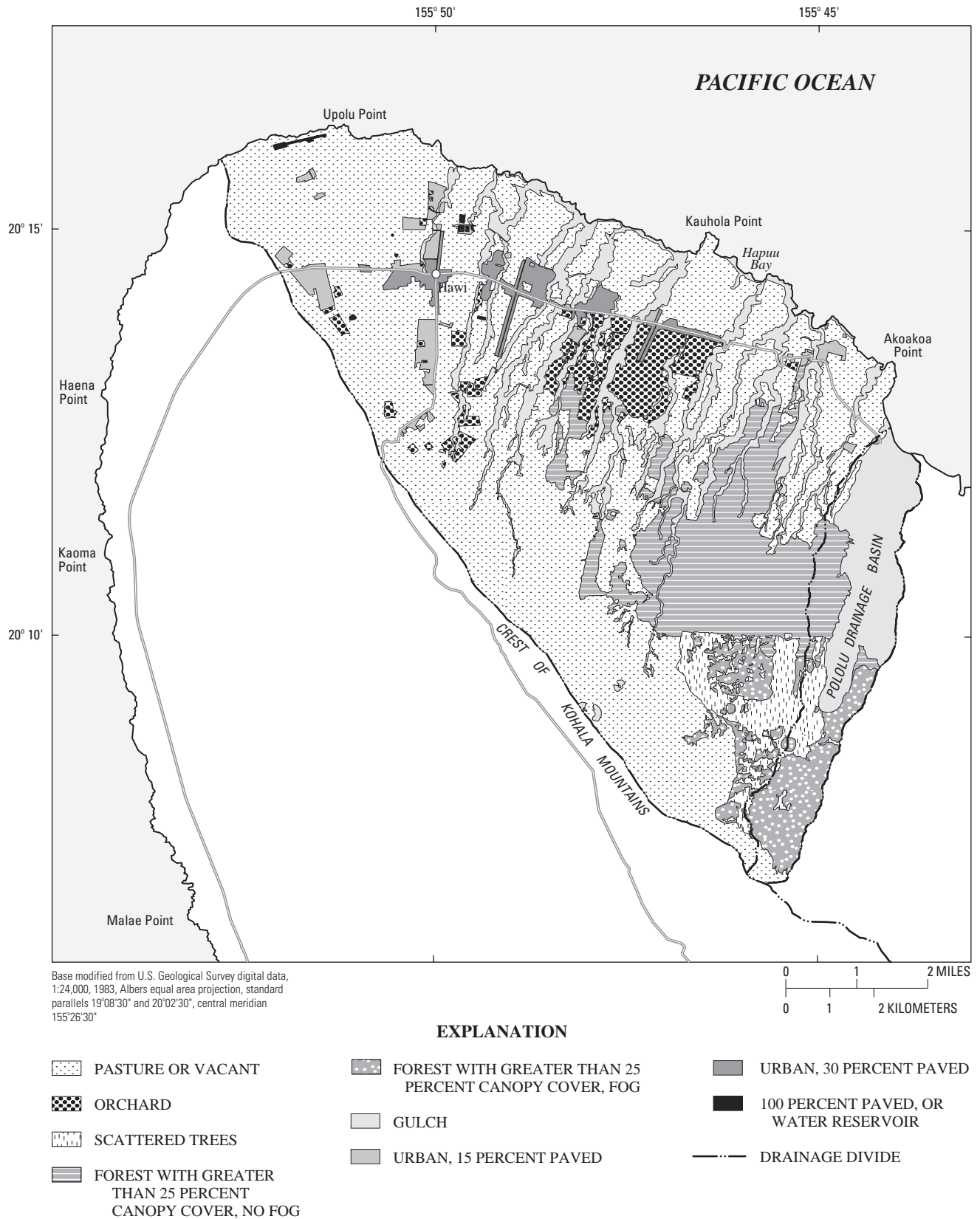


Figure 2. Land cover in the Hawi area, north Kohala, Hawaii.

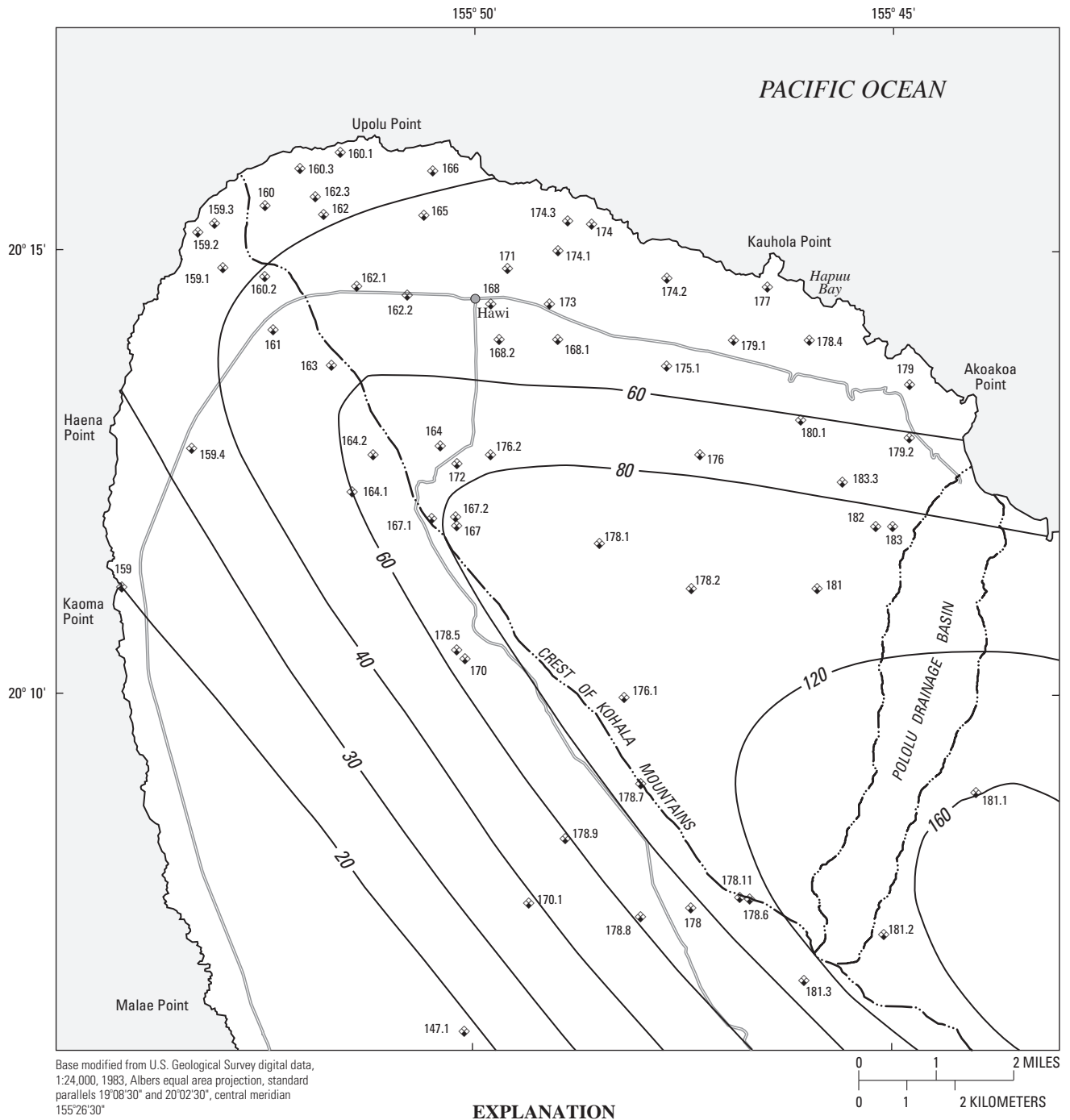


Figure 3. Average annual rainfall, north Kohala, Hawaii (modified from Giambelluca and others, 1986).

10.7 in. of fog drip was collected during the 100-day period.

Davis and Yamanaga (1963) indicated that there are no perennial streams in the study area west of Pololu Stream, although data from continuous-record gaging stations are not available to characterize streamflow in the area. Presley (1999) measured flow at various sites on Pololu Stream following a period of dry weather in 1996 and indicated that Pololu Stream was dry along its entire length except in two places: where water from the Kohala ditch was leaking into an unnamed eastern tributary that flows into the main channel, and in a wetland area near the ocean.

HYDROGEOLOGIC SETTING

Younger Hawi Volcanics and older Pololu Volcanics underlie the Hawi study area. Within the study area, the Hawi Volcanics is separated from the underlying Pololu Volcanics by a buried soil layer a few inches to 3 ft thick (Stearns and Macdonald, 1946, p. 177). The permeability of the volcanic rocks is spatially variable. Most of the soils exposed at the ground surface are in the Inceptisols order, which is characterized by soils that are on young land surfaces and have weakly developed horizons (Sato and others, 1973).

Kohala Volcano

Kohala Volcano was formed by thousands of lava flows that erupted from two main rift zones and possibly from a caldera that may have existed but that is now buried. The Kohala Volcano presently has a peak altitude of about 5,480 ft. The rift zones of Kohala Volcano trend northwest and southeast, extend from near the summit of the volcano, and are marked by numerous cinder cones and lava domes (fig. 4). Faults near the summit of the volcano indicate that a caldera may have formed during the principal stage of volcano building (shield stage), but the caldera was subsequently buried by younger lava flows.

Eruptions on Kohala Volcano were fed by magma rising in fissures. Lava flows emanated from the rift zones and central caldera where rising magma reached the land surface. Rising magma that does not erupt at the land surface may cool within the fissures, forming intrusive dikes. Dikes are thin, near-vertical sheets of massive, low-permeability rock that intrude existing

rocks, commonly permeable lava flows. Dikes are exposed in deeply eroded valleys on the northeastern part of the volcano. The number of dikes generally increases with depth and with proximity to the caldera.

The northeastern side of Kohala Volcano has undergone a major slope failure that produced a marked reentrant of the shoreline 12 mi long and extending 1 mi inland between Pololu Stream Valley and a stream valley to the southeast (Moore and others, 1989). Deeply eroded stream valleys are found within the length of the reentrant shoreline.

Pololu Volcanics.—Pololu Volcanics consists of the shield-stage tholeiitic basalt, which forms the bulk of Kohala Volcano, overlain by younger, postshield-stage transitional basalt and alkalic basalt (Wolfe and Morris, 1996). Exposed dikes of the Pololu Volcanics range in width from a few inches to 10 ft, and average about 2 ft. Individual pahoehoe and aa lava flows range from a few to 50 ft in thickness, and dip 3 to 10 degrees away from their sources where unaffected by faults (Stearns and Macdonald, 1946). Many of the surface flows can be traced to their source vents (Wolfe and Morris, 1996). Lava flows of tholeiitic basalt exposed in a valley on the northeastern part of Kohala Volcano have a weighted mean age of about 700 thousand years (ka) (Dalrymple, 1971). The tholeiitic basalt likely extends thousands of feet below sea level. Potassium-argon ages indicate that the transition from eruption of tholeiitic basalt to eruption of transitional and alkalic basalt occurred by about 400,000 years ago, and eruption of transitional and alkalic basalt continued until at least about 250,000 years ago (Wolfe and Morris, 1996).

Hawi Volcanics.—Hawi Volcanics consists of postshield-stage hawaiite, mugearite, benmoreite, and trachyte and overlies the Pololu Volcanics (Wolfe and Morris, 1996). The exposed dikes of the Hawi Volcanics range in width from 3 to 40 ft, but widths greater than 10 ft are rare (Stearns and Macdonald, 1946). Lava flows originated from numerous vents, marked by cinder cones and lava domes, near the rift zones of the volcano. The flows were fairly viscous and range from 10 to 150 ft in thickness, averaging about 40 ft. Most of the flows are massive aa flows. The composite thickness of layered flows of Hawi Volcanics may be as great as 500 ft near the summit. Lava flows dip 3 to 12 degrees except where they flowed into deeply eroded valleys (Stearns and Macdonald, 1946). Only a few flows of the

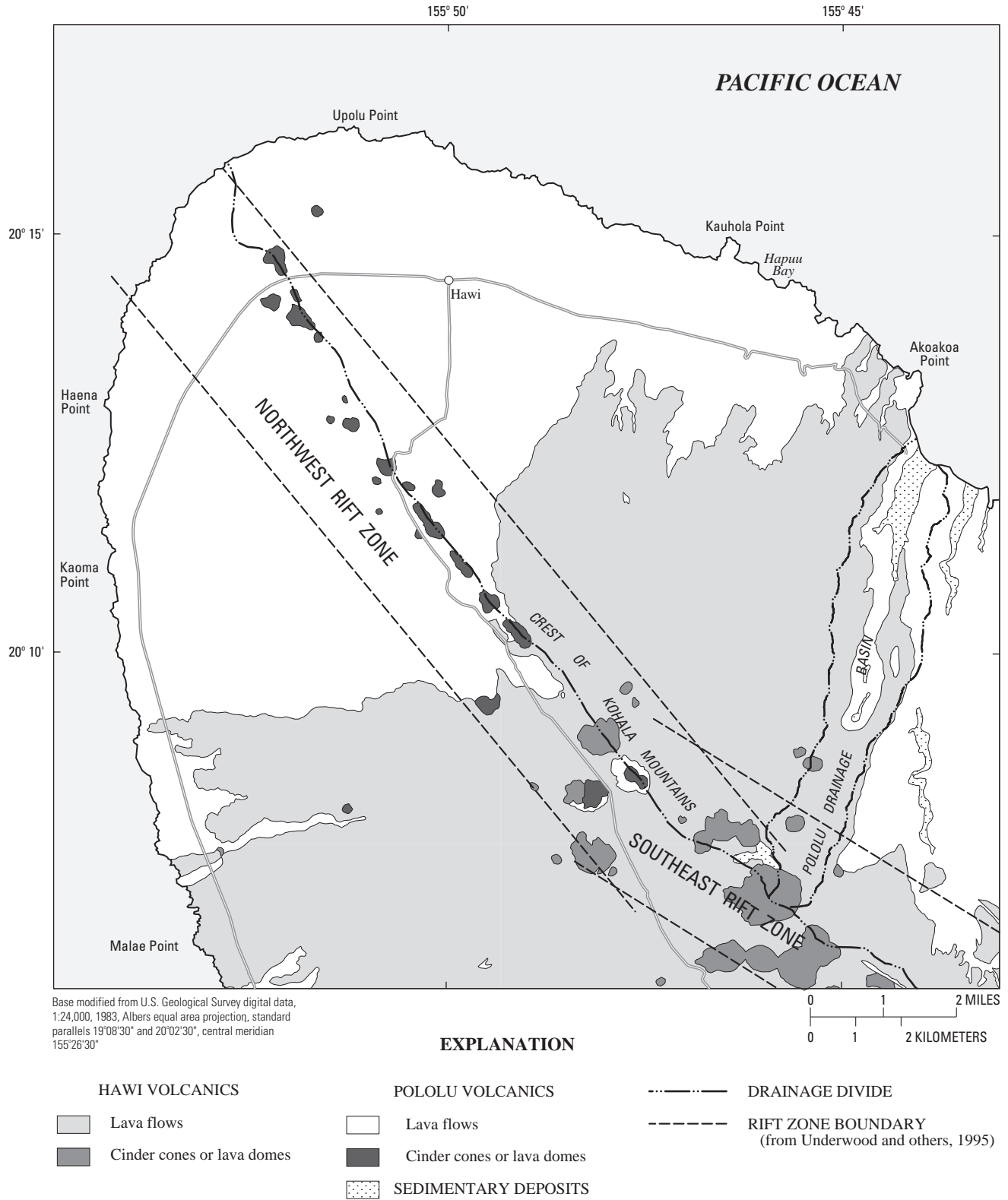


Figure 4. Surficial geology of north Kohala, Hawaii (modified from Wolfe and Morris, 1996).

Hawi Volcanics reached the coast. Potassium-argon ages of lava flows from the Hawi Volcanics range from about 230 to 120 ka (Wolfe and Morris, 1996).

Sedimentary deposits.—Unconsolidated younger alluvium, consisting of poorly sorted silts, sands, and boulders and landslide deposits, lies in streambeds and forms lowlands at the mouths of large valleys on the northeastern side of Kohala Volcano. Consolidated older alluvium, consisting of poorly sorted boulder conglomerates, lies in the larger northeastern valleys and crops out from 50 to 1,200 ft above sea level (Stearns and Macdonald, 1946).

Hydraulic Conductivity of the Rocks

Hydraulic conductivity is a quantitative measure of the capacity of a rock to transmit water. In qualitative terms, the ease with which fluid can move through a porous rock is described by permeability (see for example Domenico and Schwartz, 1990). The permeability of volcanic rocks is variable and depends partly on the mode of emplacement of the rocks. Sedimentary deposits are of limited areal extent within the study area and are not a significant controlling factor on the regional ground-water flow system.

Lava Flows.—The layered sequence of thin-bedded lava flows of Pololu Volcanics, where dike intrusions are absent, is highly permeable (Stearns and Macdonald, 1946). The main features of lava flows contributing to the high permeability are (1) clinker zones associated with aa flows, (2) voids along the contacts between flows, (3) cooling joints normal to flow surfaces, and (4) lava tubes associated with pahoehoe flows. Using aquifer tests, Underwood and others (1995) estimated the horizontal hydraulic conductivity of the dike-free Pololu Volcanics to range from 610 to 6,400 ft/d, with values increasing in a northwesterly direction within the Hawi study area. The lower hydraulic-conductivity values in the southeastern part of the study area may be associated with weathering because of higher rainfall. Within the study area, the Hawi Volcanics is probably less permeable than the Pololu Volcanics. However, the Hawi Volcanics lies above the main ground-water body and does not impede the flow of water in the aquifer formed by the Pololu Volcanics.

Dikes.—Intrusive dikes are hydrologically important because they have low permeability and can extend vertically and laterally for thousands of feet. Dikes

intersect at various angles and compartmentalize the more permeable intruded rock so that ground water can be impounded to high altitudes. Because dikes lower overall rock porosity and permeability, the bulk hydraulic conductivity of the volcanic rocks decreases as the number of dike intrusions increases. No published estimates are available for the hydraulic conductivity of the dike-intruded part of the study area near the rift zones and caldera area.

Weathering.—Weathering tends to reduce the permeability of the volcanic rocks. In general, weathering is more extensive in areas of higher rainfall to the southeast of the study area. The zone of weathered Pololu Volcanics and soil near the contact of the Hawi and Pololu Volcanics likely impedes the downward flow of water to the underlying ground-water body.

Soils

The basalts of the Pololu Volcanics weather to deep red-brown soils. In places on the lower northeast slopes of the Kohala Mountains, the Pololu Volcanics is almost completely decomposed down to depths of 50 to 200 ft. Soils on the Hawi Volcanics are generally a few inches to 3 ft thick, and are commonly rocky in dry areas. Sugarcane was grown on the soils overlying the Hawi Volcanics west of Pololu Stream Valley, but the soil is thin and plowed fields exposed gray, incompletely weathered volcanic rock (Stearns and Macdonald, 1946).

GROUND WATER

Precipitation (rainfall and fog drip) is the main source of freshwater in the study area. The precipitation either (1) runs off, (2) evaporates or is transpired by vegetation, (3) recharges the ground-water system, or (4) is stored in the soil. Ground water flows from areas of higher to lower hydraulic head, as measured by water levels in wells, shafts, and tunnels. Water levels are highest in the mountainous interior parts of the study area and lowest near the coast and, thus, fresh ground water flows from the mountainous interior areas to coastal discharge areas (fig. 5). Fresh ground water that is not withdrawn from wells and tunnels discharges naturally from the aquifer at subaerial and submarine springs and seeps.

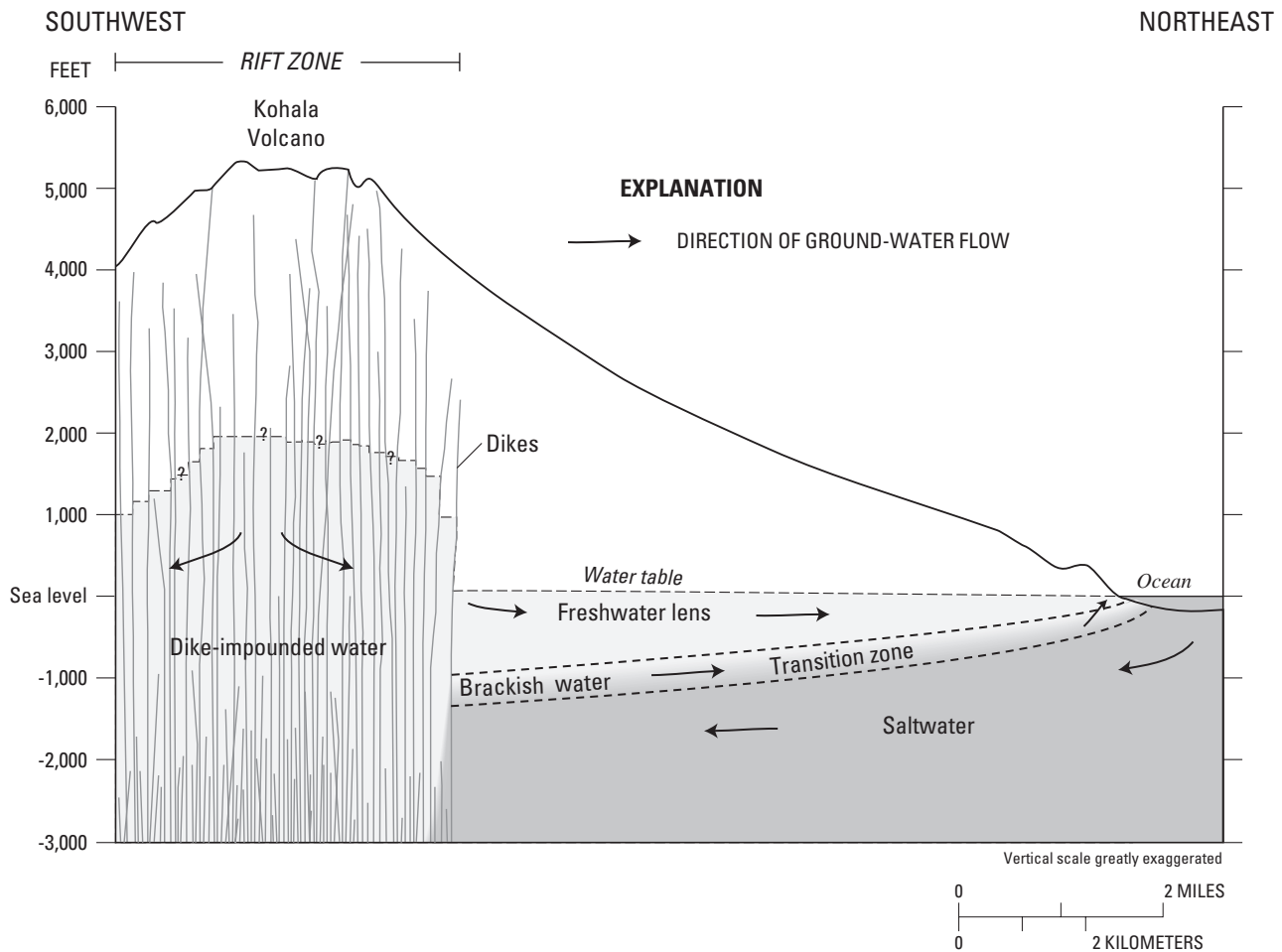


Figure 5. Schematic cross section showing generalized directions of ground-water flow in the dike-impounded and freshwater-lens systems of the Hawi area, north Kohala, Hawaii (modified from Underwood and others, 1995).

Fresh ground water in the study area is found in two main forms: (1) as a freshwater-lens system in the dike-free lava flows, and (2) as a dike-impounded system where overall permeability is reduced because of the presence of dikes. Perched water also exists near the contact between Pololu Volcanics and Hawi Volcanics.

Dike-Impounded System

A dike-impounded system is found within and near the rift zones of Kohala Volcano, where low-permeability dikes have intruded other rocks. The boundary between the dike-impounded system and the freshwater-lens system, as indicated by Underwood and others (1995), generally corresponds to the seaward extent of mapped volcanic vents represented by cinder cones and lava domes (fig. 4). Near-vertical dikes tend to compart-

mentalize areas of permeable volcanic rocks. The dike-impounded flow system includes a freshwater body, and where they exist, underlying brackish water and saltwater. Information is unavailable to determine where saltwater exists beneath the freshwater body within the dike-impounded system. However, because the dike-impounded system extends to the coast between Haena and Upolu Points and the general strikes of dikes are roughly perpendicular to the coast, saltwater can probably be found at shallow depths near the coastal part of the dike-impounded system.

Water enters the dike-impounded system mainly by infiltration of some part of rainfall and fog drip. Water discharges from the system as springs and ground-water flow to the downgradient freshwater-lens system.

Freshwater-Lens System

The freshwater-lens system includes a lens-shaped freshwater body, an intermediate transition zone of brackish water, and underlying saltwater. The freshwater lens floats on the denser saltwater. Mixing of seaward-flowing freshwater with landward-flowing saltwater forms the brackish-water transition zone. The freshwater-lens system occurs within the high-permeability, dike-free volcanic rocks.

The thickness of the freshwater lens can be estimated from monitor wells that are open to the aquifer below the water table and that penetrate into the transition zone. Two such wells were drilled in the study area. Well D (7445-01) was drilled in the northeastern part of the study area, about 0.4 mi from the coast at an altitude of 108.5 ft, to a depth of 352 ft below sea level; well I (7549-03) was drilled in the northwestern part of the study area, about 0.7 mi from the coast at an altitude of 299.5 ft, to a depth of 137 ft below sea level (fig. 6). To estimate the thickness of the freshwater lens and the upper transition zone, water samples were collected in March 1990 from several depths in each well and analyzed for chloride concentration (an indicator of salinity) (Underwood and others, 1995). For this report, freshwater is defined as water having a chloride concentration less than 250 mg/L. The chloride concentration of seawater is about 19,500 mg/L (Wentworth, 1939). The brackish-water transition zone contains water with chloride concentrations between 250 and 19,500 mg/L. The upper part of the transition zone contains water with chloride concentrations between 250 and 9,750 mg/L, whereas the lower part of the transition zone contains water with chloride concentrations between 9,750 and 19,500 mg/L. In well D, the estimated thickness of the freshwater lens was 265 ft, and the thickness of the upper part of the transition zone was about 80 ft (fig. 7). In well I, the estimated thickness of the freshwater lens was 83 ft, and the thickness of the upper part of the transition zone was about 62 ft (fig. 7). The freshwater lens is thicker in well D even though it is located closer to the coast than well I. This can be explained by (1) greater recharge, (2) lower aquifer permeability, and (3) greater resistance to discharge from the aquifer to the ocean near well D relative to well I, although regional saltwater intrusion near well I also could reduce the freshwater-lens thickness near well I.

Because wells D and I are open to the aquifer throughout their entire depths below the water table,

water from the aquifer can enter and exit the borehole at different depths, and this flow within the borehole may affect the salinity profile in the well. Underwood and others (1995) suggested that if borehole flow exists in the wells, the borehole salinity profiles would tend to indicate a shallower transition zone than actually exists in the aquifer because the wells are near the coastal discharge area where flow in the aquifer has an upward component.

Water enters the freshwater-lens system by infiltration of rainfall, fog drip, and irrigation water, and as inflow from upgradient ground-water bodies. Ground-water flow from the dike-impounded system and downward moving water from perched water bodies recharge the freshwater lens. Two additional sources of water from outside the study area include about 2.0 Mgal/d seepage losses from the Kohala ditch in the study area and injection of about 8 Mgal/d at the Hawi hydroelectric plant (Underwood and others, 1995). Discharge from the freshwater lens is by subaerial and submarine coastal springs, and by diffuse seepage near the coast. Discharge of freshwater and inflow of saltwater to the dike-free volcanic rocks may be impeded by weathered volcanic rocks that extend to sea level (Stearns and Macdonald, 1946).

Perched System

Within the study area, perched water occurs near the base of the Hawi Volcanics, where the Hawi Volcanics are underlain by low-permeability soil and weathered Pololu Volcanics (Stearns and Macdonald, 1946). Beneath the weathered Pololu Volcanics and above the water table of the freshwater-lens system, a zone of unsaturated volcanic rocks exists. Recharge to the perched system is from infiltration of precipitation and irrigation water. Discharge from the perched system is downward to the freshwater-lens system and to springs, particularly where the base of the Hawi Volcanics has been exposed.

Ground-Water Levels

Dike-impounded system.—The highest ground-water levels in the study area are likely in the interior part where dikes are present. Although no water-level measurements are available to indicate the altitude of the water table in the dike-impounded system, water levels are probably several hundreds of feet or more

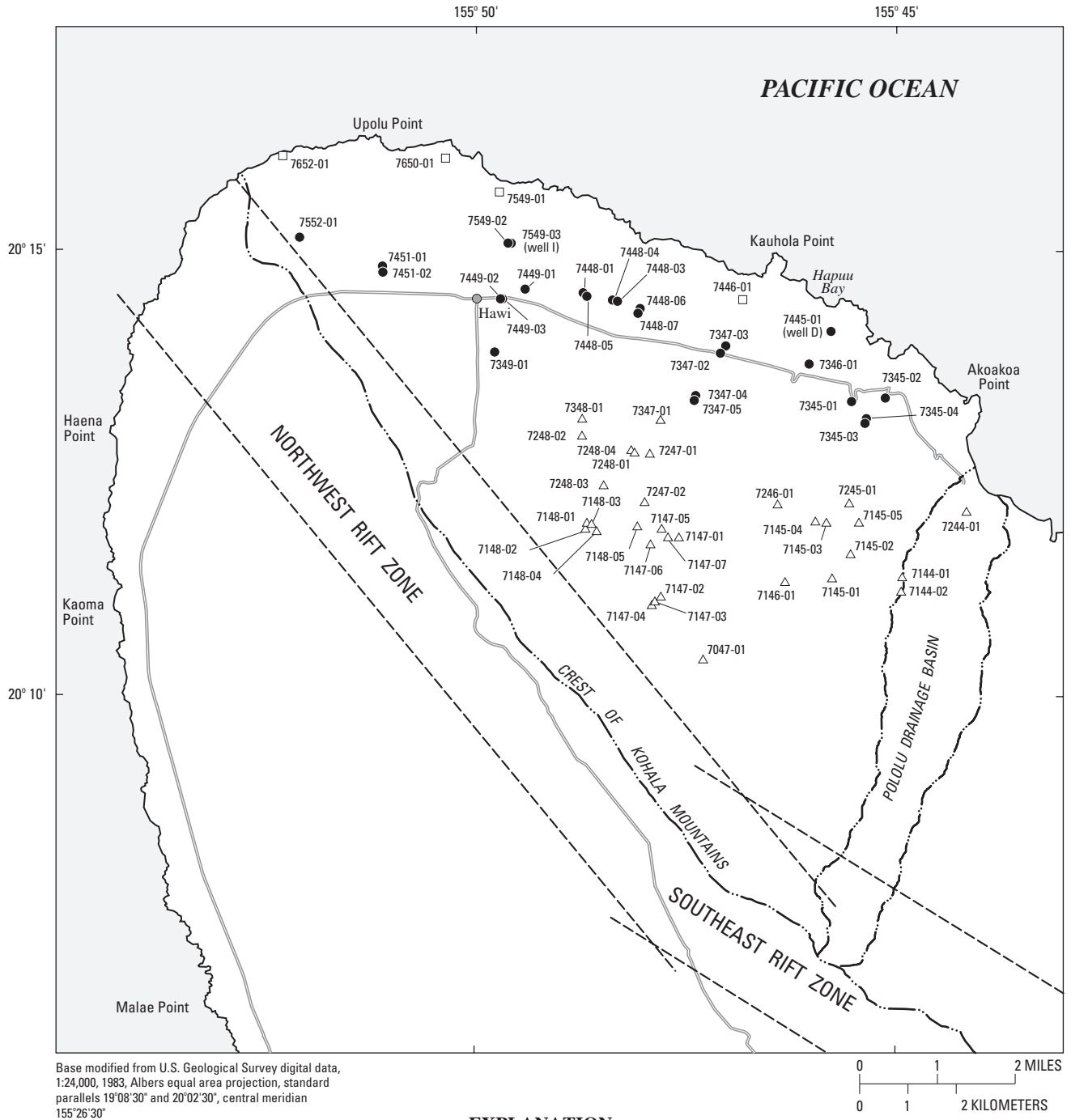


Figure 6. Selected wells, shafts, and tunnels in the Hawi area, north Kohala, Hawaii.

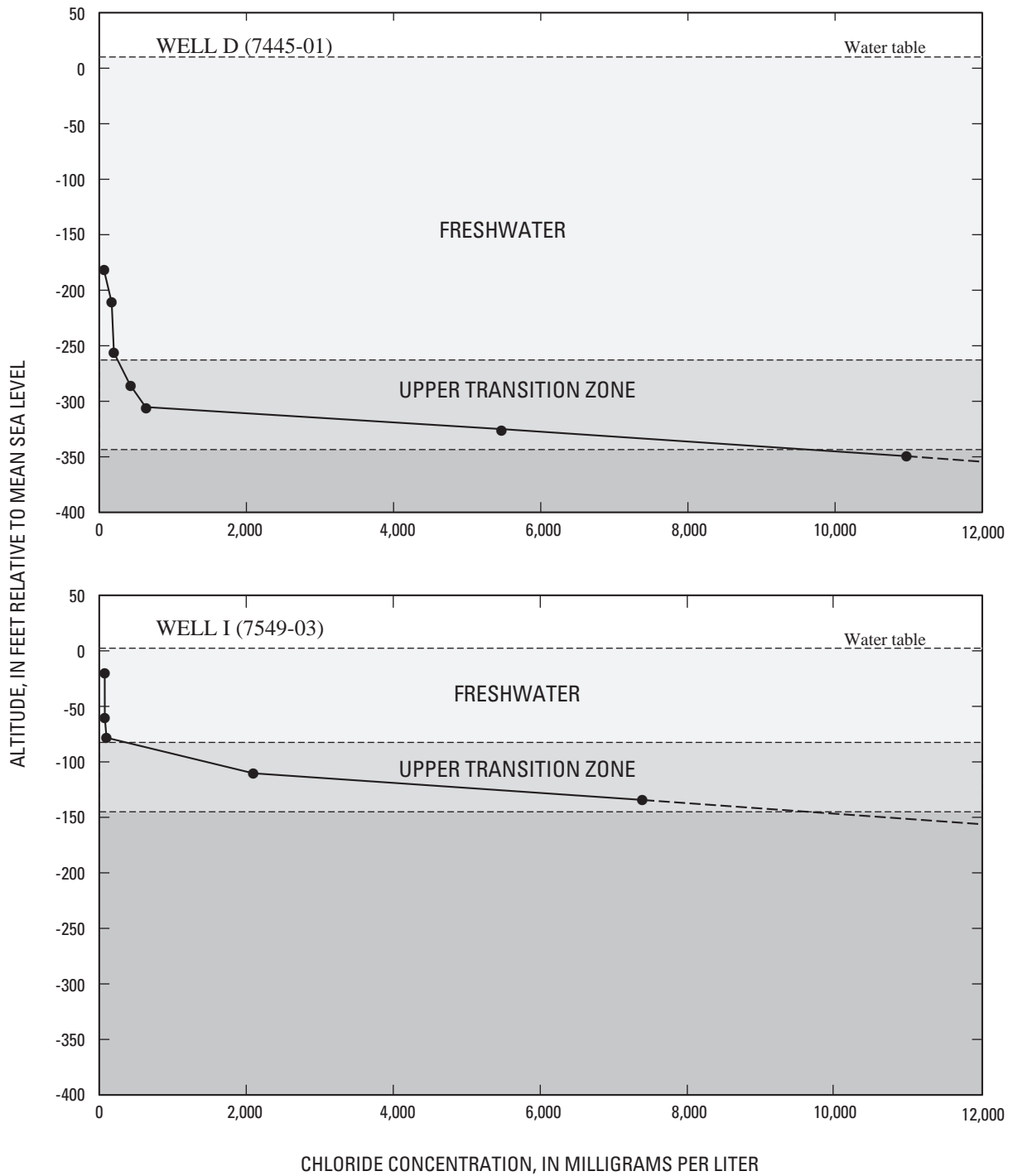


Figure 7. Chloride-concentration profiles from wells D (7445-01) and I (7549-03) in the Hawi area, north Kohala, Hawaii, March 1990 (modified from Underwood and others, 1995).

above sea level in the interior part of the system. To the southeast of the study area, dike-impounded ground water discharges from springs at altitudes higher than 2,000 ft, where dike compartments have been exposed by erosion and where rainfall is high. Near the summit of Kohala Volcano, Stearns and Macdonald (1946) indicated that ground-water levels may be as high as 3,000 ft. Near the coastal part of the dike-impounded system, water levels probably decline to a few feet or a few tens of feet above sea level.

Freshwater-lens system.—Measured water levels from wells drilled into the freshwater lens range from a few feet above sea level at shaft 7652-01 (near the coast at Upolu Point) to about 11 ft above sea level at wells 7347-04 and -05 (2 mi inland from Kauhola Point). Measured water levels (fig. 8) indicate that there is a general northerly movement of ground water in the freshwater lens. Measured water levels vary with time because of variations in rainfall but do not indicate significant long-term trends (fig. 9).

Ground-Water Withdrawals

In the Hawi area, ground water is withdrawn from the freshwater-lens and perched ground-water systems. No known wells or tunnels develop water from the dike-impounded system in the Hawi area, although the dike-impounded system southeast of the study area contributes to the flow of an irrigation ditch constructed in the early 1900's.

Freshwater-lens system.—In the late 1890's, the first successful well was drilled in the Hawi area (Union Mill well 7448-01) to about 13 ft below sea level. Although the well was eventually abandoned, it was used to supply water for sugar mill operations and produced water with a chloride concentration of about 40 mg/L (Davis and Yamanaga, 1963).

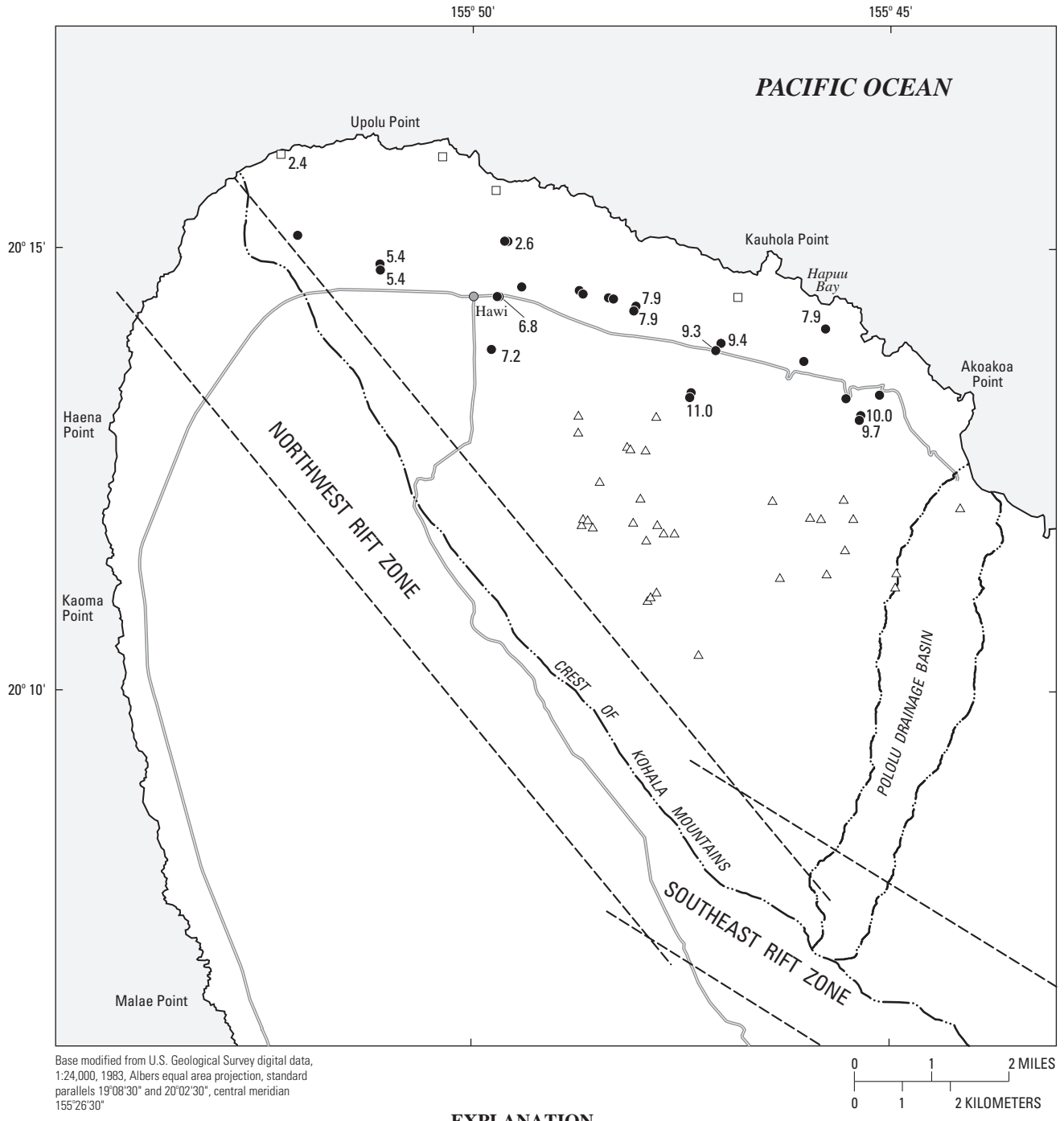
Prior to 1975, withdrawal from the freshwater-lens system was from four Maui-type wells (consisting of a shaft excavated from the ground surface to near sea level and one or more horizontal tunnels extending near the water table out from the bottom of the shaft) and three drilled wells owned by Kohala Sugar Company. Three Maui-type wells (Kohala shaft 7446-01, Alaalae shaft 7549-01, and Hoea shaft 7650-01) were completed by about 1900, and a fourth Maui-type well (Waikane shaft 7652-01) was completed in 1920. These Maui-type wells, which were used for irrigation of sugarcane

by Kohala Sugar Company, produced water with chloride concentrations ranging from 88 to 1,580 mg/L (Stearns and Macdonald, 1946). Alaalae shaft (7549-01) was abandoned prior to 1940. In 1948, Halaula well 7347-02 was drilled for domestic supply to a depth of 168 ft below sea level, and this well produced water with chloride concentrations ranging from 20 to 30 mg/L. Kohala Sugar Company drilled two irrigation wells, Union Mill well 1 (7448-04) in 1965 and Union Mill well 2 (7448-05) in 1969, to depths of 100 ft below sea level. From 1940 through 1975, annual combined withdrawal from the Kohala Sugar Company wells (7446-01, 7650-01, 7652-01, 7347-02, 7448-04, and 7448-05) averaged 7.9 Mgal/d, ranging from a low of 2.3 Mgal/d in 1975 to a high of 14.4 Mgal/d in 1962 (fig. 10) (computed from unpublished data, provided by Kohala Sugar Company, in USGS Hawaii District well files). From 1949 through 1975, withdrawal from the domestic well (7347-02) averaged about 5 percent of the total withdrawal from all wells. After 1975, Kohala Sugar Company stopped withdrawing ground water because cultivation of sugarcane in the area ceased at about that time.

The first well drilled for the Hawaii County Department of Water Supply (DWS) was the Hawi well 1 (7449-02) in 1975, which was drilled to a depth of 50 ft below sea level. The DWS had a second well drilled (Hawi well 2, 7349-01) in 1993 to a depth of 56 ft below sea level. From 1978 through 1999, annual combined withdrawal from these two DWS wells averaged 0.13 Mgal/d (fig. 10). During the 1990's, withdrawals from DWS wells 7449-02 and 7349-01 averaged 0.21 and 0.05 Mgal/d, respectively (computed from data provided by DWS).

Perched system.—Development of perched ground water by tunnels in the Hawi area began in the late 1800's (Davis and Yamanaga, 1963). Tunnels, ranging in length from a few tens of feet to about 1,600 ft, commonly were excavated near the base of the Hawi Volcanics, where water is perched on weathered Pololu Volcanics and soil, and intercepted water that discharged at springs (Stearns and Macdonald, 1946). Discharge from the tunnels was used for irrigation and domestic water systems.

The volume of perched water and the discharge from tunnels and springs fluctuated greatly, increasing during periods of high rainfall and decreasing during dry periods. For example, Stearns and Macdonald



EXPLANATION

- DRAINAGE DIVIDE
- RIFT ZONE BOUNDARY (from Underwood and others, 1995)
- 8.0 WELL AND AVERAGE 1990'S WATER LEVEL (WHERE AVAILABLE)--Datum is mean sea level
- 2.4 MAUI SHAFT AND AVERAGE 1990'S WATER LEVEL (WHERE AVAILABLE)--Datum is mean sea level
- △ TUNNEL

Figure 8. Average 1990's water levels measured in wells and shafts in the Hawi area, north Kohala, Hawaii.

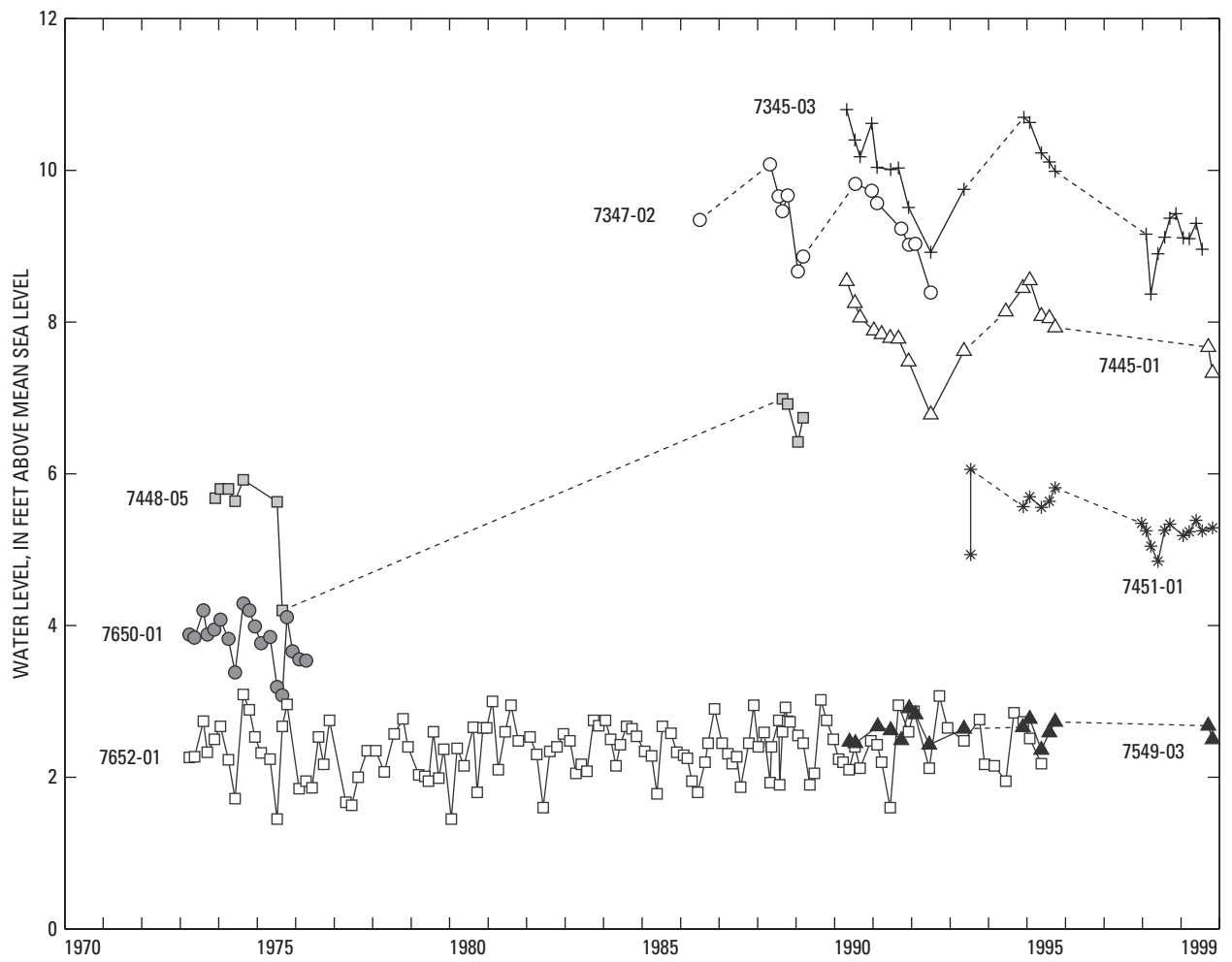


Figure 9. Water levels measured under nonpumped conditions in selected wells in the Hawi area, north Kohala, Hawaii. Data points are connected by dashed lines if successive measurements were made more than one year apart. (Data from USGS Hawaii District well files.)

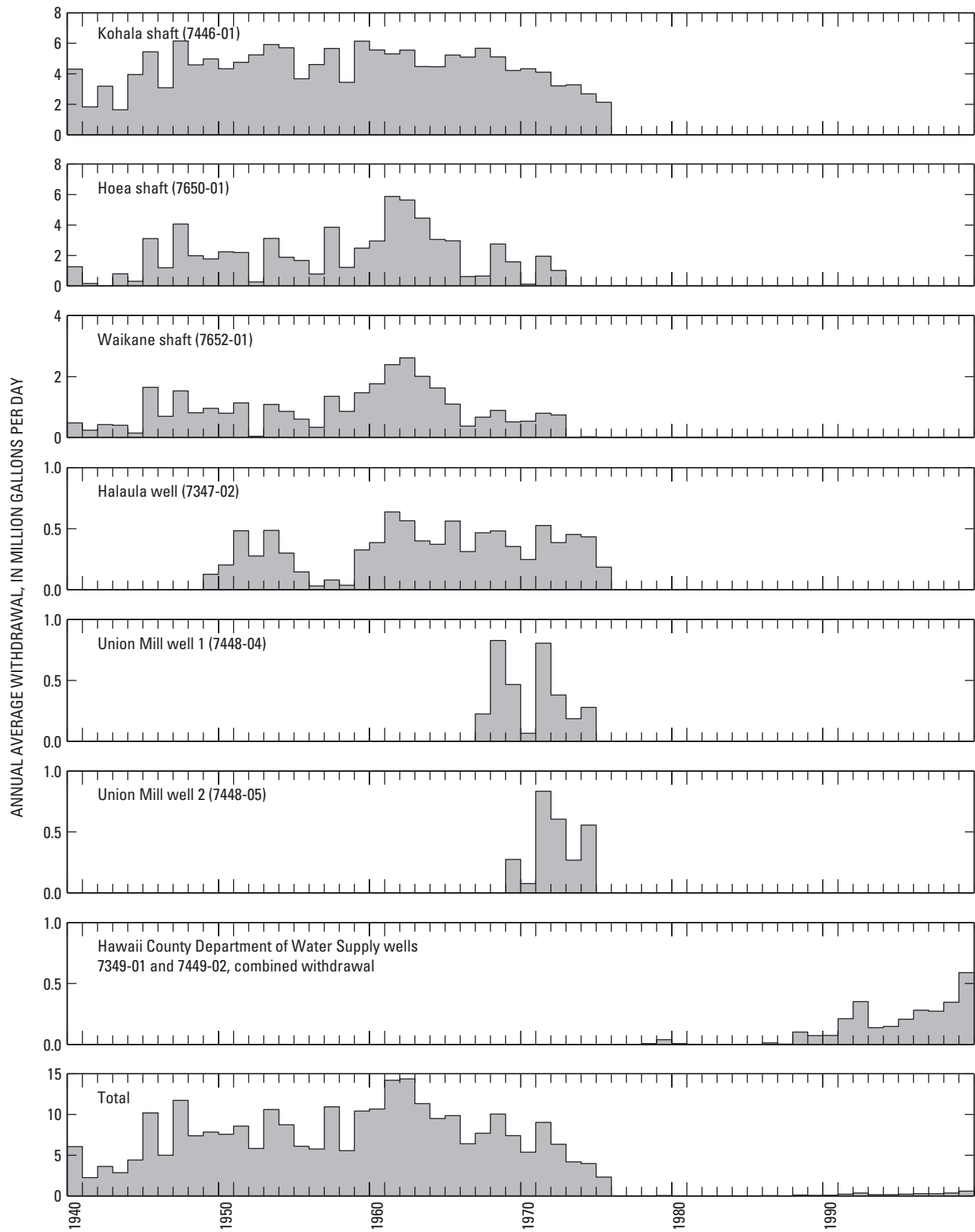


Figure 10. Ground-water withdrawal during 1940–99 from wells and shafts in the Hawi area, north Kohala, Hawaii. (Data from Kohala Sugar Company and Maui County Department of Water Supply.)

(1946) reported that discharge from the Bond 1 tunnel (7247-01) ranged from 0.2 to 4.2 Mgal/d. Data from Stearns and Macdonald (1946) indicate that average discharge from tunnels and springs in the Hawi area was about 5 Mgal/d, although an inventory of water use from the early 1990's indicates only about 0.4 Mgal/d of water withdrawn from 4 tunnels (Lindsay, 7047-01; Watt 1, 7148-04; Bond 1, 7247-01; and Murphy, 7145-02) (State of Hawaii, 1991).

Irrigation ditches.—Two irrigation ditches, Kohala and Kahena, were constructed in the early 1900's to transport water from the area east of Pololu Stream to the Hawi area for agriculture (fig. 1). The Kohala ditch was constructed between 1905 and 1907 (Wilcox, 1996), and consists of a system of diversions, ditches, tunnels, and flumes that collected and conveyed both surface water and ground water for sugarcane irrigation. Ground water conveyed by the Kohala ditch consists of both dike-impounded water from the East Branch of Honokane Nui Stream and perched water (Stearns and Macdonald, 1946). The Kohala ditch currently conveys water over a distance of about 18 mi northwest mainly for hydroelectric power near Hawi. Flow rates in the mid-1990's were about 10 to 15 Mgal/d (Underwood and others, 1995).

The Kahena ditch was constructed between 1912 and 1914 (Wilcox, 1996) and conveyed water westward over a distance of about 8 mi. Kahena ditch diverts water from an altitude of 4,200 ft from Honokane Nui Stream. During the period of record of discharge measurements for Kahena ditch (1918–19, 1928–65), average discharge was 7.4 Mgal/d (U.S. Geological Survey, 1977). The Kahena ditch did not flow continuously and in recent years has fallen into disrepair.

WATER BUDGET

A daily water budget was used for this study to estimate long-term mean annual recharge for 1990's land-use conditions. A daily water budget was used rather than a monthly water budget to avoid possible errors associated with the longer computation interval. To estimate long-term average recharge, it was necessary to compute the daily water budget for a period long enough to achieve a steady, long-term mean recharge value given representative interannual variations in rainfall. The method and data used to compute the water budget are described below.

Daily Water-Budget Method

The daily water-budget method used in this study is a variant of the Thornthwaite and Mather (1955) bookkeeping procedure. A water-budget of the plant-soil system was computed on a daily basis in the following manner. For a given area, daily runoff was subtracted from daily water input (rainfall plus irrigation plus fog drip), and this volume was added to the ending soil-moisture storage for the previous day to determine interim soil-moisture storage:

$$X_i = P_i + I_i + F_i - R_i + S_{i-1} \quad (1)$$

where:

X_i = interim soil-moisture storage for current day [L],

S_{i-1} = ending soil-moisture storage from previous day (i-1) [L],

P_i = rainfall for current day [L],

I_i = irrigation for current day [L],

F_i = fog drip for current day [L],

R_i = runoff for current day [L], and

i = subscript designating current day.

All volumes of water are expressed as an equivalent depth of water over an area by dividing by the total plan area.

In general, runoff in the study area occurs rapidly in response to rainfall. There are no known perennial streams in the study area, which indicates that runoff is not significantly enhanced by water that previously recharged to the water table. Thus, in the water budget, runoff is assumed to be an instantaneous response to rainfall and is removed before accounting for recharge.

For a given day, evapotranspiration was subtracted from the interim soil-moisture storage, and any soil moisture remaining above the maximum soil-moisture storage was assumed to be recharge. Recharge and soil-moisture storage at the end of a given day were assigned according to the following equations:

$$\begin{array}{ll} \text{for } X_i - E_i \leq S_m & \text{for } X_i - E_i > S_m \\ Q_i = 0 & Q_i = X_i - E_i - S_m \\ S_i = X_i - E_i & S_i = S_m \end{array} \quad (2)$$

where:

E_i = depth of water lost to evapotranspiration during the day [L],

Q_i = ground-water recharge during the day [L],

S_i = soil-moisture storage [L] (≥ 0) at the end of the current day, i , and

S_m = maximum soil-moisture storage [L].

Ending soil-moisture storage for the current day, expressed as a depth of water, is equal to the root depth multiplied by the difference between the ending volumetric soil moisture content within the root zone for the current day and the volumetric wilting-point moisture content.

$$S_i = D \times (\theta_i - \theta_{wp}) \quad (3)$$

where:

D = plant root depth [L],

θ_i = ending volumetric soil-moisture content for the current day, i , [L^3/L^3], and

θ_{wp} = volumetric wilting-point moisture content [L^3/L^3].

The maximum soil-moisture storage, S_m , expressed as a depth of water, is equal to the root depth multiplied by the available water capacity, ϕ , which is the difference between the volumetric field-capacity moisture content and the volumetric wilting-point moisture content.

$$S_m = D \times \phi \quad (4)$$

where:

$\phi = \theta_{fc} - \theta_{wp}$ [L^3/L^3], and

θ_{fc} = volumetric field-capacity moisture content [L^3/L^3].

Evapotranspiration was determined as a function of the potential-evapotranspiration rate and soil moisture. A vegetated surface loses water to the atmosphere at the potential-evapotranspiration rate if available water is non-limiting (see for example Thornthwaite, 1948). Although Penman (1956) defined potential transpiration as “the amount of water transpired in unit time by a short green crop, completely shading the ground, of uniform height and never short of water,” in this study the potential-evapotranspiration concept was applied to all vegetated surfaces and was not restricted to a reference short green crop.

At all sites, the potential evapotranspiration was assumed to be equal to pan evaporation multiplied by an appropriate vegetation factor. For soil-moisture contents greater than or equal to a threshold value, C_i , the rate of evapotranspiration was assumed to be equal to the potential-evapotranspiration rate. For soil-moisture contents below C_i , the rate of evapotranspiration was

assumed to occur at a reduced rate that declines linearly with soil moisture content:

$$\begin{aligned} E &= PE_i && \text{for } S \geq C_i \\ E &= S \times PE_i/C_i && \text{for } S < C_i \end{aligned} \quad (5)$$

where:

E = instantaneous rate of evapotranspiration [L/T],

PE_i = potential-evapotranspiration rate for current day [L/T],

S = instantaneous soil-moisture storage [L], and

C_i = threshold soil-moisture content below which evapotranspiration is reduced below the potential-evapotranspiration rate [L].

The threshold soil moisture, C_i , was estimated from an empirical model (Giambelluca, 1983) having the form:

$$\begin{aligned} C_i &= [a + bD + cPE_i] \times S_m && \text{for } [a + bD + cPE_i] < 1 \\ C_i &= S_m && \text{for } [a + bD + cPE_i] \geq 1 \end{aligned} \quad (6)$$

The calibration coefficients a , b , and c were determined by Giambelluca (1983) partly on the basis of lysimeter studies from Hawaii (Ekern, 1966). For D expressed in millimeters (mm), and PE_i expressed in mm per day, the calibration coefficients were determined to be:

for $PE_i \leq 6$ mm/d	for $PE_i > 6$ mm/d
$a = 1.25$	$a = 1.41$
$b = -1.87 \times 10^{-3}$	$b = -1.87 \times 10^{-3}$
$c = 5.20 \times 10^{-2}$	$c = 2.20 \times 10^{-2}$

In the water budget, the evapotranspiration rate may (1) be equal to the potential-evapotranspiration rate for part of the day and less than the potential-evapotranspiration rate for the remainder of the day, (2) be equal to the potential-evapotranspiration rate for the entire day, or (3) be less than the potential-evapotranspiration rate for the entire day. The total evapotranspiration during a day is a function of the potential-evapotranspiration rate, interim soil-moisture storage, and threshold soil-moisture content, C_i . By recognizing that $E = -dS/dt$, the total depth of water lost to evapotranspiration during a day, E_i , was determined as:

$$\begin{aligned}
E_i &= PE_i t_i + C_i \{1 - \exp[-PE_i(1-t_i)/C_i]\} & \text{for } X_i > C_i, t_i < 1 \\
E_i &= PE_i & \text{for } X_i > C_i, t_i = 1 \\
E_i &= X_i \{1 - \exp[-PE_i/C_i]\} & \text{for } X_i \leq C_i
\end{aligned} \tag{7}$$

$$\begin{aligned}
t_i &= (X_i - C_i)/PE_i & \text{for } X_i - C_i < PE_i \\
t_i &= 1 & \text{for } X_i - C_i \geq PE_i
\end{aligned} \tag{8}$$

where:

t_i = time during which soil-moisture storage is above C_i [T].

The spatial distributions of land cover, rainfall, irrigation, fog drip, runoff, potential evapotranspiration, soil properties, and vegetation root depths were incorporated into a geographic-information system (GIS) model.

Rainfall

Long-term daily rainfall data in the study area are limited, but estimates of daily rainfall are needed for the daily water budget. For this study, existing mean monthly rainfall maps (Giambelluca and others, 1986) were used as the basis for the synthesis of daily rainfall sequences. Mean monthly rainfall maps were digitized (Shade, 1995) and used to represent the spatial distribution of rainfall for this study. The mean monthly rainfall maps are representative of the period 1916 through 1983. Areas between adjacent lines of equal rainfall were assigned the average of the rainfall values for the bounding lines. Mean monthly rainfall values were modified to account for interannual and daily variations in rainfall. Rather than attempting to estimate the actual daily rainfall at a site for a given time period on the basis of limited data, a representative daily rainfall sequence was synthesized and used to estimate average annual recharge.

Interannual rainfall variability.—Annual variations in rainfall in the study area were represented by data from rain gage 168 for the period 1888 to 1983 (figs. 3 and 11). Although annual rainfall departures from mean annual rainfall are not constant over the study area, the overall interannual variability in rainfall is assumed to be reasonably represented by data from rain gage 168. The assumption is valid because the approach does not require a precise representation of the actual time series of daily rainfall to estimate long-term mean annual recharge. Monthly rainfall values from the

mean monthly rainfall maps (Giambelluca and others, 1986) were multiplied by an annual rainfall factor, equal to the annual rainfall at rain gage 168 divided by the mean annual rainfall at rain gage 168, to produce a sequence of 96 years of monthly rainfall maps in the study area.

Daily rainfall.—Daily rainfall was synthesized by disaggregating the monthly rainfall values described in the preceding section using the method of fragments (see, for example, Srikanthan and McMahon, 1982). The method creates a synthetic sequence of daily rainfall from monthly data by imposing the rainfall pattern from a rain gage with daily data. The method assumes that the rainfall pattern at a selected gage with daily data is a reasonable representation of the daily rainfall pattern for the area near the gage. The synthesized daily data approximate the long-term average character of daily rainfall, such as frequency, duration, and intensity, but do not reproduce the actual historical daily rainfall record.

Daily rainfall from nine rain gages (160.1, 167, 168, 175.1, 176, 176.1, 179, 179.1, and 181.1) (fig. 12) was used to represent the pattern of daily rainfall for the study area. Thiessen polygons were drawn around each of the nine gages, and the daily rainfall pattern from the gage within each Thiessen polygon was assumed to be a reasonable representation of the daily rainfall pattern throughout that polygon.

In the method of fragments, daily rainfall for a month is generated by multiplying the monthly rainfall total by numbers called fragments, with values greater than or equal to zero, and less than or equal to one. The fragments form a set of size n , where n is equal to the number of days in the month, and the n fragments in the set sum to one. Thus, the sum of the synthesized daily rainfall values for the month is equal to the monthly rainfall total.

In this study, measured daily rainfall values from nine selected gages (fig. 12) (Hydrosphere, 1996) were normalized by dividing the daily rainfall by the corresponding monthly rainfall total. Each normalized daily rainfall value is a rainfall fragment. Thus, as applied in this study, monthly sets of rainfall fragments were computed using daily rainfall measurements with the following equation:

$$Y_i = P_i / P_m \tag{9}$$

where:

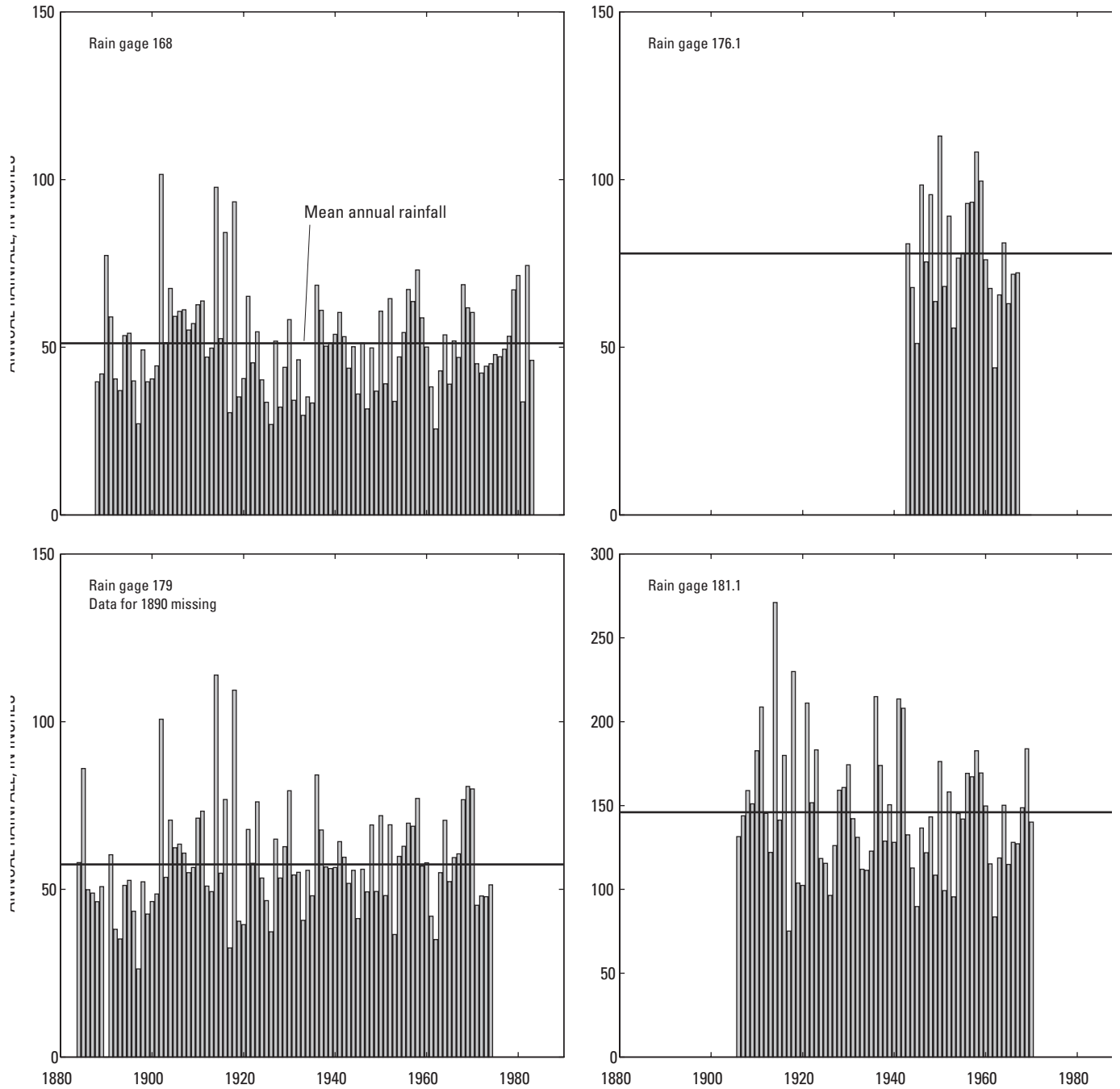


Figure 11. Annual rainfall measured at selected rain gauges in the Hawi area, north Kohala, Hawaii. (Data from Hawaii State Commission on Water Resource Management.)

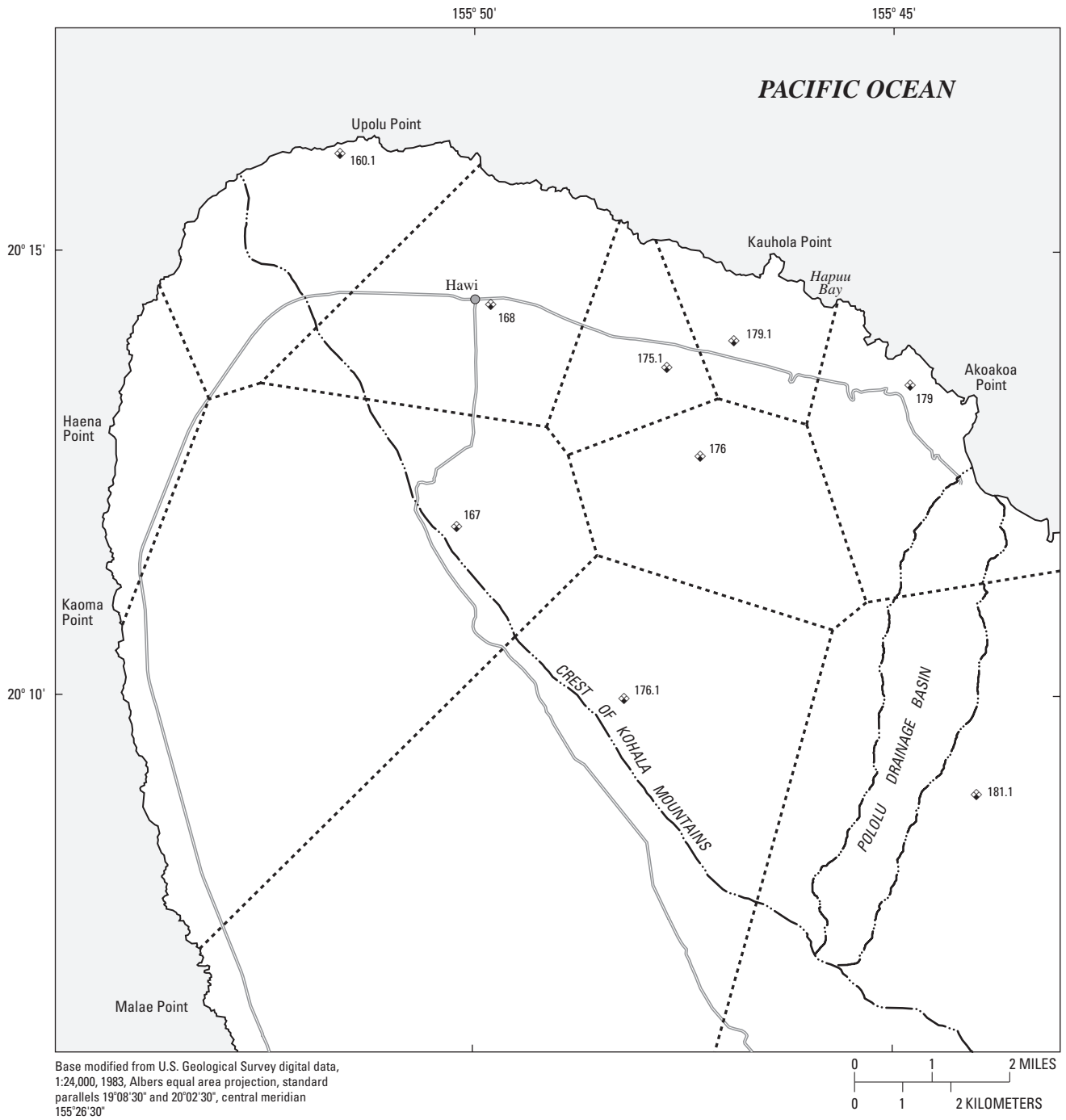


Figure 12. Thiessen polygons around selected rain gages with daily rainfall data in the Hawi area, north Kohala, Hawaii.

Table 1. Periods of record used to develop monthly fragment sets for selected rain gages in the Hawi area, north Kohala, Hawaii
[Data from Hydrosphere, 1996]

Rain gage number	Period of record	Number of usable monthly fragment sets											
		Jan	Feb	Mar	Apr	May	June	July	Aug	Sep	Oct	Nov	Dec
160.1	10/49 to 8/56	6	7	7	6	6	7	6	7	6	6	7	7
167	10/49 to 9/65	7	7	7	6	7	8	7	7	7	7	7	7
168	10/49 to 6/85	16	17	14	17	15	12	12	10	13	16	16	16
175.1	10/49 to 2/89	35	33	32	33	33	31	29	31	33	34	32	32
176	10/49 to 5/74	6	7	7	6	8	7	7	7	6	7	7	7
176.1	10/49 to 9/65	5	7	7	7	7	8	7	6	7	6	7	7
179	10/49 to 8/65	7	7	7	7	7	7	7	7	6	7	7	6
179.1	10/49 to 8/65	6	7	7	6	6	7	7	7	6	7	7	7
181.1	10/49 to 8/65	16	15	15	13	13	14	16	15	15	14	16	13

Y_i = rainfall fragment for the i th day of the month [L/L],

P_i = rainfall for the i th day of the month [L], and

P_m = rainfall for month [L].

To synthesize daily rainfall values in a particular month, a set of fragments for the appropriate site and month is randomly selected from those available for that site and month (table 1). This is done on the basis of a random number, greater than or equal to zero and less than one, from a uniform distribution of numbers. For example, a set of fragments for February at rain gage 175.1 would be selected randomly from 33 sets of fragments. Then each fragment in the set is multiplied by the monthly rainfall total. Because the sum of the fragments in each monthly set is equal to one, the rainfall model preserves (exactly) each monthly rainfall total and, thus, the mean of the synthesized daily rainfall will always equal the mean of the measured daily rainfall.

To test the method of fragments, daily rainfall was synthesized at a site where measured daily rainfall data were available. Three sequences of daily rainfall were synthesized using monthly rainfall and fragment data from rain gage 175.1. The number of rainy days, standard deviation of daily rainfall, coefficient of skew of daily rainfall, and maximum daily rainfall from the synthesized sequences are in general agreement with the values from the observed data (fig. 13). Although the observed and synthesized rainfall distributions are both positively skewed, the magnitudes of the maximum daily rainfall values may differ slightly because of the randomness associated with the selection of fragments.

For this study, the monthly sets of fragments computed using data from the rain gage within a given Thiessen polygon (fig. 12) were used to disaggregate

monthly rainfall throughout that polygon. Because of a paucity of data, it was necessary to use nonconcurrent periods of record from the nine rain gages used to generate the fragments (fig. 12, table 1). However, because sets of fragments are selected randomly during the synthesis of daily rainfall sequences, and because it was not the intent of this study to attempt to simulate the actual time series of daily rainfall, the use of nonconcurrent periods of record is not considered to be a severe limitation.

Irrigation

Estimated water use for agricultural irrigation is about 1 Mgal/d in the study area (State of Hawaii, 1991). This rate of application is equal to about 10 in/yr if it is assumed that water is uniformly distributed over the 2 square miles of land used for agriculture (fig. 2). For the water budget, it was assumed that crops were irrigated with 0.42 in. of water on the first and fifteenth days of each month. Irrigation in residential areas was considered small and was not included in the water budget.

Fog Drip

Fog that is intercepted by vegetation and that drips to the ground, also known as fog drip, can be a significant component of the water budget in Hawaii. Limited fog data for Kohala just southeast of the study area indicate a significant presence of fog at an altitude of 3,800 ft (Juvik and Nullet, 1995). Data from the islands of Lanai, Hawaii, and Oahu indicate that fog occurs above altitudes of about 2,000 to 3,000 ft (Ekern, 1964; Juvik

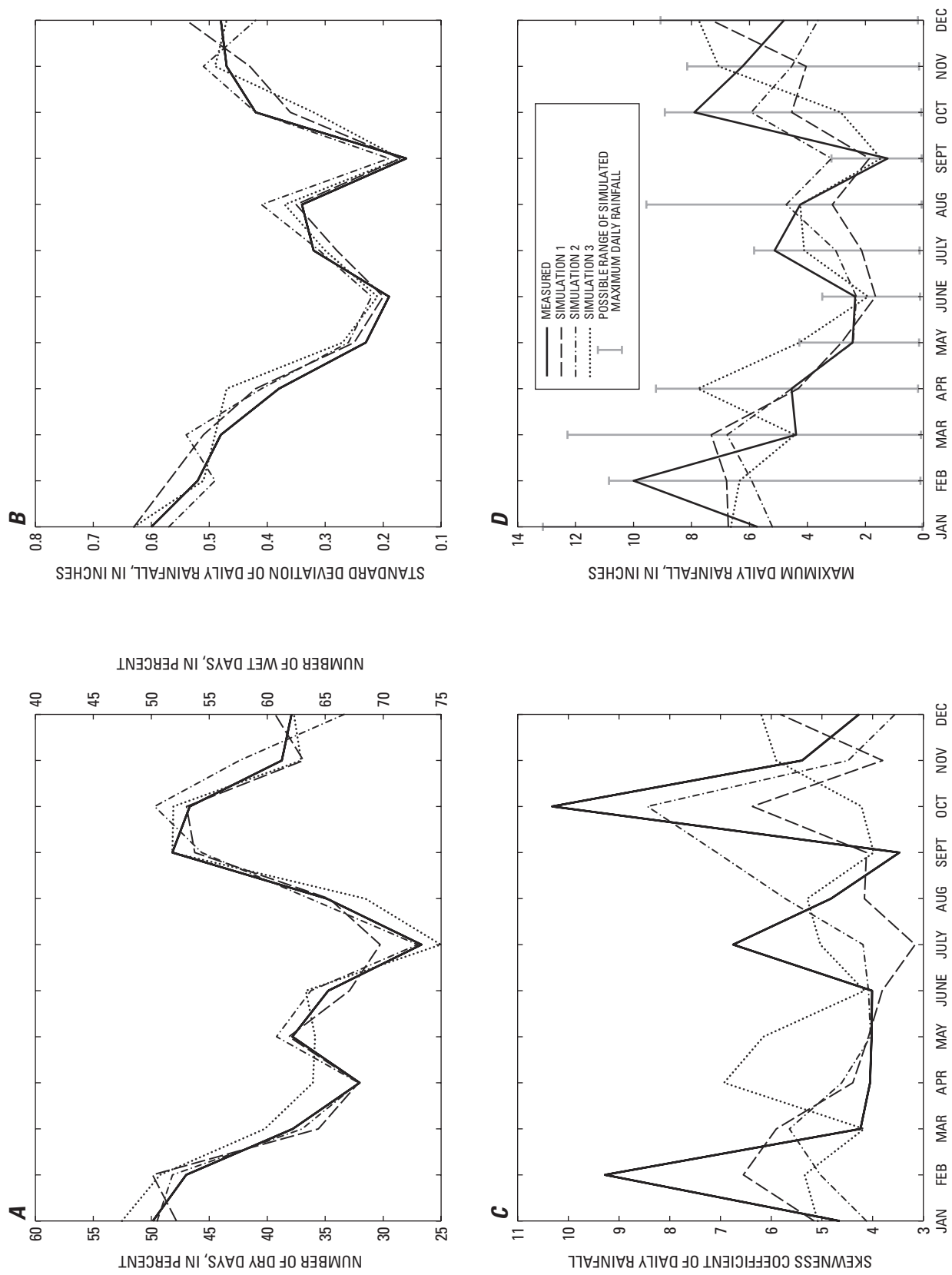


Figure 13. Measured and simulated daily rainfall at rain gage 175.1, north Kohala, Hawaii, in terms of **(A)** number of dry (or wet) days in a month, **(B)** standard deviation, **(C)** skewness coefficient, and **(D)** maximum daily rainfall.

and Ekern, 1978; Ekern, 1983). For the study area, it was assumed that fog exists much of the time in forested areas above an altitude of 2,500 ft (fig. 2). Monthly fog-to-rain ratios were estimated on the basis of information from a generalized model of seasonal fog on the windward slope of Mauna Loa (Juvik and Ekern, 1978) (table 2). Monthly fog-to-rain ratios are highest during the dry months (June through October) and lowest during the wet months (November through May). Daily fog-to-rain ratios for a given month were assumed to be equal to the monthly fog-to-rain ratio. The contribution of fog drip to the daily water budget was estimated by multiplying the fog-to-rain ratio by the daily rainfall.

Table 2. Estimated fog-drip to rainfall ratios for the Hawi area, north Kohala, Hawaii
[Estimated from Juvik and Ekern, 1978, fig. 9]

Month	Fog-drip:rainfall ratio
January	0.02
February	0.03
March	0.05
April	0.10
May	0.13
June	0.19
July	0.25
August	0.33
September	0.27
October	0.22
November	0.13
December	0.07

Runoff

Although there are no continuous stream-gaging stations in the study area, Shade (1995) estimated monthly ratios of direct runoff to rainfall on the basis of data from comparable areas on Oahu with similar mean annual rainfall and soil properties. The monthly runoff-to-rainfall ratios from Shade (1995) were also used in this study (fig. 14; table 3). The daily runoff-rainfall relation is dependent on factors including the amount, intensity, and spatial distribution of rainfall as well as antecedent rainfall. Because data were not available to develop a detailed runoff-rainfall relation, it was assumed that the daily runoff-to-rainfall ratio within a given month was constant and equal to the monthly ratio estimated by Shade (1995). Uncertainty in the runoff estimate is addressed in the “Recharge Uncertainty” section.

Potential Evapotranspiration

Although evapotranspiration rates generally are poorly known in Hawaii because of a lack of data, a significant amount of pan-evaporation data is available (Ekern and Chang, 1985), and thus, pan evaporation may be the best available indicator of evapotranspiration. Annual pan-evaporation rates in the study area range from about 95 in. near the coast to between 60 and 70 in. inland, near the headwater of Pololu Stream (fig. 15) (Ekern and Chang, 1985). Pan-evaporation rates are highest during June through September, and lowest during November through March (fig. 16). The seasonal pattern of pan-evaporation rates is fairly consistent at all of the measurement sites within the study area.

The annual pan-evaporation map developed by Ekern and Chang (1985) was digitized (Shade, 1995) and used to represent the spatial distribution of pan evaporation for this study. The mean ratios of monthly pan evaporation to annual pan evaporation (fig. 16), determined from nine sites, were multiplied by the annual pan-evaporation distribution to determine the distribution of monthly pan evaporation. Monthly pan-evaporation totals were uniformly distributed to each day of the month. The error associated with this distribution is probably small because daily pan evaporation is generally less than a few tenths of an inch and much less variable than daily rainfall.

For this study, potential evapotranspiration is estimated from pan evaporation multiplied by an appropriate vegetation factor. In Hawaii, studies of furrow- and sprinkler-irrigated sugarcane indicated that potential evapotranspiration for this crop is about equal to pan evaporation (Jones, 1980). Although sugarcane was previously grown in the study area, much of the land is now covered with pasture grass. A study on Oahu with Bermuda grass sod planted in a lysimeter that was weighed with a hydraulic scale indicated that evapotranspiration was about equal to pan evaporation when soil-moisture stress was small (Ekern, 1966). Similarly, a percolate-lysimeter study on Oahu in which Californiagrass (paragrass) was irrigated with sewage effluent indicated that evapotranspiration was about 10 percent higher than pan evaporation when the grass was kept fully wetted and was not lodged beyond the lysimeter borders (Ekern, 1983). Percolate-lysimeters planted with Panicum grass at two sites on Oahu indicated that annual evapotranspiration was about 20 to 70 percent higher than measured pan evaporation (Stearns, 1940).

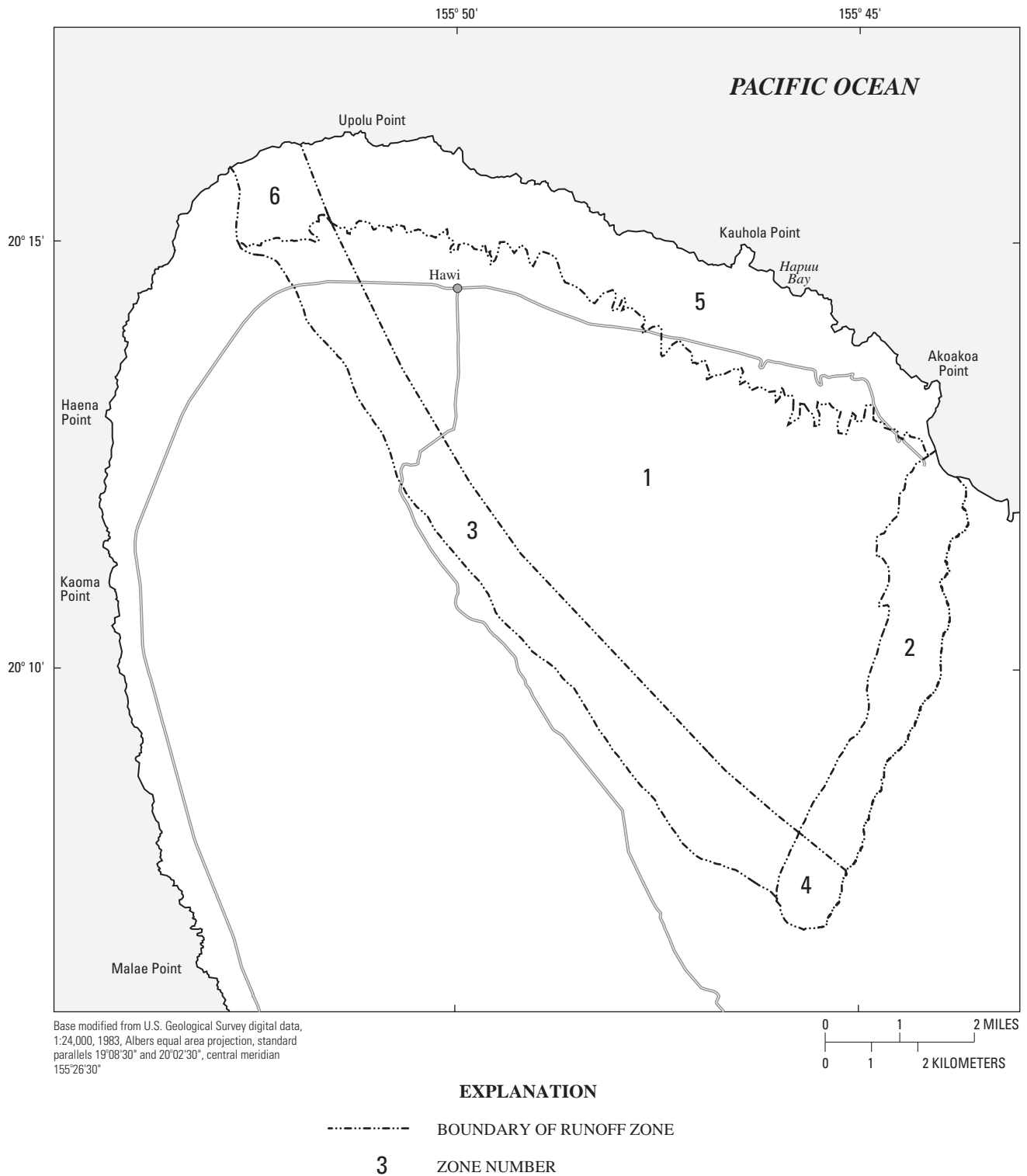


Figure 14. Runoff zones in the Hawi study area, north Kohala, Hawaii (Shade, 1995).

Table 3. Estimated runoff-to-rainfall ratios in the Hawi area, north Kohala, Hawaii
 [See figure 14 for zones; runoff:rainfall ratios and zones from Shade, 1995, table 1, fig. 3]

Zone	Corresponding zone from Shade, 1995	Runoff:rainfall ratio											
		Jan	Feb	Mar	Apr	May	June	July	Aug	Sept	Oct	Nov	Dec
1	1	0.18	0.17	0.18	0.18	0.07	0.07	0.08	0.08	0.06	0.07	0.17	0.18
2	2	0.27	0.26	0.40	0.39	0.34	0.32	0.41	0.30	0.25	0.32	0.35	0.33
3	7	0.18	0.17	0.18	0.18	0.07	0.07	0.08	0.08	0.06	0.07	0.17	0.18
4	8	0.27	0.26	0.40	0.39	0.34	0.32	0.41	0.30	0.25	0.32	0.35	0.33
5	5	0.11	0.07	0.12	0.12	0.06	0.01	0.07	0.09	0.01	0.06	0.11	0.11
6	6	0.13	0.07	0.10	0.06	0.03	0.01	0.01	0.01	0.02	0.04	0.10	0.09

However, Ekern (1983) indicated that lodged grass may have received extra radiant energy from outside the lysimeter boundaries, resulting in increased evapotranspiration.

Although most studies in Hawaii indicate that potential evapotranspiration of grass is about equal to pan evaporation, data from other sources indicate that evapotranspiration from an extensive surface of green grass (of uniform height, actively growing, completely shading the ground, and with adequate water) may be less than pan evaporation (Allen and others, 1998; Doorenbos and Pruitt, 1977). For relative humidity and wind conditions typical of the study area, recommended ratios of pan evaporation to potential evapotranspiration for an extensive surface of green grass range from about 0.7 to 0.8 (Allen and others, 1998; Doorenbos and Pruitt, 1977).

Evapotranspiration rates from wet forested areas below the clouds are largely unknown, but available information from Hawaii (Giambelluca, 1983) and other tropical islands (Dykes, 1997; Shellekens and others, 1999; Shellekens and others, 2000) indicates that rates may be high. On the basis of the Priestley-Taylor equation (Priestley and Taylor, 1972), Giambelluca (1983) estimated that potential evapotranspiration in wet forested areas on Oahu is 1.3 times pan evaporation. Although Shuttleworth and Calder (1979) warned against the indiscriminate use of the Priestley-Taylor equation for estimating forest evapotranspiration because of the dependence of forest evapotranspiration on surface controls and possible advection in high rainfall areas, estimates of evapotranspiration from a rain forest in Puerto Rico (Schellekens and others, 2000) tend to support the assessment by Giambelluca (1983). Schellekens and others (2000) estimated annual evapo-

transpiration for a rain forest in Puerto Rico to be between 85 and 95 in., whereas open-water evaporation was estimated to be about 43 in./yr. In Fiji, Waterloo and others (1999) estimated that the evapotranspiration rate from pine forest plots was about 2.3 to 2.6 times the evapotranspiration rate from a nearby grassland plot. High evapotranspiration rates in wet tropical rainforests may be caused by (1) frequent occurrence of storms of low intensity combined with large interception capacity, and (2) advected warm air from a nearby water body (Shellekens and others, 2000).

Tropical forests frequently subjected to low clouds have lower evapotranspiration rates than forests that are infrequently subjected to clouds (Bruijnzeel and Veneklaas, 1998; Bruijnzeel and Proctor, 1993). Although the reasons for the difference in evapotranspiration are not fully understood, Bruijnzeel and Veneklaas (1998) suggested that evapotranspiration in tropical montane cloud forests is limited by both climatic conditions and canopy conductance.

For this study, the ratio of potential evapotranspiration to pan evaporation was assumed to be 0.85, representing the average of the range of 0.7 (Allen and others, 1998; Doorenbos and Pruitt, 1977) to 1.0 (Ekern, 1966; Jones, 1980), for all areas except forested areas that are below the fog zone and that receive annual rainfall greater than 80 in. The ratio of potential evapotranspiration to pan evaporation was assumed to be 1.1 ($=0.85 \times 1.3$) in forested areas that are below the fog zone and that receive annual rainfall greater than 80 in. Because these potential evapotranspiration estimates are uncertain, lower and higher ratios of potential evapotranspiration to pan evaporation were explored in the "Recharge Uncertainty" section.



Figure 15. Average annual pan evaporation, north Kohala, Hawaii (modified from Ekern and Chang, 1985).

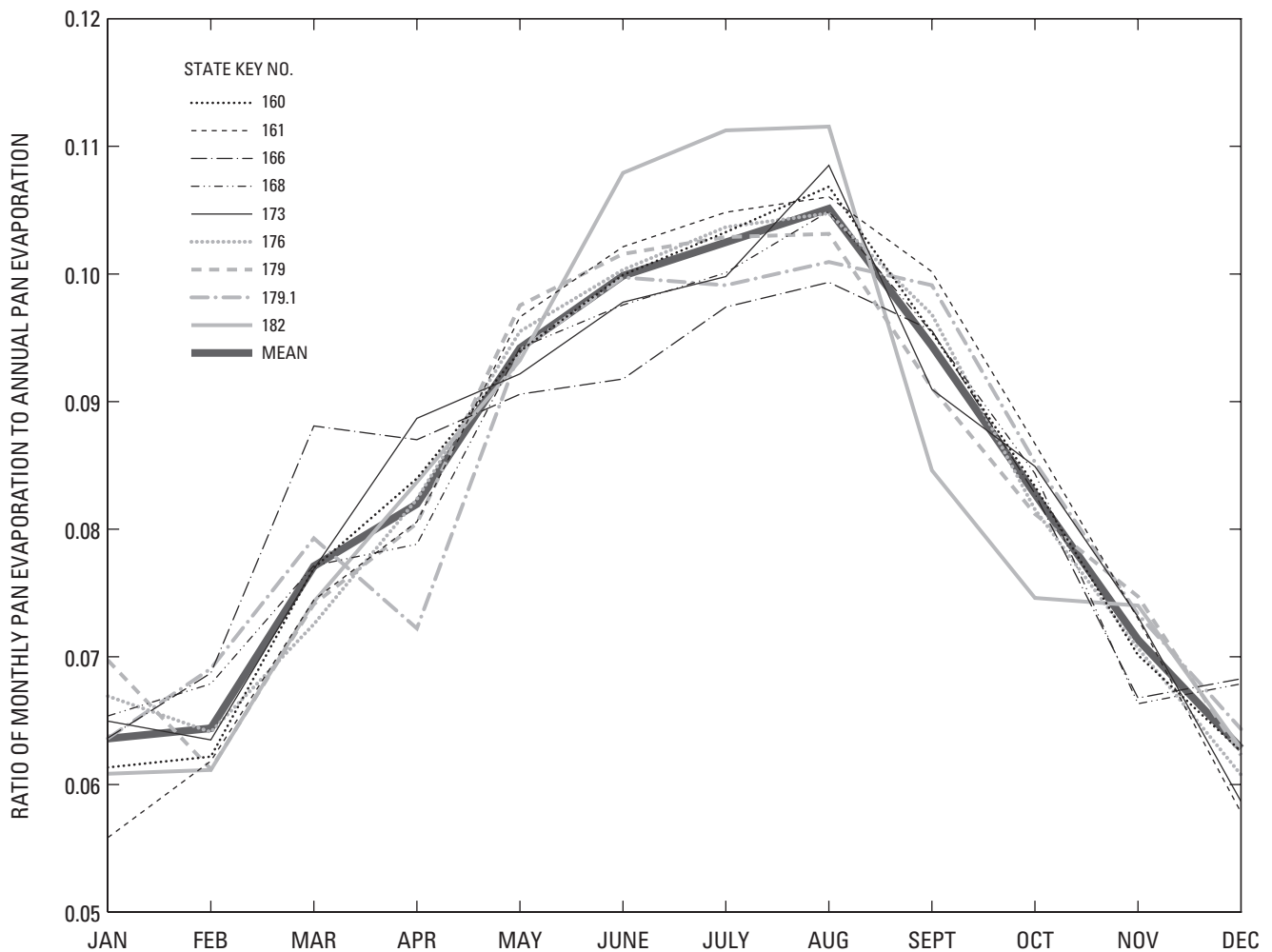


Figure 16. Ratios of monthly mean pan evaporation to annual pan evaporation at selected sites in the Hawi area, north Kohala, Hawaii.

Soil-Moisture Storage Capacity

Soil-moisture storage capacity is computed from the product of available water capacity and root depth. The distribution of available water capacity is dependent on soil type, whereas the root depth is mainly dependent on vegetation type. The digital soil map of the island of Hawaii used in this study was obtained from the U.S. Department of Agriculture, Natural Resource Conservation Service (P.J. Shade, Natural Resource Conservation Service, unpub. data, 2000).

The distribution of vegetation in the study area was digitized from orthophoto-quadrangle data.

For most of the soil series in the study area, Sato and others (1973) estimated a range of values for available water capacity. For the soil series in the study area, the maximum and minimum values of available water capacity (Sato and others, 1973) are within 10 percent of the average value of the reported range. For this study, the average value of the reported range for each soil series was used in the water budget (table 4). For the soil series that Sato and others (1973) did not estimate

available water capacity, values reported by Shade (1995, 1999) were used. If no information was available, a value of 0.14 was assumed for available water capacity.

Table 4. Estimated available water-capacity values for soils in the Hawi area, north Kohala, Hawaii
[From Sato and others, 1973; Shade, 1995; Shade, 1999]

Soil series	Available water capacity, in inches per inch of soil
Ainakea	0.18
Amalu	0.12
Beaches	0.04
Cinder land	0.04
Fill land	0.15
Hawi	0.14
Kahua	0.17
Kaiwiki	0.14
Kamakoa	0.14
Kawaihae	0.12
Kehena	0.18
Kikoni	0.14
Kohala	0.14
Mahukona	0.12
Maile	0.15
Manahaa	0.15
Mixed alluvial land	0.12
Niulii	0.18
Palapalai	0.15
Puu Pa	0.15
Rough broken land	0.12
Tropaquepts	0.12
Waimea	0.15

Vegetation root depths were estimated on the basis of available information. For grazing pasture, Allen and others (1998) indicated a root depth of 20 to 59 in. However, profiles for soils in the study area (Sato and others, 1973) indicated that the depth at which the description changes from “many roots” to “few roots” is generally between 14 and 30 in. For this study, areas in pasture were assumed to have a root depth of 22 in. The forested areas with greater than 25 percent canopy cover are primarily ohia lehua (*Metrosideros polymorpha*) (Jacobi, 1989) and have an estimated root depth of 30 in. (Shade, 1995). In forested areas with scattered trees (less than 25 percent canopy cover), a root depth of 26 in. was estimated from the average root depths for pasture areas and the forested areas with greater than 25

percent canopy cover. Steeply sloping surfaces generally cannot support deep soils. On steeply sloping surfaces on Oahu, Scott (1975) measured root depths of 6 in. to more than 20 in. depending on vegetation type. For this study, a root depth of 12 in. was used for gulch areas, which generally have steeper slopes than adjacent ridges. For rural and urbanized areas, a root depth of 12 in. was used (Giambelluca, 1983). For the agricultural areas (primarily orchards) the root depth was assumed to be 30 in.

Soil-moisture storage capacity (fig. 17) was estimated for each area formed by superimposing the vegetation information (root depths) on the soils information (available water capacity). The estimated soil-moisture storage capacity values in the study area range from 0.5 to 5.4 in.

Recharge

Recharge was computed for each area formed by overlaying digital maps of land cover, rainfall, fog drip, runoff, potential evapotranspiration, soils, and vegetation type. The initial soil moisture in each area was assumed to equal half of the soil-moisture storage capacity value. The daily water budget was computed for a period of 96 years, which was determined to be adequate to compute a steady average annual recharge (fig. 18). For urban areas, estimated recharge over the area was adjusted to account for paved and roofed surfaces that do not contribute to recharge; that is, estimated recharge over the urban area was multiplied by a factor equal to the fraction of the total area that is not paved or roofed (fig. 2). Because rainfall on many of the paved and roofed surfaces in the study area runs on to permeable surfaces that contribute to recharge, multiplying recharge in urban areas by the fraction of the total area that is not paved or roofed may slightly underestimate recharge. However, it is also likely that these areas have lower infiltration capacities and greater runoff-to-rainfall ratios than similar areas that have not been urbanized. For water reservoirs, annual recharge was conservatively estimated to be 12 in. on the basis of estimates for the saturated hydraulic conductivity of weathered basalt ranging from 12 to 1.2×10^6 in/yr (Miller, 1987), and assuming vertical flow just beneath the reservoirs.

Estimated average annual recharge in the study area is 37.5 Mgal/d, which represents about 18 percent

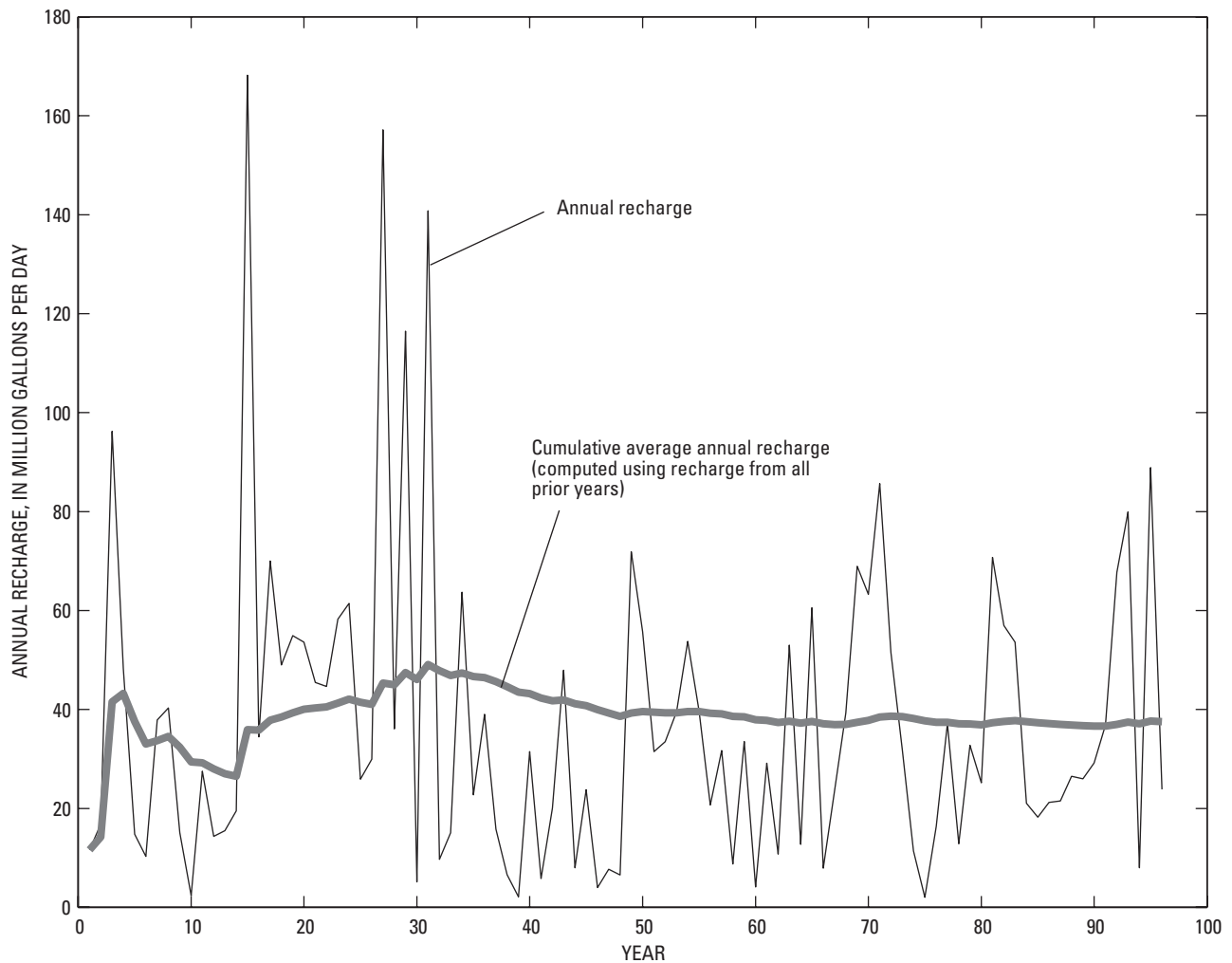


Figure 18. Variations in estimated annual recharge and cumulative average annual recharge with number of years of recharge simulation for the Hawi area, north Kohala, Hawaii.

of the average annual rainfall (208 Mgal/d). However, average annual recharge is spatially variable, ranging from less than 5 to more than 50 percent of average annual rainfall. Recharge is lowest in the drier northwest part of the study area and highest in the wetter southeast part (fig. 19).

Average annual recharge from the direct infiltration of rainfall in the study area was previously estimated to be 68.4 Mgal/d using a monthly water bud-

get that accounts for recharge before evapotranspiration (Underwood and others, 1995; Shade, 1995). Average annual recharge estimated from a daily water budget (this study) is 55 percent of the recharge estimated from the monthly water budget (Shade, 1995). As expected, the estimated recharge from a daily water budget is lower than the estimated recharge from a monthly budget that accounts for recharge before evapotranspiration.

Recharge Uncertainty

Estimated errors in the values of potential evapotranspiration, available water capacity, root depth, runoff, irrigation, and fog drip were incorporated in the daily water budget to quantify uncertainty in the recharge estimate. Although uncertainty in the rainfall distribution also contributes to uncertainty in the recharge estimate, rainfall in the Hawi area is generally better known than the other factors mentioned above. For this study, uncertainty in recharge caused by uncertainty in potential evapotranspiration, available water capacity, root depth, runoff, irrigation, and fog drip was estimated using a sensitivity analysis approach in each area formed by overlaying digital maps of land cover, rainfall, fog drip, runoff, potential evapotranspiration, soils, and vegetation type. For each of these areas, uncertainty in recharge was estimated from the component uncertainties using the following equation:

$$U = [u_p^2 + u_a^2 + u_d^2 + u_r^2 + u_i^2 + u_f^2]^{1/2} \quad (10)$$

where:

- U = total uncertainty in recharge [L/T],
- u_p = recharge uncertainty associated with potential-evapotranspiration estimate [L/T],
- u_a = recharge uncertainty associated with available-water-capacity estimate [L/T],
- u_d = recharge uncertainty associated with root-depth estimate [L/T],
- u_r = recharge uncertainty associated with runoff estimate [L/T],
- u_i = recharge uncertainty associated with irrigation estimate [L/T], and
- u_f = recharge uncertainty associated with fog-drip estimate [L/T].

Each of the component uncertainties, u , is estimated from the sensitivity analysis results:

$$u = [u_2 - u_1]/2 \quad (11)$$

where:

- u = component uncertainty in recharge ($u_p, u_a, u_d, u_r, u_i,$ or u_f) [L/T],
- u_1 = recharge obtained by decreasing the water-budget component (potential evapotranspiration, available water capacity, root depth, runoff, irrigation, or fog drip) to the lower value of the estimated plausible range [L/T], and

u_2 = recharge obtained by increasing the water-budget component (potential evapotranspiration, available water capacity, root depth, runoff, irrigation, or fog drip) to the upper value of the estimated plausible range [L/T].

For a given water-budget component, the values for u_2 and u_1 are commonly determined by adjusting the mean value of the water-budget component by adding or subtracting one standard deviation (see for example Giambelluca and others, 1996). For this study, values for u_1 and u_2 associated with potential evapotranspiration, available water capacity, and runoff were estimated on the basis of available information. Values for u_1 and u_2 associated with irrigation and fog drip were estimated by covering the range over which these components may vary.

Potential evapotranspiration.—For this study, the ratio of potential evapotranspiration to pan evaporation was assumed to be 0.85 for all areas except forested areas that are below the fog zone and that receive annual rainfall greater than 80 in., where the ratio of potential evapotranspiration to pan evaporation was assumed to be 1.1 (=0.85 × 1.3). On the basis of available information, the ratio of potential evapotranspiration to pan evaporation may range from 0.7 (Allen and others, 1998; Doorenbos and Pruitt, 1977) to 1.0 (Ekern, 1966; Jones, 1980) for all areas except forested areas that are below the fog zone and that receive average annual rainfall greater than 80 in. For forested areas that are below the fog zone and that receive average annual rainfall greater than 80 in., the ratio of potential evapotranspiration to pan evaporation may range from 0.91 (=0.7 × 1.3) to 1.3 (=1.0 × 1.3).

Holding all other factors at their original values and using the lower potential evapotranspiration to pan evaporation ratios resulted in an average annual recharge estimate of 49.0 Mgal/d (table 5), which is 31 percent higher than the average estimate of 37.5 Mgal/d. Holding all other factors at their original values and using the higher potential evapotranspiration to pan evaporation ratios resulted in an average annual recharge estimate of 29.3 Mgal/d, which is 22 percent lower than the average estimate of 37.5 Mgal/d.

Available water capacity.—For the soil series in the study area, the maximum and minimum values of available water capacity (Sato and others, 1973) are within 10 percent of the average value of the reported

Table 5. Sensitivity of the water-budget estimate of average annual recharge to potential evapotranspiration, available water capacity, root depth, runoff, fog drip, and irrigation in the Hawi area, north Kohala, Hawaii [Mgal/d, million gallons per day]

Average annual recharge, in Mgal/d	^a PE:pan evaporation ratio	Base case multiplier					Description
		Available water capacity	Root depth	Runoff	Fog drip	Irrigation	
37.5	1.0	1.0	1.0	1.0	1.0	1.0	base case
49.0	0.7/0.85	1.0	1.0	1.0	1.0	1.0	reduce ^a PE 18 percent
29.3	1.0/0.85	1.0	1.0	1.0	1.0	1.0	increase ^a PE 18 percent
38.7	1.0	0.9	1.0	1.0	1.0	1.0	reduce ^b AWC 10 percent
36.5	1.0	1.1	1.0	1.0	1.0	1.0	increase ^b AWC 10 percent
45.3	1.0	1.0	0.7	1.0	1.0	1.0	reduce root depth 30 percent
33.2	1.0	1.0	1.3	1.0	1.0	1.0	increase root depth 30 percent
49.3	1.0	1.0	1.0	0.5	1.0	1.0	reduce runoff 50 percent
26.8	1.0	1.0	1.0	1.5	1.0	1.0	increase runoff 50 percent
35.8	1.0	1.0	1.0	1.0	0.0	1.0	no fog drip
39.5	1.0	1.0	1.0	1.0	2.0	1.0	double fog drip
37.3	1.0	1.0	1.0	1.0	1.0	0.0	no irrigation
37.9	1.0	1.0	1.0	1.0	1.0	2.0	double irrigation

^aPE = potential evapotranspiration

^bAWC = available water capacity

range, which represents the original value used in the water budget. Thus, varying the original available water-capacity values upward or downward by 10 percent was assumed to provide an estimate of the uncertainty in the available water capacity. Holding all other factors at their original values and decreasing the original available water-capacity values by 10 percent resulted in a 3 percent increase in total recharge to 38.7 Mgal/d, whereas increasing the original available water-capacity values by 10 percent resulted in a 3 percent decrease in total recharge to 36.5 Mgal/d.

Root depth.—No published values are available to estimate the range of plausible root depths in the study area. On the basis of an assumed uniform distribution with range equal to the mean (Giambelluca and others, 1996), the estimated standard deviation of each original root-depth value for a particular area is equal to 30 percent of that root-depth value. Holding all other factors at their original values and decreasing the original root-depth values by 30 percent resulted in a 21 percent increase in total recharge to 45.3 Mgal/d, whereas increasing the root-depth values by 30 percent resulted in an 11 percent decrease in total recharge to 33.2 Mgal/d.

Runoff.—Runoff in the Hawi area is poorly known because there are no continuous stream-gaging stations in the area. Shade (1995) estimated monthly ratios of direct runoff to rainfall on the basis of information from comparable areas on Oahu (Giambelluca, 1983). Giambelluca (1983) quantified the standard error of the runoff estimate for a bivariate linear regression between monthly rainfall and monthly runoff for basins in southern Oahu. The standard error of the runoff estimate generally was about 50 percent of the mean value. This error estimate was used for the Hawi area for this study. Holding all other factors at their original values and decreasing the original runoff estimates by 50 percent resulted in a 31 percent increase in total recharge to 49.3 Mgal/d, whereas increasing the runoff by 50 percent resulted in a 29 percent decrease in total recharge to 26.8 Mgal/d.

Irrigation and fog drip.—Uncertainty in estimated irrigation amounts and fog drip is unknown. For this study, sensitivity of the recharge estimate to irrigation was tested by holding all other factors at their original values and either (1) setting irrigation equal to zero or (2) doubling the irrigation. Similarly, sensitivity of the recharge estimate to fog drip was tested by either

(1) setting fog drip equal to zero or (2) doubling fog drip. Changes in irrigation or fog drip within the specified ranges caused a change of less than 2 Mgal/d in the total recharge estimate for the study area.

Recharge estimates.— For each area formed by overlaying digital maps of land cover, rainfall, fog drip, runoff, potential evapotranspiration, soils, and vegetation type, the estimated total recharge uncertainty was added to the original recharge value to provide an upper recharge estimate for that area. Similarly, the estimated total recharge uncertainty was subtracted from the original recharge value to provide a lower recharge estimate. If the lower recharge estimate for an area was less than zero, the recharge for that area was assigned a value of zero. For the Hawi area, the average annual recharge was estimated to be 37.5 Mgal/d with a daily water budget. Lower and upper annual recharge estimates that incorporate the estimated uncertainty respectively are 19.9 Mgal/d (fig. 20) and 55.4 Mgal/d (fig. 21).

Because it is unlikely that all of the water-budget components are biased in a common direction, total recharge from infiltration of rainfall, fog drip, and irrigation is probably not as low as 19.9 Mgal/d nor as high as 55.4 Mgal/d. However, for the purposes of the numerical ground-water flow simulations described in the next section of this report, the range of recharge values was tested.

NUMERICAL GROUND-WATER FLOW MODELS

A numerical ground-water flow model was previously developed to simulate steady-state regional ground-water flow in the Hawi area (Underwood and others, 1995). The model developed by Underwood and others (1995) was modified to account for new estimates of recharge and formed the basis of the steady-state regional models developed for this study.

The regional models used the two-dimensional (areal) finite-element code AQUIFEM-SALT (Voss, 1984), which was modified to account for the saltwater column overlying the aquifer offshore (Oki, 1997). The AQUIFEM-SALT code was designed to simulate flow of confined or unconfined fresh ground water in systems that may have a freshwater body floating on denser underlying saltwater. AQUIFEM-SALT treats freshwater and saltwater as immiscible fluids separated by a

sharp interface. The depth of the interface is determined by the Ghyben-Herzberg relation, which predicts, for hydrostatic conditions, that every foot of freshwater above sea level must be balanced by 40 ft of freshwater below sea level. In reality, a diffuse brackish-water transition zone exists between the freshwater and underlying saltwater. Furthermore, the Ghyben-Herzberg relation tends to underestimate freshwater-lens thickness in the coastal discharge zone (Bear, 1979) and overestimate freshwater-lens thickness in the mountainous interior area. In this study, it was assumed that the position of the surface of 50-percent seawater salinity is approximated by the sharp-interface position. AQUIFEM-SALT simulates the vertically averaged freshwater head in the aquifer and assumes that flow is horizontal and all withdrawal and injection wells fully penetrate the freshwater body.

Model Construction

Three ground-water models, corresponding to three different estimated recharge distributions (figs. 19–21), were developed for the Hawi area to simulate ground-water levels and discharges for the 1990's. The models account for spatially varying hydraulic characteristics of the geologic materials, recharge, and ground-water withdrawals. The hydraulic characteristics were estimated from available data and were modified by varying them in the model to obtain acceptable agreement between measured and model-calculated water levels. Water levels from the 1990's were available at 14 wells.

Recharge to and discharge from the freshwater lens have not changed significantly for many years, indicating that the measured water levels (fig. 9) represent equilibrium or near-equilibrium conditions, although seasonal variations in water levels are expected (Underwood and others, 1995). Extensive agriculture and irrigation of crops ceased in the mid-1970's and water previously used for irrigation has been injected at the Hawi hydroelectric plant since about 1979. The only regularly pumped wells in the area are two Hawaii Department of Water Supply wells (7449-02 and 7349-01). Although withdrawal from these wells has increased slightly with time, the 1990's average combined withdrawal of 0.26 Mgal/d is much less than the total recharge to the aquifer.

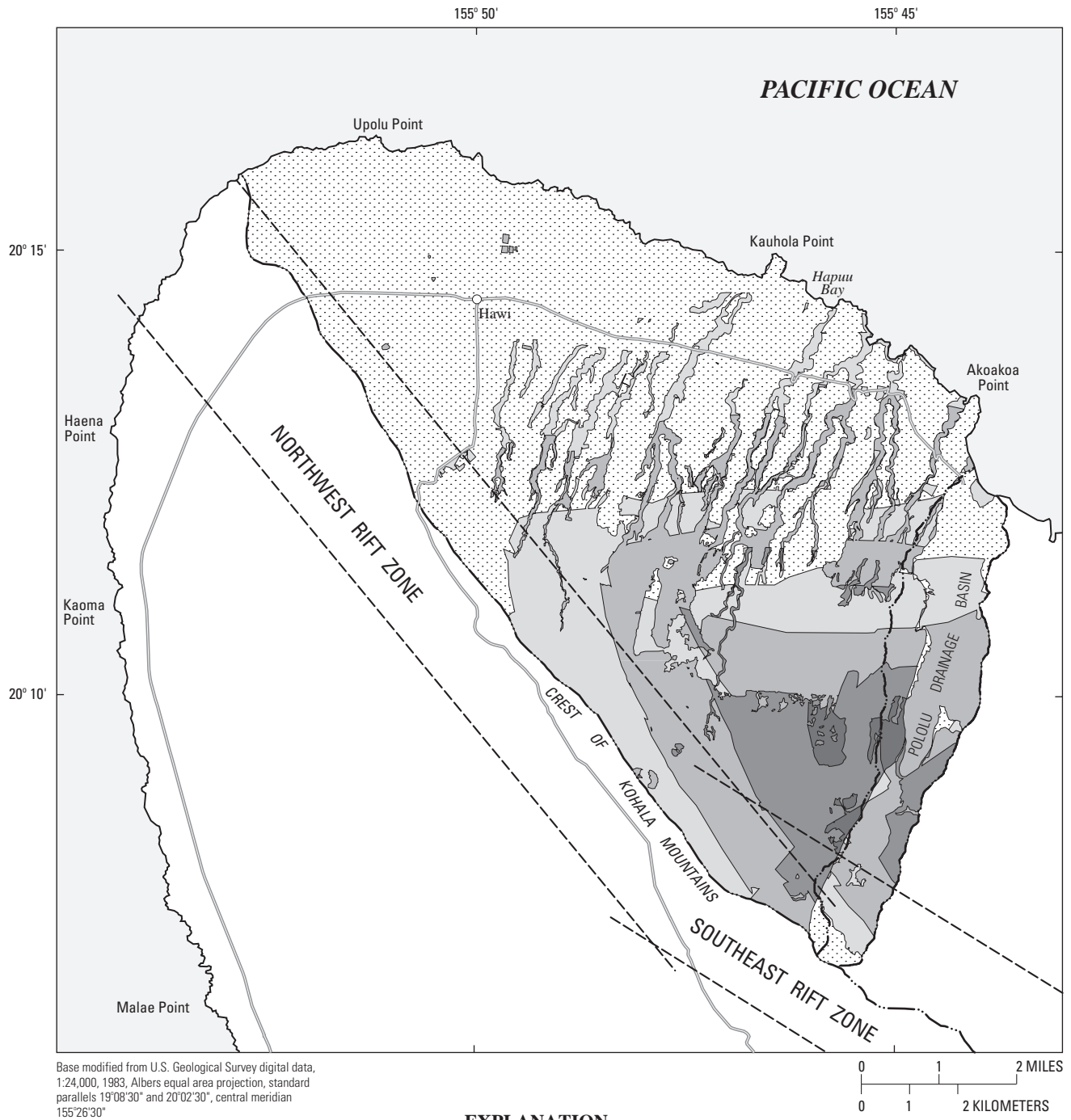


Figure 20. Estimated average annual ground-water recharge (low estimate of 19.9 million gallons per day) in the Hawi area, north Kohala, Hawaii, computed with a water budget.

Model Mesh

The finite-element mesh used in this study consists of 397 nodes and 348 elements (fig. 22). The mesh covers the part of the study area underlain by a freshwater lens, and extends offshore to include the zone where fresh ground water discharges to the ocean. The rift zones were excluded from the model mesh because no water-level information was available to characterize the hydraulic properties of the dike-impounded ground-water flow system. The perched-water system was not simulated in this study, although withdrawals from the perched-water system were taken into account. Perched water that is not withdrawn generally recharges the freshwater-lens system, and this recharge also was taken into account. Discharge from the perched-water system to streams has not been quantified, but was assumed to be small in this study.

Boundary Conditions

AQUIFEM-SALT supports three types of boundary conditions: (1) specified head, (2) specified flow (which includes no flow), and (3) head-dependent discharge. Specified-head boundary conditions were not used for this study. The perimeter of the active mesh is a no-flow boundary. The aquifer bottom was treated as a no-flow boundary located 3,000 ft below sea level. The aquifer bottom is deep enough to include the entire freshwater-lens thickness.

All elements representing onshore areas were modeled as unconfined, water-table elements. All elements representing offshore areas were modeled using a head-dependent discharge boundary condition. Flow out of the aquifer at head-dependent discharge elements was assumed to be linearly related to the difference between the head in the aquifer and the equivalent freshwater head of the ocean overlying the aquifer at the discharge site according to the equation:

$$Q = (K'/B)A(h - h_0) \quad (12)$$

where:

Q = rate of discharge from a model element [L³/T],

K' = vertical hydraulic conductivity of the confining unit overlying the aquifer [L/T],

B' = thickness of the confining unit overlying the aquifer [L],

A = area of the model element [L²],

h = head, relative to mean sea level, in the aquifer [L], and

h_0 = equivalent freshwater head, relative to mean sea level, of the ocean overlying the aquifer [L].

The confining-unit vertical hydraulic conductivity divided by the confining-unit thickness forms a lumped parameter known as leakance. Although a low-permeability confining unit may not exist offshore of the study area, the volcanic rocks impede the discharge of ground water to the ocean because the resistance to movement of ground water across the layering of lava flows generally is much greater than the resistance to movement along the direction of the lava flows. Near coastal discharge areas, ground-water flow is expected to be upward and across the layering of the lava flows. In the model, the vertical hydraulic conductivity of the confining unit represents the vertical hydraulic conductivity of the volcanic-rock aquifer, and the confining-unit thickness represents the aquifer thickness over which vertical discharge occurs. No attempt was made to estimate separate values for aquifer thickness over which vertical discharge occurs and vertical hydraulic conductivity for the study area; instead, the leakance was estimated.

For this study, the head, h_0 , overlying the aquifer for offshore elements was assigned a value corresponding to the freshwater-equivalent head of the saltwater column overlying the ocean floor within the element. Because saltwater has a greater density than freshwater, the freshwater-equivalent head, measured relative to a mean sea-level datum, was computed from the equation:

$$h_0 = -Z/40 \quad (13)$$

where Z is the altitude of the ocean floor (fig. 22).

Underwood and others (1995) assumed that h_0 was equal to zero for all offshore elements to avoid introducing anomalous offshore sources of freshwater. This assumption tends to make the model overestimate water-level declines associated with withdrawals. Because a modified version of AQUIFEM-SALT (Oki, 1997) was used for this study, the necessity to set h_0 equal to zero was avoided, and a more realistic representation of the offshore boundary was possible.

Model Zones

The modeled area was divided into two zones to account for the difference in hydraulic conductivity

between the southeastern and northwestern parts (fig. 23) (Underwood and others, 1995). In the model, leakage also was allowed to differ between the two zones. Two was the minimum number of zones considered necessary to adequately represent the system.

Recharge

Because of the uncertainty in the recharge estimate, three different recharge distributions (from infiltration of rainfall, fog drip, and irrigation) were used in the numerical ground-water flow model; a low estimate of 19.9 Mgal/d (fig. 24), an intermediate estimate of 37.5 Mgal/d (fig. 25), and a high estimate of 55.4 Mgal/d (fig. 26). Recharge to elements at the inland boundary of the mesh was augmented to account for recharge outside of the mesh but within the study area. For example, although the rift-zone areas were not included in the mesh, recharge to the rift zones was added to the elements at the mesh boundary. Recharge outside the mesh was assigned to elements at the mesh boundary by artificially extending the mesh lines to the boundary of the study area and assuming that recharge enters the mesh parallel to the mesh lines. For recharge in the rift zones, the mesh lines were artificially extended in a southwest direction to the boundary of the study area and recharge between any two lines in the rift zone was summed, and assigned to the element at the mesh boundary between the same two lines. For recharge to the Pololu drainage basin, the mesh lines were artificially extended in a southeast direction to the eastern drainage divide, and recharge to the mesh boundary elements was treated similarly as for the rift zone.

Recharge in each of 20 model elements representing the Kohala ditch was increased by 0.1 Mgal/d to account for a total estimated 2 Mgal/d seepage loss from the ditch. Also, 8 Mgal/d recharge was added to a single model node to account for injection at the Hawi hydroelectric plant (figs. 24 through 26).

Withdrawals

Average 1990's withdrawal rates from DWS wells 7449-02 and 7349-01 were 0.21 and 0.05 Mgal/d, respectively. These withdrawals were represented at two model nodes (figs. 24 through 26). Estimated withdrawals of 0.12, 0.16, 0.11, and 0.03 Mgal/d (State of Hawaii, 1991) from the Lindsay, Watt 1, Bond 1, and Murphy tunnels, respectively, were represented by

reduced recharge from model elements near these tunnels (figs. 24 through 26).

Estimation of Hydraulic Characteristics

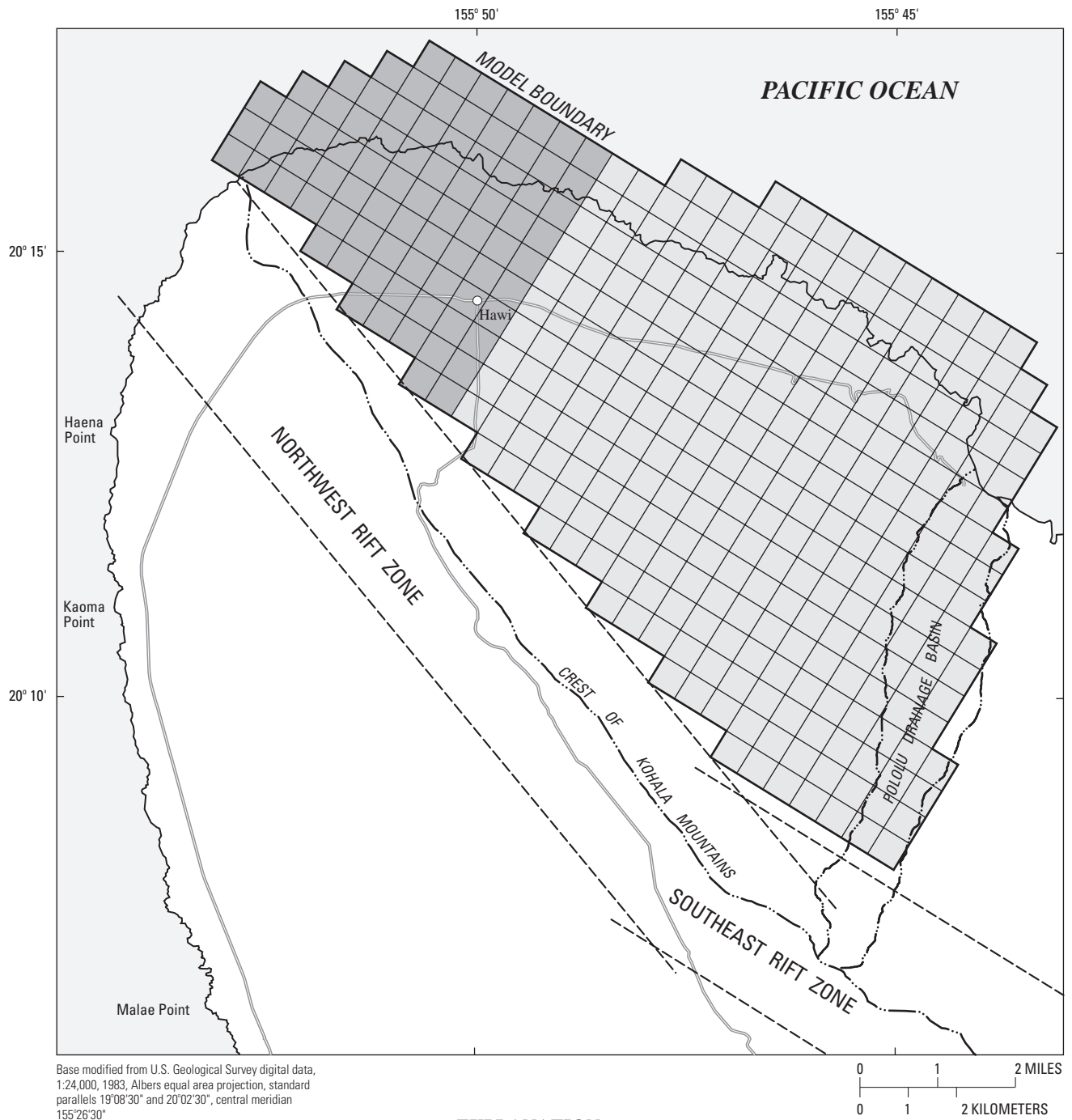
For each of the three recharge distributions considered, 81 different combinations of leakage and hydraulic-conductivity values were tested. All combinations of three different hydraulic-conductivity values and three different leakage values for each of the two zones were tested. The same model zones were used for each recharge distribution. All simulations were run to steady-state conditions. Model-calculated water levels for each run were compared to measured water levels from the 1990's available from 14 wells.

Model 1, Low Recharge

Model 1 included 19.9 Mgal/d recharge from infiltration of rainfall, fog drip, and irrigation, 8 Mgal/d recharge from injected water at the Hawi hydroelectric plant, and 2 Mgal/d recharge from seepage from Kohala ditch (table 6). All combinations of three hydraulic-conductivity values for the northwestern model zone (750; 1,500; and 2,250 ft/d), three hydraulic-conductivity values for the southeastern model zone (100, 300, and 500 ft/d), three leakage values for the northwestern model zone (0.05, 0.1, and 0.2 ft/d/ft), and three leakage values for the southeastern model zone (0.0025, 0.005, and 0.01 ft/d/ft) were tested. The combination of values that produced the lowest average-absolute error between measured and model-calculated water levels was a hydraulic conductivity of 1,500 ft/d and a leakage of 0.1 ft/d/ft for the northwestern zone, and a hydraulic conductivity of 300 ft/d and a leakage of 0.005 ft/d/ft for the southeastern zone. For this combination of hydraulic characteristics, the average and average-absolute errors were 0.21 and 0.55 ft, respectively. Model-calculated water levels are in general agreement with the available measured water levels (figs. 27 and 28).

Model 2, Intermediate Recharge

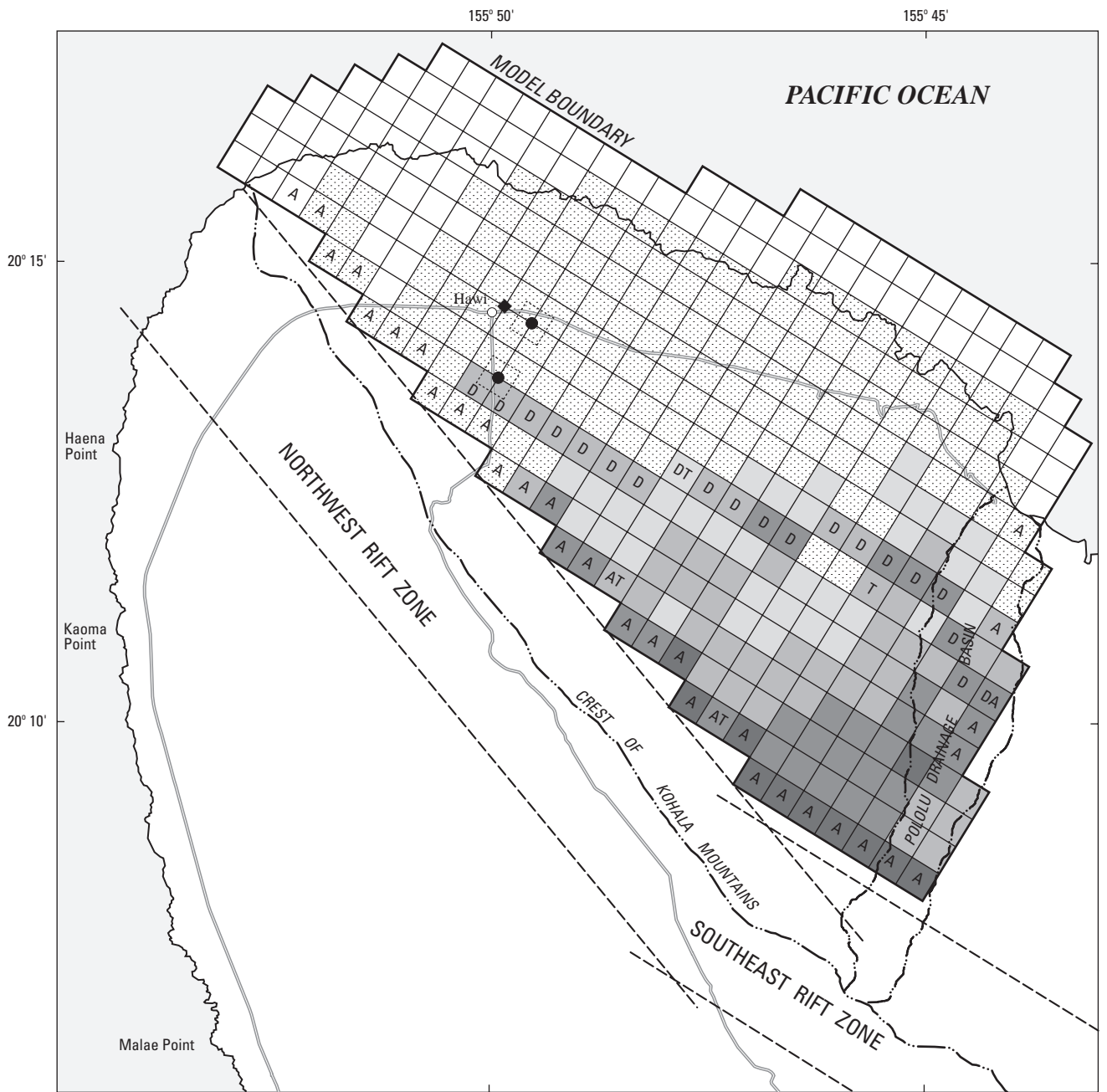
Model 2 included 37.5 Mgal/d recharge from infiltration of rainfall, fog drip, and irrigation, 8 Mgal/d recharge from injected water at the Hawi hydroelectric plant, and 2 Mgal/d recharge from seepage from Kohala ditch (table 6). All combinations of three hydraulic-conductivity values for the northwestern model zone (1,500; 2,250; and 3,000 ft/d), three hydraulic-



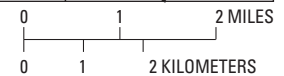
EXPLANATION

- NORTHWEST ZONE (HIGHER PERMEABILITY)
- SOUTHEAST ZONE (LOWER PERMEABILITY)
- DRAINAGE DIVIDE
- RIFT ZONE BOUNDARY (from Underwood and others, 1995)

Figure 23. Hydraulic-conductivity zones used in the numerical ground-water flow model for the Hawi area, north Kohala, Hawaii. In the model mesh, hydraulic-conductivity values are assigned to nodes. If a node is associated with elements in two zones in the figure, the hydraulic conductivity assigned to that node is the lower value for the two zones.



Base modified from U.S. Geological Survey digital data, 1:24,000, 1983, Albers equal area projection, standard parallels 19°08'30" and 20°02'30", central meridian 155°26'30"



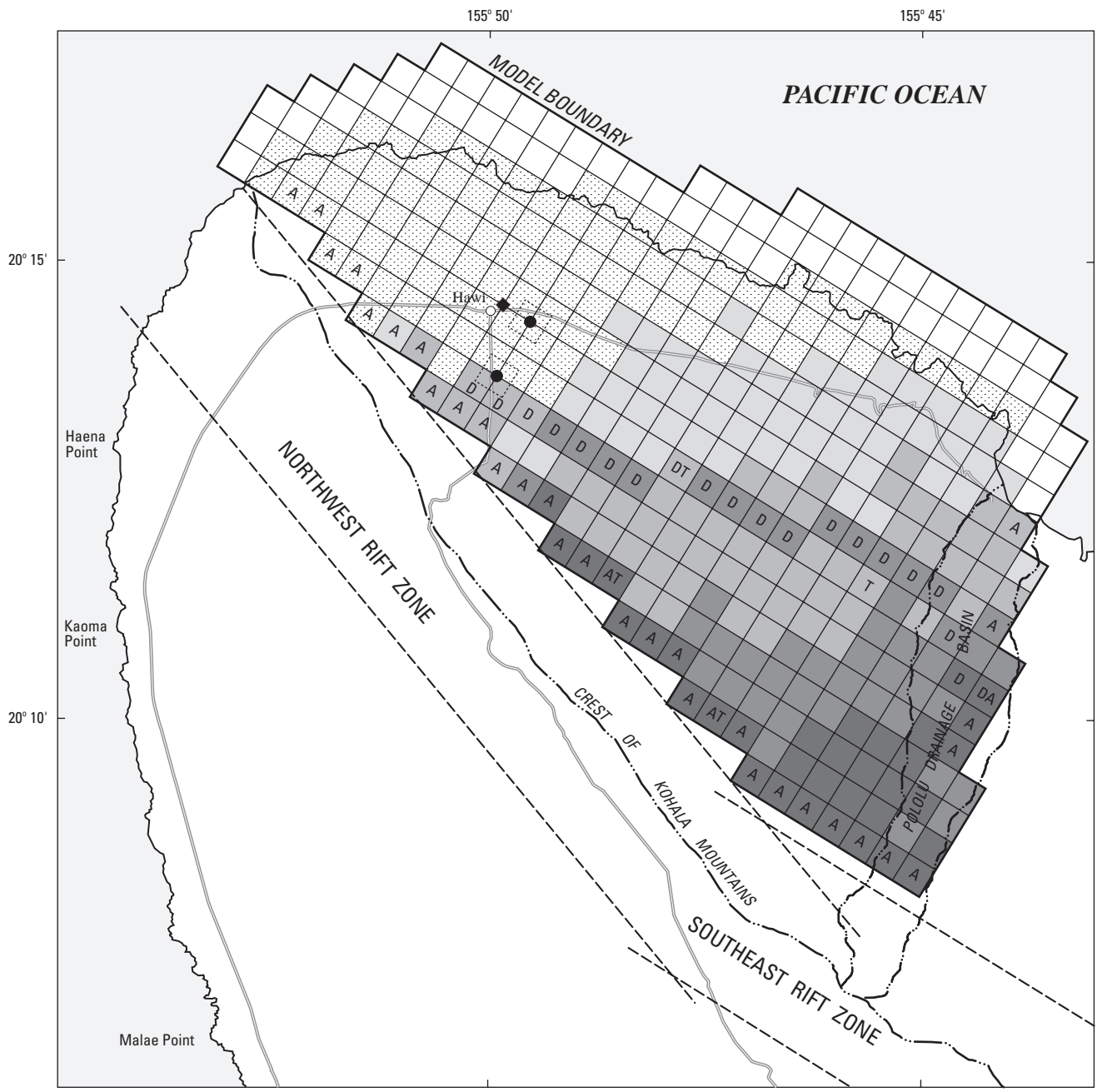
EXPLANATION

- GROUND-WATER RECHARGE, IN INCHES PER YEAR
- Zero
 - Greater than 0 and less than or equal to 5
 - Greater than 5 and less than or equal to 10
 - Greater than 10 and less than or equal to 20
 - Greater than 20 and less than or equal to 40
 - Greater than 40

- ELEMENT WITH RECHARGE FROM OUTSIDE MODEL MESH
- ELEMENT WITH RECHARGE FROM KOHALA DITCH
- ELEMENT WITH TUNNEL DISCHARGE
- AREA REPRESENTED BY WITHDRAWAL NODE

- DRAINAGE DIVIDE
- RIFT ZONE BOUNDARY (from Underwood and others, 1995)
- INJECTION NODE
- WITHDRAWAL NODE

Figure 24. Low estimate of average annual ground-water recharge (19.9 million gallons per day from infiltration of rain-fall, fog drip, and irrigation) used in the numerical ground-water flow model (model 1) for the Hawi area, north Kohala, Hawaii.



Base modified from U.S. Geological Survey digital data, 1:24,000, 1983, Albers equal area projection, standard parallels 19°08'30" and 20°02'30", central meridian 155°26'30"

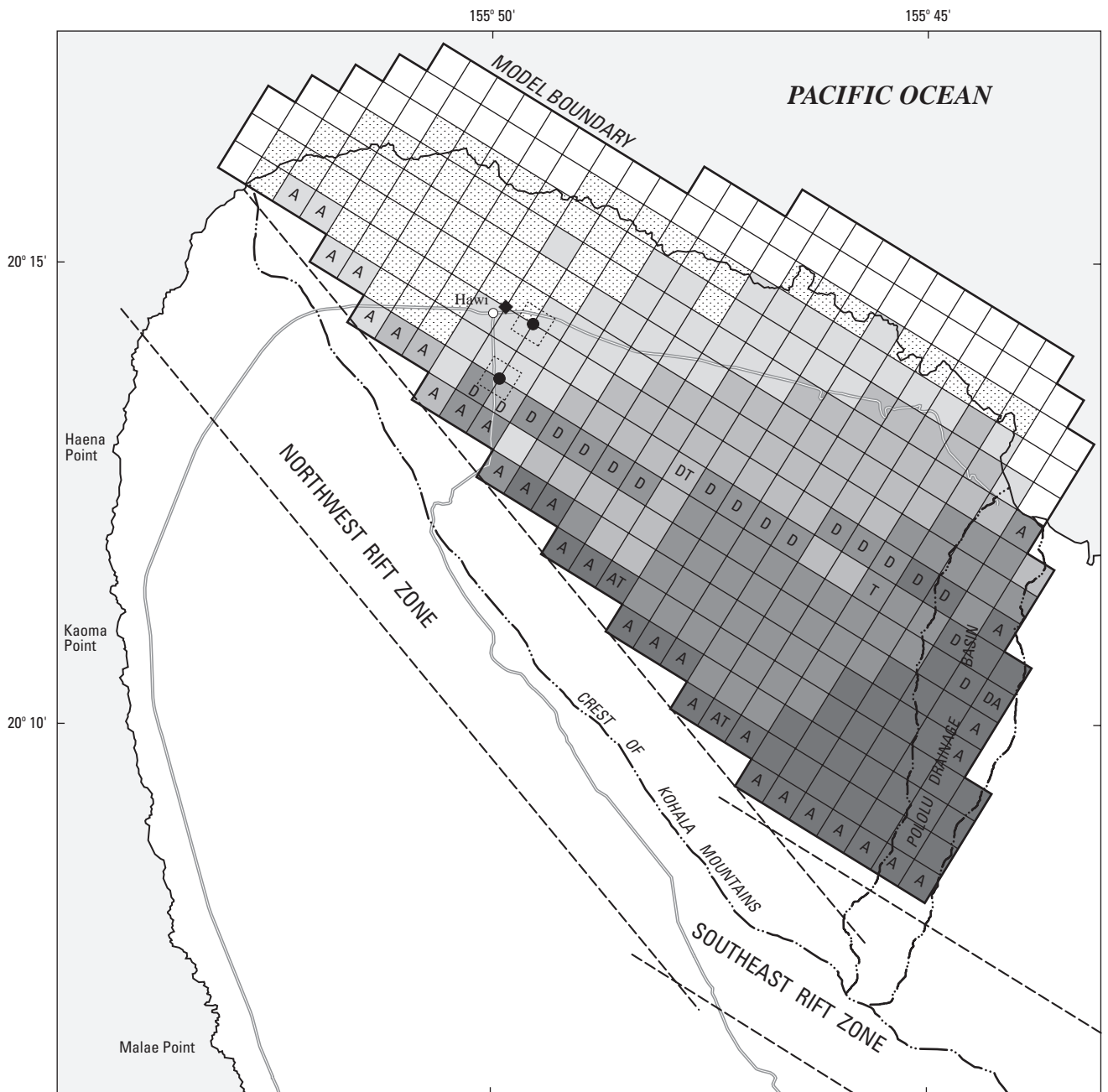
GROUND-WATER RECHARGE, IN INCHES PER YEAR

- Zero
- Greater than 0 and less than or equal to 5
- Greater than 5 and less than or equal to 10
- Greater than 10 and less than or equal to 20
- Greater than 20 and less than or equal to 40
- Greater than 40

EXPLANATION

- A ELEMENT WITH RECHARGE FROM OUTSIDE MODEL MESH
- D ELEMENT WITH RECHARGE FROM KOHALA DITCH
- T ELEMENT WITH TUNNEL DISCHARGE
- AREA REPRESENTED BY WITHDRAWAL NODE
- DRAINAGE DIVIDE
- RIFT ZONE BOUNDARY (from Underwood and others, 1995)
- INJECTION NODE
- WITHDRAWAL NODE

Figure 25. Intermediate estimate of average annual ground-water recharge (37.5 million gallons per day from infiltration of rainfall, fog drip, and irrigation) used in the numerical ground-water flow model (model 2) for the Hawi area, north Kohala, Hawaii.



Base modified from U.S. Geological Survey digital data, 1:24,000, 1983, Albers equal area projection, standard parallels 19°08'30" and 20°02'30", central meridian 155°26'30"

GROUND-WATER RECHARGE, IN INCHES PER YEAR

	Zero
	Greater than 0 and less than or equal to 5
	Greater than 5 and less than or equal to 10
	Greater than 10 and less than or equal to 20
	Greater than 20 and less than or equal to 40
	Greater than 40

EXPLANATION

	ELEMENT WITH RECHARGE FROM OUTSIDE MODEL MESH		DRAINAGE DIVIDE
	ELEMENT WITH RECHARGE FROM KOHALA DITCH		RIFT ZONE BOUNDARY (from Underwood and others, 1995)
	ELEMENT WITH TUNNEL DISCHARGE		INJECTION NODE
	AREA REPRESENTED BY WITHDRAWAL NODE		WITHDRAWAL NODE

Figure 26. High estimate of average annual ground-water recharge (55.4 million gallons per day from infiltration of rainfall, fog drip, and irrigation) used in the numerical ground-water flow model (model 3) for the Hawi area, north Kohala, Hawaii.

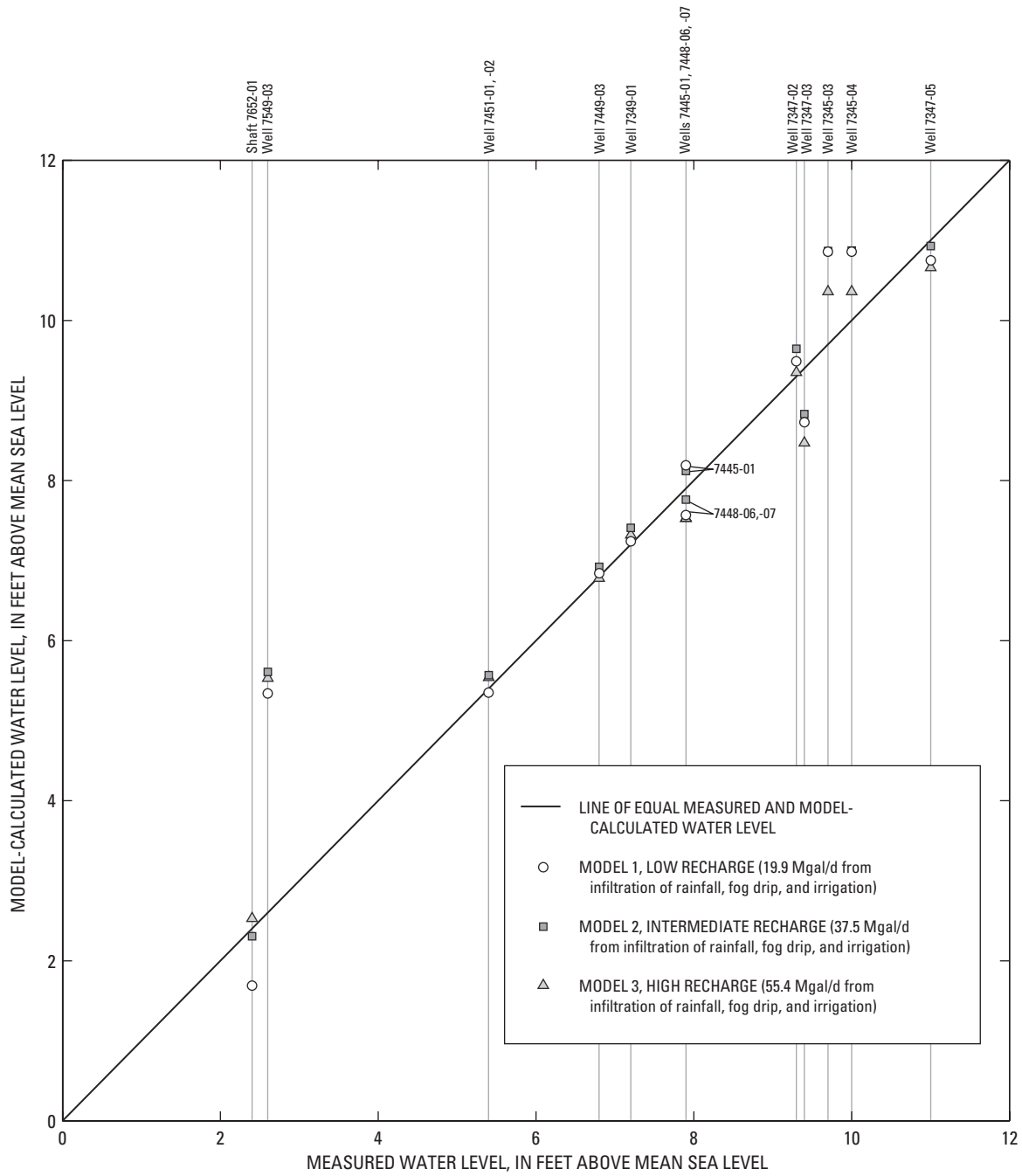


Figure 27. Measured and model-calculated water levels for 1990's pumping conditions and three estimated recharge distributions, Hawi area, north Kohala, Hawaii.

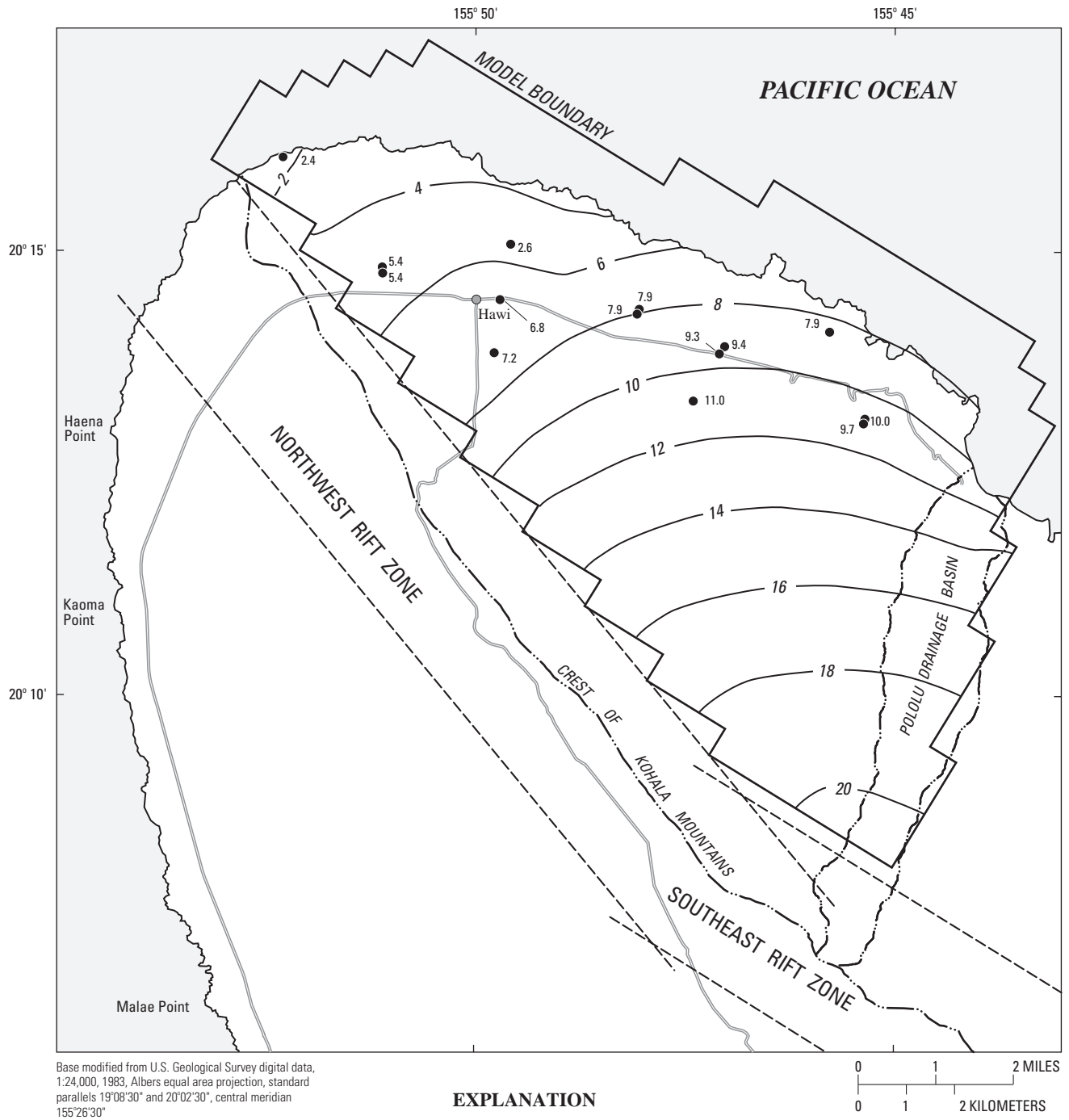


Figure 28. Measured and model-calculated water levels in the Hawi area, north Kohala, Hawaii, using the low recharge estimate (19.9 million gallons per day from infiltration of rainfall, fog drip, and irrigation).

Table 6. Steady-state ground-water budget (1990's withdrawal conditions) for the numerical ground-water flow models, Hawi area, north Kohala, Hawaii

[Values in million gallons per day. Total ground-water sources may not equal total ground-water discharges because of rounding errors]

	Model 1, low recharge	Model 2, intermediate recharge	Model 3, high recharge
Ground-water sources			
Infiltration of rainfall, fog drip, and irrigation	19.9	37.5	55.4
Seepage from Kohala ditch	8.0	8.0	8.0
Hydroelectric plant injection wells	2.0	2.0	2.0
Total	29.9	47.5	65.4
Ground-water discharges			
Withdrawals from wells	0.26	0.26	0.26
Withdrawals from tunnels	0.42	0.42	0.42
Freshwater discharge to ocean	29.2	46.9	64.7
Total	29.9	47.6	65.4

conductivity values for the southeastern model zone (300, 500, and 700 ft/d), three leakance values for the northwestern model zone (0.025, 0.05, and 0.10 ft/d/ft), and three leakance values for the southeastern model zone (0.005, 0.01, and 0.02 ft/d/ft) were tested. The combination of values that produced the lowest average-absolute error between measured and model-calculated water levels was a hydraulic conductivity of 2,250 ft/d and a leakance of 0.05 ft/d/ft for the northwestern zone, and a hydraulic conductivity of 500 ft/d and a leakance of 0.01 ft/d/ft for the southeastern zone. For this combination of hydraulic characteristics, the average and average-absolute errors were 0.38 and 0.52 ft, respectively. Model-calculated water levels are in general agreement with average measured water levels from the 1990's (figs. 27 and 29).

Model 3, High Recharge

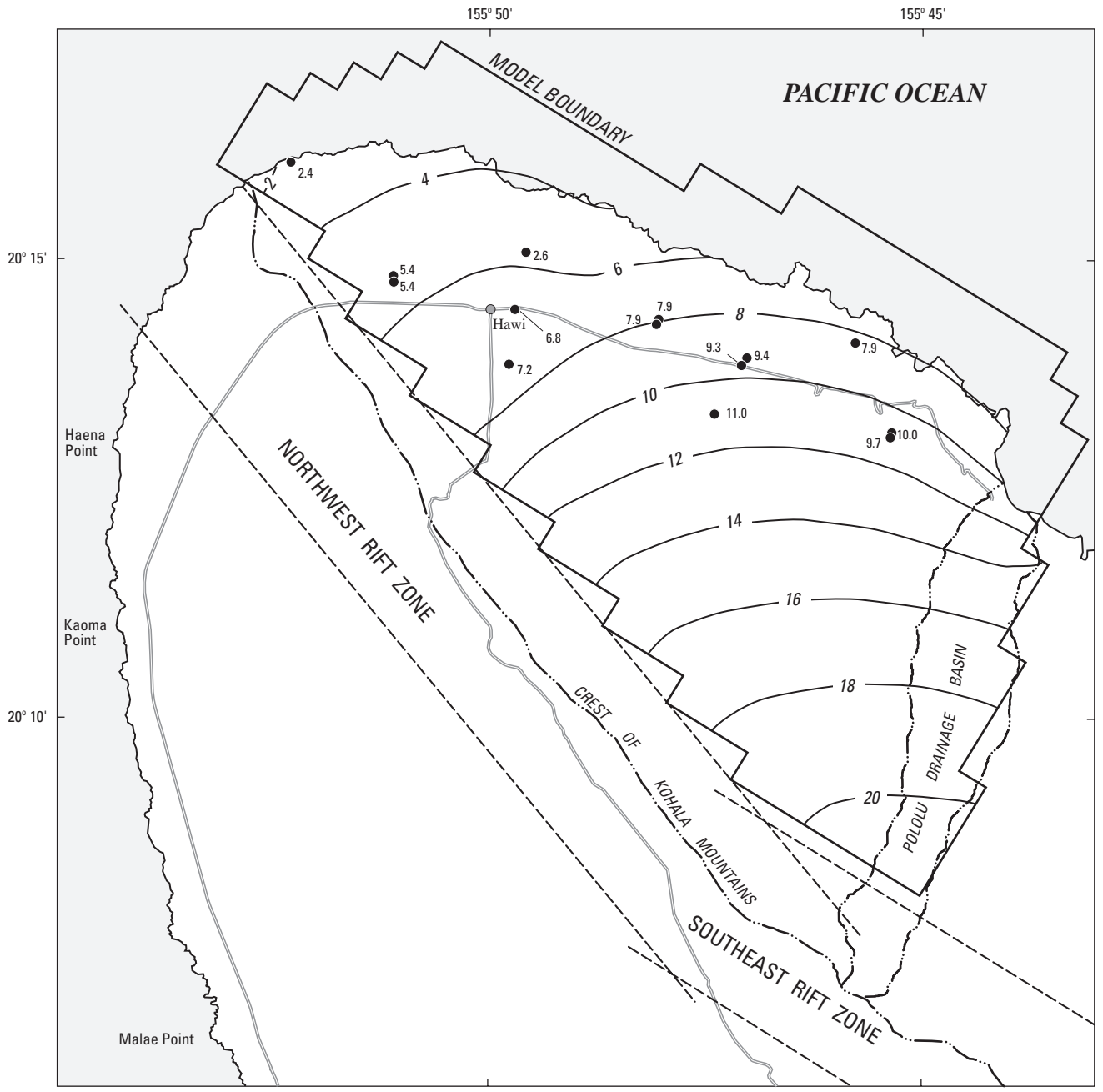
Model 3 included 55.4 Mgal/d recharge from infiltration of rainfall, fog drip, and irrigation, 8 Mgal/d recharge from injected water at the Hawi hydroelectric plant, and 2 Mgal/d recharge from seepage from Kohala ditch (table 6). All combinations of three hydraulic-conductivity values for the northwestern model zone (2,250; 3,000; and 3,750 ft/d), three hydraulic-conductivity values for the southeastern model zone (500, 700, and 900 ft/d), three leakance values for the northwestern model zone (0.025, 0.05, and 0.1 ft/d/ft), and three leakance values for the southeastern model zone (0.01, 0.02, and 0.04 ft/d/ft) were tested. The combination of values that produced the lowest average-absolute error between measured and model-calculated water levels was a hydraulic conductivity of 3,000 ft/d and a leak-

ance of 0.05 ft/d/ft for the northwestern zone, and a hydraulic conductivity of 700 ft/d and a leakance of 0.02 ft/d/ft for the southeastern zone. For this combination of hydraulic characteristics, the average and average-absolute errors were 0.15 and 0.49 ft, respectively. Model-calculated water levels are in general agreement with average measured water levels from the 1990's (figs. 27 and 30).

EFFECTS OF PROPOSED WITHDRAWALS

For steady-state conditions, withdrawal from a freshwater-lens system will cause a decline in water levels, a rise in the transition zone, and a decrease in discharge to the ocean. For steady-state conditions, ground-water withdrawal causes natural discharge to the ocean to decrease by an amount equal to the withdrawal.

The three numerical ground-water flow models developed for this study were used to simulate the steady-state response of the freshwater-lens system to withdrawals at rates in excess of the average 1990's withdrawal rates. Each of two withdrawal rates (above average 1990's withdrawal rates) and two distributions of withdrawal sites were tested in each of the three models. Thus, a total of 12 (=2 × 2 × 3) scenarios were tested (table 7). The first distribution of withdrawal sites corresponds to the well locations in scenario 1 of Underwood and others (1995). The second distribution is similar to the first, but three of the six withdrawal sites were moved farther inland, where the freshwater lens is thicker and the possibility of saltwater intrusion less likely.



Base modified from U.S. Geological Survey digital data, 1:24,000, 1983, Albers equal area projection, standard parallels 19°08'30" and 20°02'30", central meridian 155°26'30"

EXPLANATION



- 4 — LINE OF EQUAL MODEL-CALCULATED WATER LEVEL-- Interval 2 feet. Datum is mean sea level
- DRAINAGE DIVIDE
- - - - RIFT ZONE BOUNDARY (from Underwood and others, 1995)
- 6.8 WELL LOCATION AND AVERAGE 1990'S WATER LEVEL, IN FEET ABOVE MEAN SEA LEVEL

Figure 29. Measured and model-calculated water levels in the Hawi area, north Kohala, Hawaii, using the intermediate recharge estimate (37.5 million gallons per day from infiltration of rainfall, fog drip, and irrigation).

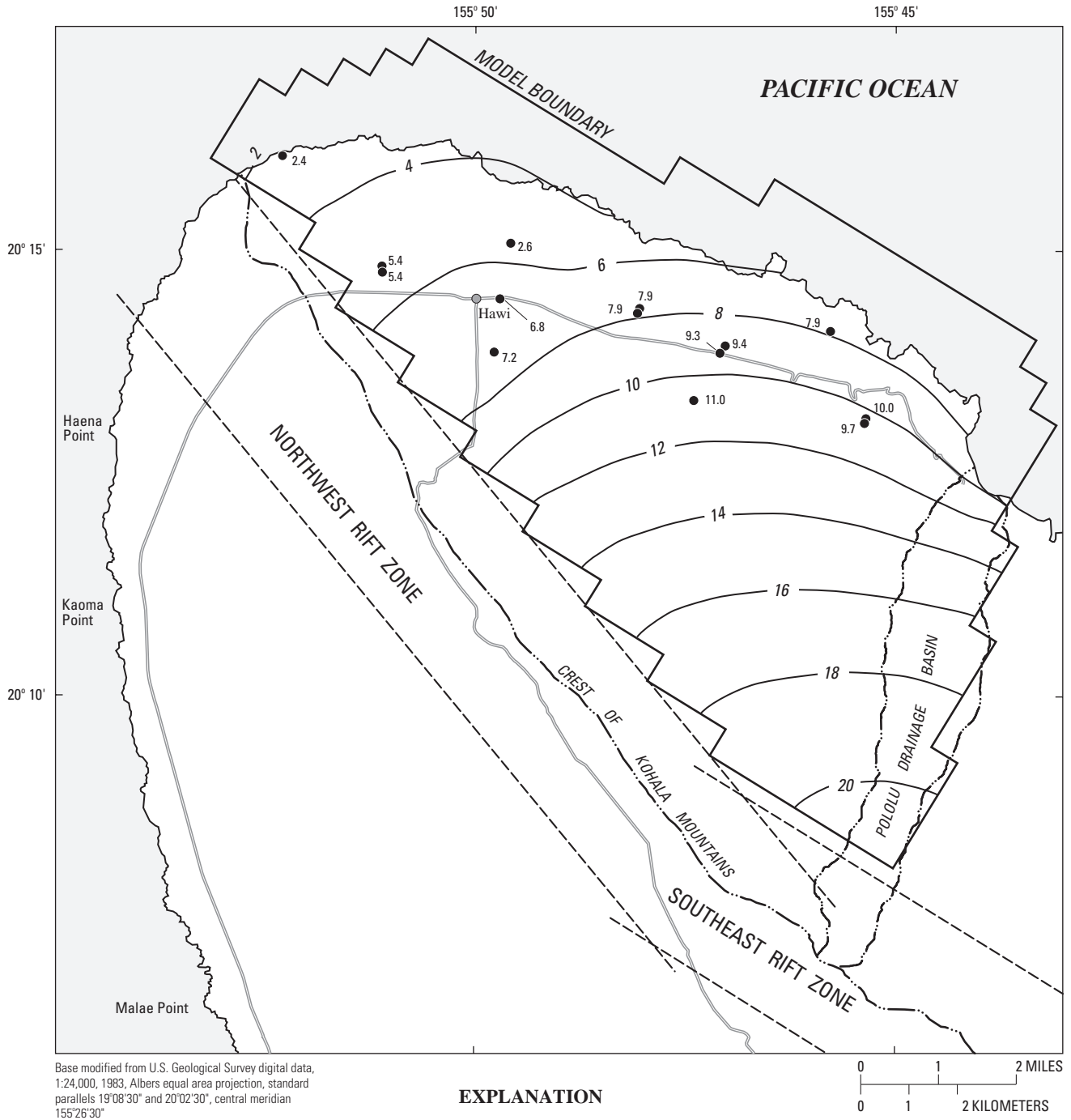


Figure 30. Measured and model-calculated water levels in the Hawi area, north Kohala, Hawaii, using the high recharge estimate (55.4 million gallons per day from infiltration of rainfall, fog drip, and irrigation).

Table 7. Recharge and withdrawal (scenarios 1 to 12) for the numerical ground-water flow models, Hawi area, north Kohala, Hawaii [Mgal/d, million gallons per day]

Scenario	^a Recharge, in Mgal/d	^b Distribution of withdrawal sites	^c Withdrawal, in Mgal/d									
			Withdrawal site									Total
			P-1	P-2	P-3	P-4	P-5	P-6	P-7	P-8	P-9	
1	19.9	1	1.0	2.0	2.0	2.0	2.0	1.0	0.0	0.0	0.0	10
2	19.9	2	1.0	2.0	2.0	0.0	0.0	0.0	2.0	2.0	1.0	10
3	19.9	1	1.5	3.0	3.0	3.0	3.0	1.5	0.0	0.0	0.0	15
4	19.9	2	1.5	3.0	3.0	0.0	0.0	0.0	3.0	3.0	1.5	15
5	37.5	1	1.5	3.0	3.0	3.0	3.0	1.5	0.0	0.0	0.0	15
6	37.5	2	1.5	3.0	3.0	0.0	0.0	0.0	3.0	3.0	1.5	15
7	37.5	1	2.0	4.0	4.0	4.0	4.0	2.0	0.0	0.0	0.0	20
8	37.5	2	2.0	4.0	4.0	0.0	0.0	0.0	4.0	4.0	2.0	20
9	55.4	1	1.5	3.0	3.0	3.0	3.0	1.5	0.0	0.0	0.0	15
10	55.4	2	1.5	3.0	3.0	0.0	0.0	0.0	3.0	3.0	1.5	15
11	55.4	1	2.0	4.0	4.0	4.0	4.0	2.0	0.0	0.0	0.0	20
12	55.4	2	2.0	4.0	4.0	0.0	0.0	0.0	4.0	4.0	2.0	20

^aRecharge from infiltration of rainfall, fog drip, and irrigation. An additional 10 Mgal/d recharge from injection at the Hawi hydroelectric plant and seepage from Kohala ditch is included in scenarios 1 to 8.

^bThe sites in distribution 1 correspond to scenario 1 from Underwood and others (1995). Sites P-7 to P-9 in distribution 2 are located farther inland than sites P-4 to P-6 in distribution 1.

^cWithdrawal above the average 1990's rates.

The location of the model-calculated freshwater-saltwater interface is important because it is an indicator of freshwater-lens thickness and, thus, the limits on available water at withdrawal sites. If the model-calculated freshwater-saltwater interface rises near or into wells, saltwater intrusion may be a problem. For the Kohala study area, Underwood and others (1995) estimated that the thickness of the upper part of the transition zone (above the freshwater-saltwater interface) is about 80 ft and, on the basis of this estimate, determined the thickness of the freshwater above the transition zone at simulated withdrawal sites. The approach of Underwood and others (1995) for estimating the thickness of freshwater from the water table to the upper part of the transition zone (80 ft above the model-calculated freshwater-saltwater interface) was used in this study.

In Hawaii, wells tapping freshwater-lens systems commonly are drilled to depths of 50 to 200 ft below sea level. Deep wells are more likely to be affected by saltwater intrusion, whereas shallow wells would tend to maintain a greater buffer of freshwater between the wells and the transition zone. The amount of freshwater

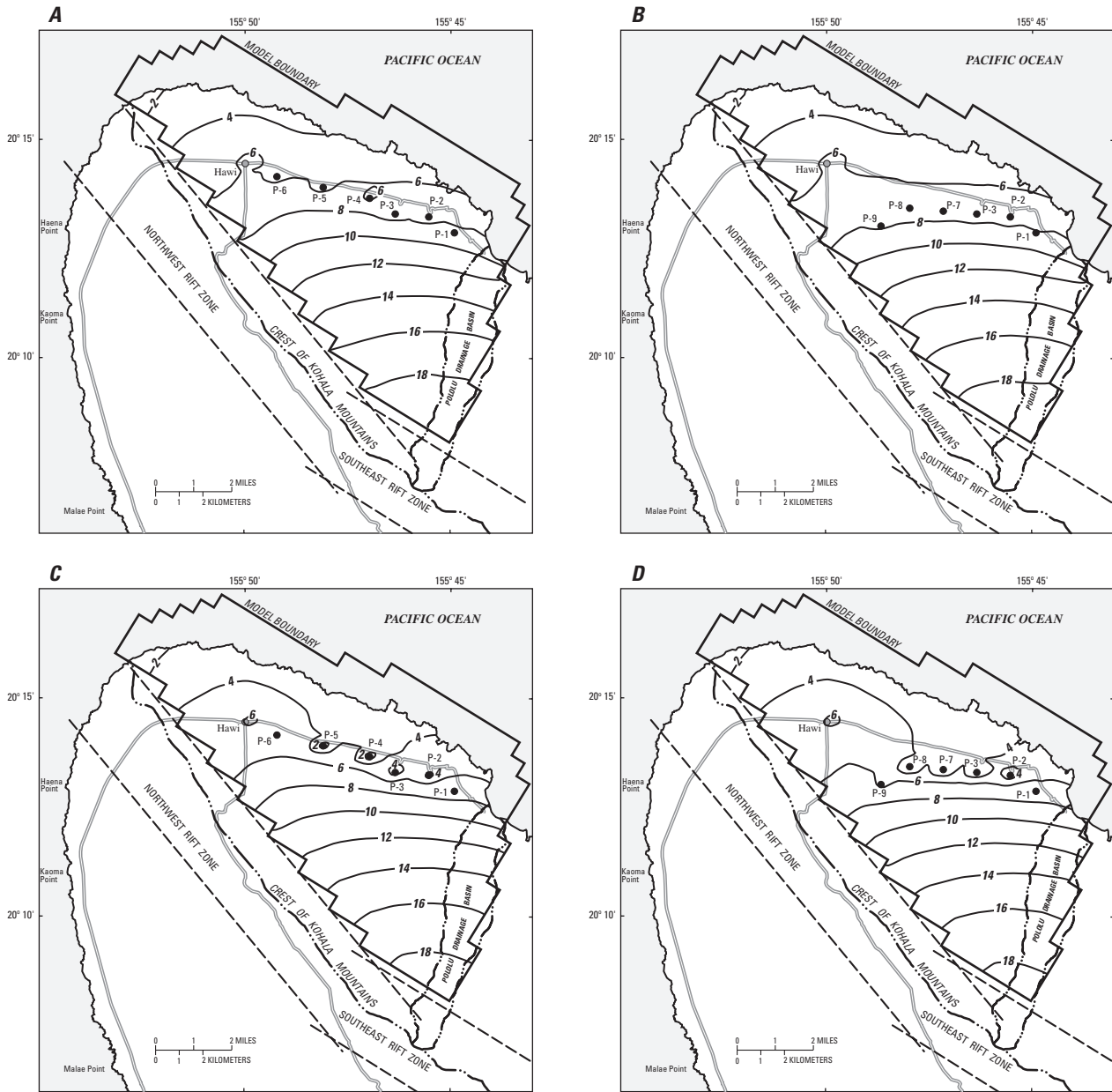
buffer would depend on the actual depth, spacing, and withdrawal rates of the wells and the location of the wells.

Model 1

Model 1 includes 19.9 Mgal/d recharge from infiltration of rainfall, fog drip, and irrigation, plus 10 Mgal/d combined recharge from injection at the Hawi hydroelectric plant and seepage from Kohala ditch. The model 1 hydraulic characteristics, estimated from average 1990's water levels and withdrawals, were used to simulate four scenarios (scenarios 1 to 4).

Scenario 1.— 10 Mgal/d Withdrawal, Distribution 1

In scenario 1, 10 Mgal/d (above the 1990's average withdrawal rates) was withdrawn from six sites (fig. 31A). At both the easternmost site (P-1) and the westernmost site (P-6), simulated withdrawal was 1.0 Mgal/d. Simulated withdrawal at each of the four other sites (P-2 to P-5) was 2.0 Mgal/d (table 7).



Base modified from U.S. Geological Survey digital data, 1:24,000, 1983, Albers equal area projection, standard parallels 19°08'30" and 20°02'30", central meridian 155°26'30"

EXPLANATION

- | | | | |
|-------|--|-------|--|
| — 4 — | LINE OF EQUAL MODEL-CALCULATED WATER LEVEL--Interval 2 feet. Datum is mean sea level | ----- | RIFT ZONE BOUNDARY (from Underwood and others, 1995) |
| ----- | DRAINAGE DIVIDE | ● P-3 | WITHDRAWAL SITE AND IDENTIFIER |

Figure 31. Model-calculated water levels in the Hawi area, north Kohala, Hawaii, with 19.9 million gallons per day recharge from infiltration of rainfall, fog drip, and irrigation and different withdrawal rates and distributions: **(A)** 10 million gallons per day withdrawal using well distribution 1; **(B)** 10 million gallons per day withdrawal using well distribution 2; **(C)** 15 million gallons per day withdrawal using well distribution 1; **(D)** 15 million gallons per day withdrawal using well distribution 2. Specified withdrawals are at rates above the average 1990's rates. Withdrawal rates at individual pumped wells are shown in table 7. Model-calculated freshwater-saltwater interface depths below sea level are equal to -40 times the indicated water levels.

Table 8. Model-calculated water levels for scenarios 1 to 12 at proposed sites of withdrawal, Hawi area, north Kohala, Hawaii [Mgal/d, million gallons per day; na, not applicable; --, zero withdrawal at site for scenarios 1 to 12; model calculated freshwater-saltwater interface depth below sea level is equal to -40 times the indicated water level; estimated freshwater thickness at the withdrawal site is equal to 41 times the indicated water level minus 80 feet]

Scenario	^a Recharge, in Mgal/d	^b Withdrawal, in Mgal/d	^c Distribution	Model-calculated water level at site of proposed withdrawal, in feet above mean sea level								
				P-1	P-2	P-3	P-4	P-5	P-6	P-7	P-8	P-9
Model 1 (low recharge), zero withdrawal from P-1 to P-9	19.9	0	na	11.0	10.7	10.9	10.0	8.9	7.1	10.8	10.2	10.6
1	19.9	10	1	8.3	6.8	6.8	5.7	5.1	5.6	--	--	--
2	19.9	10	2	8.1	6.5	6.4	--	--	--	6.2	6.0	7.7
3	19.9	15	1	6.6	3.6	3.3	1.1	1.3	4.7	--	--	--
4	19.9	15	2	6.2	2.9	2.2	--	--	--	1.6	1.9	5.8
Model 2 (intermediate recharge), zero withdrawal from P-1 to P-9	37.5	0	na	11.0	10.7	11.0	10.2	9.1	7.3	10.9	10.5	10.9
5	37.5	15	1	8.7	7.4	7.5	6.5	5.9	5.7	--	--	--
6	37.5	15	2	8.5	7.2	7.3	--	--	--	7.1	6.8	8.3
7	37.5	20	1	7.8	5.9	5.9	4.8	4.3	5.2	--	--	--
8	37.5	20	2	7.5	5.6	5.5	--	--	--	5.3	5.1	7.3
Model 3 (high recharge), zero withdrawal from P-1 to P-9	55.4	0	na	10.4	10.2	10.7	9.8	8.9	7.1	10.7	10.3	10.7
9	55.4	15	1	8.9	8.1	8.4	7.5	6.8	6.1	--	--	--
10	55.4	15	2	8.8	7.9	8.2	--	--	--	8.2	7.9	9.0
11	55.4	20	1	8.4	7.2	7.5	6.5	5.9	5.7	--	--	--
12	55.4	20	2	8.2	7.0	7.2	--	--	--	7.1	6.9	8.4

^aRecharge from infiltration of rainfall, fog drip, and irrigation.

^bWithdrawal in excess of average 1990's rates.

^cDistribution of withdrawals and sites shown in table 7 and figures 31–33.

In scenario 1, model-calculated water levels at the six withdrawal sites range from 5.1 to 8.3 ft above sea level, and the water levels at these sites are 1.5 to 4.3 ft lower than the model-calculated water levels from model 1 without the 10 Mgal/d additional withdrawal (table 8). At the six withdrawal sites, the model-calculated interface in scenario 1 is 204 to 332 ft below sea level. The estimated thicknesses of freshwater from the water table to the upper part of the transition zone range from 129 to 260 ft at the six withdrawal sites in scenario 1. The freshwater thicknesses are least (129 to 154 ft) near the three westernmost withdrawal sites (P-4 to P-6) and, therefore, deeply drilled wells at these sites would more likely be affected by saltwater intrusion than at the three eastern sites. For steady-state conditions, withdrawing an additional 10 Mgal/d causes ground-water discharge to the ocean to decrease by 10 Mgal/d (compare tables 6 and 9).

Scenario 2.— 10 Mgal/d Withdrawal, Distribution 2

In scenario 2, 10 Mgal/d (above the 1990's average withdrawal rates) was withdrawn from six sites (fig. 31B). At both the easternmost site (P-1) and the westernmost site (P-9), simulated withdrawal was 1.0 Mgal/d. Simulated withdrawal at each of the four other sites (P-2, P-3, P-7, and P-8) was 2.0 Mgal/d (table 7). Relative to the three westernmost sites in scenario 1 (P-4 to P-6), the corresponding three westernmost sites in scenario 2 (P-7 to P-9) are farther inland, where the freshwater lens is thicker.

In scenario 2, model-calculated water levels at the six withdrawal sites range from 6.0 to 8.1 ft above sea level, and the water levels at these sites are 2.9 to 4.6 ft lower than the model-calculated water levels from model 1 without the 10 Mgal/d additional withdrawal (table 8). The water levels at common withdrawal sites (P-1 to P-3) are 0.2 to 0.4 ft lower in scenario 2 relative to scenario 1 (table 8).

Table 9. Steady-state ground-water budget (scenarios 1 to 12) for the numerical ground-water flow models, Hawi area, north Kohala, Hawaii [Values in million gallons per day. Total ground-water sources may not equal total ground-water discharges because of rounding errors]

	Scenario					
	1 and 2	3 and 4	5 and 6	7 and 8	9 and 10	11 and 12
Ground-water sources						
Infiltration of rainfall, fog drip, and irrigation	19.9	19.9	37.5	37.5	55.4	55.4
Seepage from Kohala ditch	2.0	2.0	2.0	2.0	2.0	2.0
Hydroelectric plant injection wells	8.0	8.0	8.0	8.0	8.0	8.0
Total	29.9	29.9	47.5	47.5	65.4	65.4
Ground-water discharges						
Withdrawals from wells	10.3	15.3	15.3	20.3	15.3	20.3
Withdrawals from tunnels	0.42	0.42	0.42	0.42	0.42	0.42
Freshwater discharge to ocean	19.2	14.2	31.9	26.9	49.7	44.7
Total	29.9	29.9	47.6	47.6	65.4	65.4

At the six withdrawal sites, the model-calculated interface in scenario 2 is 240 to 324 ft below sea level. The estimated thicknesses of freshwater from the water table to the upper part of the transition zone range from 166 to 252 ft at the six withdrawal sites in scenario 2. Relative to scenario 1, the estimated freshwater thicknesses at the three easternmost withdrawal sites (P-1 to P-3) in scenario 2 decreased by about 8 to 17 ft. However, the estimated freshwater thicknesses (166 to 236 ft) at the three westernmost withdrawal sites (P-7 to P-9) in scenario 2 are greater than the estimated freshwater thicknesses (129 to 154 ft) at the three westernmost withdrawal sites (P-4 to P-6) in scenario 1 because the three westernmost withdrawal sites in scenario 2 are farther inland (where the freshwater lens is thicker) than the three westernmost withdrawal sites in scenario 1. Thus, the potential for saltwater intrusion at the three westernmost withdrawal sites is lower in scenario 2 than scenario 1.

Scenario 3.— 15 Mgal/d Withdrawal, Distribution 1

In scenario 3, 15 Mgal/d (above the 1990's average withdrawal rates) was withdrawn from six sites (fig. 31C). At both the easternmost site (P-1) and the westernmost site (P-6), simulated withdrawal was 1.5 Mgal/d. Simulated withdrawal at each of the four other sites (P-2 to P-5) was 3.0 Mgal/d (table 7).

In scenario 3, model-calculated water levels at the six withdrawal sites range from 1.1 to 6.6 ft above sea level, and the water levels at these sites are 2.4 to 8.9 ft lower than the model-calculated water levels from

model 1 without the 15 Mgal/d additional withdrawal (table 8). At the six withdrawal sites, the model-calculated interface in scenario 3 is 44 to 264 ft below sea level. The estimated thicknesses of freshwater from the water table to the upper part of the transition zone range from 0 to 191 ft at the six withdrawal sites in scenario 3. The estimated freshwater thicknesses are zero near withdrawal sites P-4 and P-5.

Scenario 4.— 15 Mgal/d Withdrawal, Distribution 2

In scenario 4, 15 Mgal/d (above the 1990's average withdrawal rates) was withdrawn from six sites (fig. 31D). At both the easternmost site (P-1) and the westernmost site (P-9), simulated withdrawal was 1.5 Mgal/d. Simulated withdrawal at each of the four other sites (P-2, P-3, P-7, and P-8) was 3.0 Mgal/d (table 7).

In scenario 4, model-calculated water levels at the six withdrawal sites range from 1.6 to 6.2 ft above sea level, and the water levels at these sites are 4.8 to 9.2 ft lower than the model-calculated water levels from model 1 without the 15 Mgal/d additional withdrawal (table 8). The water levels at common withdrawal sites (P-1 to P-3) are 0.4 to 1.1 ft lower in scenario 4 relative to scenario 3 (table 8).

At the six withdrawal sites, the model-calculated interface in scenario 4 is 64 to 248 ft below sea level. The estimated thicknesses of freshwater from the water table to the upper part of the transition zone range from 0 to 174 ft at the six withdrawal sites in scenario 4. The estimated freshwater thicknesses are zero near withdrawal sites P-7 and P-8.

Model 2

Model 2 includes 37.5 Mgal/d recharge from infiltration of rainfall, fog drip, and irrigation, plus 10 Mgal/d combined recharge from injection at the Hawi hydroelectric plant and seepage from Kohala ditch. The model 2 hydraulic characteristics, estimated from average 1990's water levels and withdrawals, were used in four additional withdrawal scenarios (scenarios 5 to 8).

Scenario 5.— 15 Mgal/d Withdrawal, Distribution 1

In scenario 5, 15 Mgal/d (above the 1990's average withdrawal rates) was withdrawn from six sites using the same withdrawal sites and rates as in scenario 3 (fig. 32A, table 7). In scenario 5, model-calculated water levels at the six withdrawal sites range from 5.7 to 8.7 ft above sea level, and the water levels are 1.6 to 3.7 ft lower than the model-calculated water levels from model 2 without the 15 Mgal/d additional withdrawal (table 8). The water-level declines at the withdrawal sites are greater in scenario 3 than scenario 5 because the hydraulic-conductivity and leakance values estimated for model 1 (low recharge) generally are lower than those for model 2 (intermediate recharge).

At the six withdrawal sites, the model-calculated interface in scenario 5 is 228 to 348 ft below sea level. The estimated thicknesses of freshwater from the water table to the upper part of the transition zone range from 154 to 277 ft at the six withdrawal sites in scenario 5. The freshwater thicknesses are least near the three westernmost withdrawal sites (P-4 to P-6).

Scenario 6.— 15 Mgal/d Withdrawal, Distribution 2

In scenario 6, 15 Mgal/d (above the 1990's average withdrawal rates) was withdrawn from six sites using the same withdrawal sites and rates as in scenario 4 (fig. 32B, table 7). In scenario 6, model-calculated water levels at the six withdrawal sites range from 6.7 to 8.5 ft above sea level. The water levels at common withdrawal sites (P-1 to P-3) are 0.2 ft lower in scenario 6 relative to scenario 5 (table 8).

At the six withdrawal sites, the model-calculated interface in scenario 6 is 268 to 340 ft below sea level. The estimated thicknesses of freshwater from the water table to the upper part of the transition zone range from 199 to 269 ft at the six withdrawal sites in scenario 6. Relative to scenario 5, the estimated freshwater thicknesses at the three easternmost withdrawal sites (P-1 to

P-3) in scenario 6 decreased by about 8 to 9 ft. However, the estimated freshwater thicknesses at the three westernmost withdrawal sites (P-7 to P-9) in scenario 6 range from 199 to 260 ft, which are greater than the estimated freshwater thicknesses of 154 to 187 ft at the three westernmost withdrawal sites (P-4 to P-6) in scenario 5.

Scenario 7.— 20 Mgal/d Withdrawal, Distribution 1

In scenario 7, 20 Mgal/d (above the 1990's average withdrawal rates) was withdrawn from six sites (fig. 32C, table 7). At both the easternmost site (P-1) and the westernmost site (P-6), simulated withdrawal was 2.0 Mgal/d. Simulated withdrawal at each of the four other sites (P-2 to P-5) was 4.0 Mgal/d (table 7).

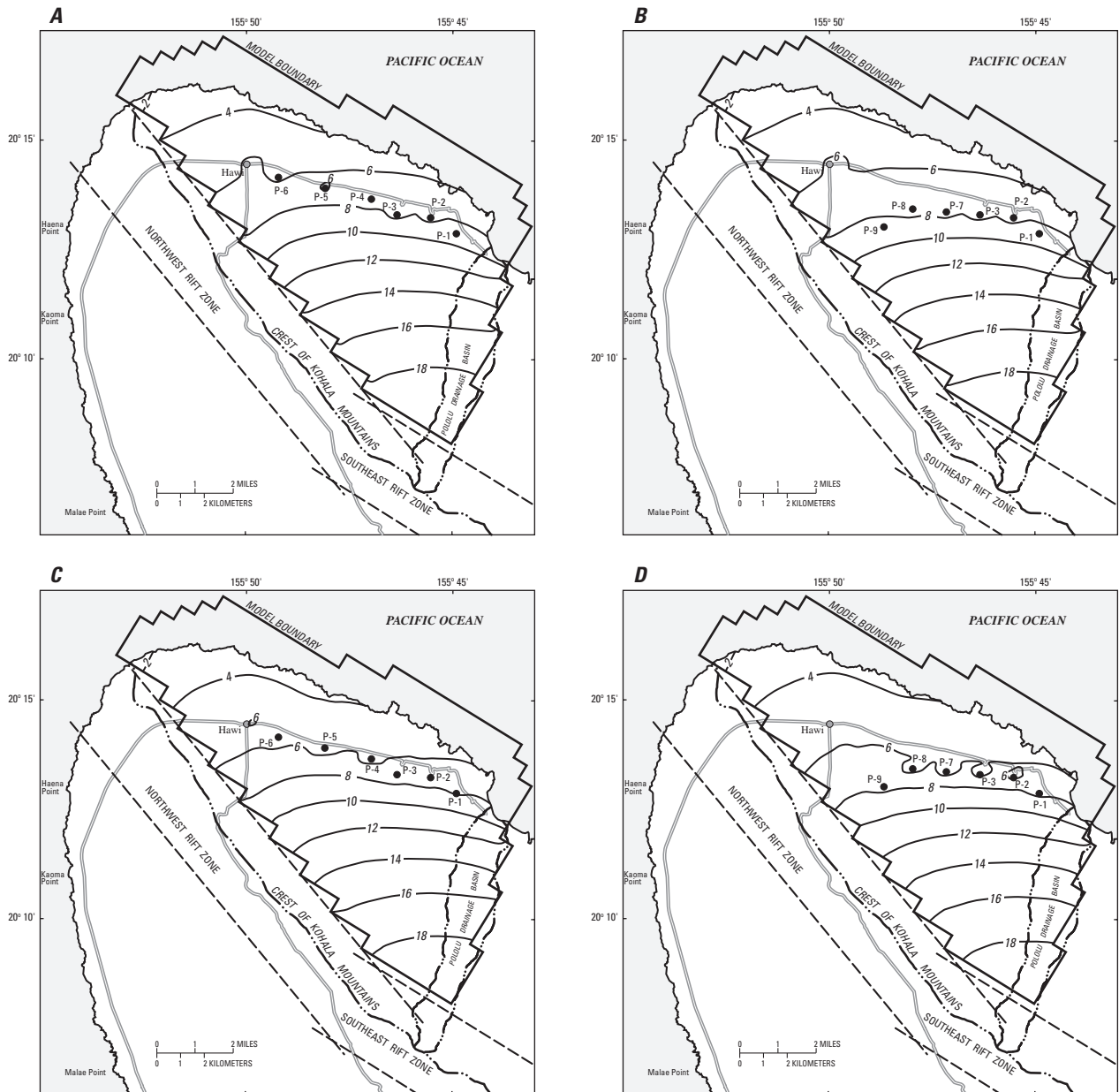
In scenario 7, model-calculated water levels at the six withdrawal sites range from 4.3 to 7.8 ft above sea level, and the water levels are 2.1 to 5.4 ft lower than the model-calculated water levels from model 2 without the 20 Mgal/d additional withdrawal (table 8). At the six withdrawal sites, the model-calculated interface in scenario 7 is 172 to 312 ft below sea level. The estimated thicknesses of freshwater from the water table to the upper part of the transition zone range from 96 to 240 ft at the six withdrawal sites in scenario 7. The freshwater thicknesses are least near the three westernmost withdrawal sites (P-4 to P-6).

Scenario 8.— 20 Mgal/d Withdrawal, Distribution 2

In scenario 8, 20 Mgal/d (above the 1990's average withdrawal rates) was withdrawn from six sites (fig. 32D). At both the easternmost site (P-1) and the westernmost site (P-9), simulated withdrawal was 2.0 Mgal/d. Simulated withdrawal at each of the four other sites (P-2, P-3, P-7, and P-8) was 4.0 Mgal/d (table 7).

In scenario 8, model-calculated water levels at the six withdrawal sites range from 5.1 to 7.5 ft above sea level. The water levels at common withdrawal sites (P-1 to P-3) are 0.3 to 0.4 ft lower in scenario 8 relative to scenario 7 (table 8).

At the six withdrawal sites, the model-calculated interface in scenario 8 is 204 to 300 ft below sea level. The estimated thicknesses of freshwater from the water table to the upper part of the transition zone range from 129 to 228 ft at the six withdrawal sites in scenario 8. Relative to scenario 7, the estimated freshwater thicknesses at the three easternmost withdrawal sites (P-1 to P-3) in scenario 8 decreased by about 12 to 16 ft.



Base modified from U.S. Geological Survey digital data, 1:24,000, 1983, Albers equal area projection, standard parallels 19°08'30" and 20°02'30", central meridian 155°26'30"

EXPLANATION

- 4 — LINE OF EQUAL MODEL-CALCULATED WATER LEVEL--Interval 2 feet. Datum is mean sea level
- RIFT ZONE BOUNDARY (from Underwood and others, 1995)
- DRAINAGE DIVIDE
- P-3 WITHDRAWAL SITE AND IDENTIFIER

Figure 32. Model-calculated water levels in the Hawi area, north Kohala, Hawaii, with 37.5 million gallons per day recharge from infiltration of rainfall, fog drip, and irrigation and different withdrawal rates and distributions: **(A)** 15 million gallons per day withdrawal using well distribution 1; **(B)** 15 million gallons per day withdrawal using well distribution 2; **(C)** 20 million gallons per day withdrawal using well distribution 1; **(D)** 20 million gallons per day withdrawal using well distribution 2. Specified withdrawals are at rates above the average 1990's rates. Withdrawal rates at individual pumped wells are shown in table 7. Model-calculated freshwater-saltwater interface depths below sea level are equal to -40 times the indicated water levels.

However, the estimated freshwater thicknesses at the three westernmost withdrawal sites (P-7 to P-9) in scenario 8 range from 129 to 219 ft, which are greater than the estimated freshwater thicknesses of 96 to 133 ft at the three westernmost withdrawal sites (P-4 to P-6) in scenario 7.

Model 3

Model 3 includes 55.4 Mgal/d recharge from infiltration of rainfall, fog drip, and irrigation, plus 10 Mgal/d combined recharge from injection at the Hawi hydroelectric plant and seepage from Kohala ditch. The model 3 hydraulic characteristics, estimated from average 1990's water levels and withdrawals, were used in four additional withdrawal scenarios (scenarios 9 to 12).

Scenario 9.— 15 Mgal/d Withdrawal, Distribution 1

In scenario 9, 15 Mgal/d (above the 1990's average withdrawal rates) was withdrawn from six sites using the same withdrawal sites and rates as in scenarios 3 and 5 (fig. 33A, table 7). In scenario 9, model-calculated water levels at the six withdrawal sites range from 6.1 to 8.9 ft above sea level, and the water levels are 1.0 to 2.3 ft lower than the model-calculated water levels from model 3 without the 15 Mgal/d additional withdrawal (table 8). The water-level declines at the withdrawal sites are greater in scenario 5 than scenario 9 because the hydraulic-conductivity and leakance values estimated for model 2 (intermediate recharge) generally are lower than those for model 3 (high recharge).

At the six withdrawal sites, the model-calculated interface in scenario 9 is 244 to 356 ft below sea level. The estimated thicknesses of freshwater from the water table to the upper part of the transition zone range from 170 to 285 ft at the six withdrawal sites in scenario 9. The freshwater thicknesses are least near the three westernmost withdrawal sites (P-4 to P-6).

Scenario 10.— 15 Mgal/d Withdrawal, Distribution 2

In scenario 10, 15 Mgal/d (above the 1990's average withdrawal rates) was withdrawn from six sites using the same withdrawal sites and rates as in scenarios 4 and 6 (fig. 33B, table 7). In scenario 10, model-calculated water levels at the six withdrawal sites range from 7.9 to 9.0 ft above sea level. The water levels at common withdrawal sites (P-1 to P-3) are 0.1 to 0.2 ft lower in scenario 10 relative to scenario 9 (table 8).

At the six withdrawal sites, the model-calculated interface in scenario 10 is 316 to 360 ft below sea level. The estimated thicknesses of freshwater from the water table to the upper part of the transition zone range from 244 to 289 ft at the six withdrawal sites in scenario 10. Relative to scenario 9, the estimated freshwater thicknesses at the three easternmost withdrawal sites (P-1 to P-3) in scenario 10 decreased by about 4 to 8 ft. However, the estimated freshwater thicknesses at the three westernmost withdrawal sites (P-7 to P-9) in scenario 10 range from 244 to 289 ft, which are greater than the estimated freshwater thicknesses of 170 to 228 ft at the three westernmost withdrawal sites (P-4 to P-6) in scenario 9.

Scenario 11.— 20 Mgal/d Withdrawal, Distribution 1

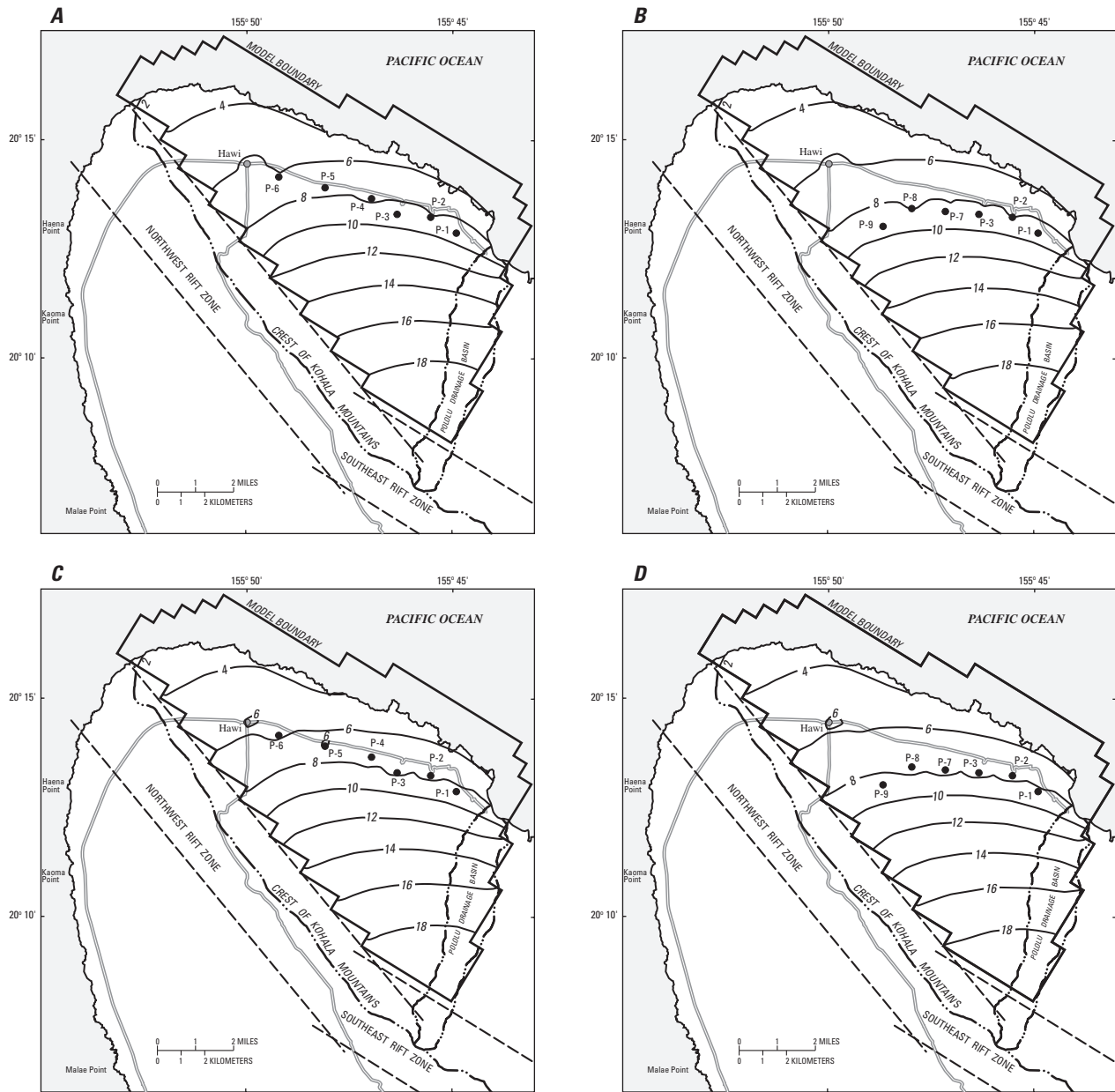
In scenario 11, 20 Mgal/d (above the 1990's average withdrawal rates) was withdrawn from six sites using the same withdrawal sites and rates as in scenario 7 (fig. 33C, table 7). In scenario 11, model-calculated water levels at the six withdrawal sites range from 5.7 to 8.4 ft above sea level, and the water levels are 1.4 to 3.3 ft lower than the model-calculated water levels from model 3 without the 20 Mgal/d additional withdrawal (table 8).

At the six withdrawal sites, the model-calculated interface in scenario 11 is 228 to 336 ft below sea level. The estimated thicknesses of freshwater from the water table to the upper part of the transition zone range from 154 to 264 ft at the six withdrawal sites in scenario 11. The freshwater thicknesses are least near the three westernmost withdrawal sites (P-4 to P-6).

Scenario 12.— 20 Mgal/d Withdrawal, Distribution 2

In scenario 12, 20 Mgal/d (above the 1990's average withdrawal rates) was withdrawn from six sites using the same withdrawal sites and rates as in scenario 8 (fig. 33D, table 7). In scenario 12, model-calculated water levels at the six withdrawal sites range from 6.9 to 8.4 ft above sea level. The water levels at common withdrawal sites (P-1 to P-3) are 0.2 to 0.3 ft lower in scenario 12 relative to scenario 11 (table 8).

At the six withdrawal sites, the model-calculated interface in scenario 12 is 276 to 336 ft below sea level. The estimated thicknesses of freshwater from the water table to the upper part of the transition zone range from 203 to 264 ft at the six withdrawal sites in scenario 12.



Base modified from U.S. Geological Survey digital data, 1:24,000, 1983, Albers equal area projection, standard parallels 19°08'30" and 20°02'30", central meridian 155°26'30"

EXPLANATION

- | | | | |
|-------|--|-------|--|
| — 4 — | LINE OF EQUAL MODEL-CALCULATED WATER LEVEL--Interval 2 feet. Datum is mean sea level | ----- | RIFT ZONE BOUNDARY (from Underwood and others, 1995) |
| ----- | DRAINAGE DIVIDE | ● P-3 | WITHDRAWAL SITE AND IDENTIFIER |

Figure 33. Model-calculated water levels in the Hawi area, north Kohala, Hawaii, with 55.4 million gallons per day recharge from infiltration of rainfall, fog drip, and irrigation and different withdrawal rates and distributions: **(A)** 15 million gallons per day withdrawal using well distribution 1; **(B)** 15 million gallons per day withdrawal using well distribution 2; **(C)** 20 million gallons per day withdrawal using well distribution 1; **(D)** 20 million gallons per day withdrawal using well distribution 2. Specified withdrawals are at rates above the average 1990's rates. Withdrawal rates at individual pumped wells are shown in table 7. Model-calculated freshwater-saltwater interface depths below sea level are equal to -40 times the indicated water levels.

Relative to scenario 11, the estimated freshwater thicknesses at the three easternmost withdrawal sites (P-1 to P-3) in scenario 12 decreased by about 8 to 13 ft. However, the estimated freshwater thicknesses at the three westernmost withdrawal sites (P-7 to P-9) in scenario 12 range from 203 to 264 ft, which are greater than the estimated freshwater thicknesses of 154 to 187 ft at the three westernmost withdrawal sites (P-4 to P-6) in scenario 11.

Ground-Water Availability

On the basis of numerical ground-water flow model results, Underwood and others (1995) indicated that withdrawal of 20 Mgal/d from the Hawi area is feasible, but depth, spacing, and withdrawal rates of individual wells are important considerations in planning ground-water development. Model results from Underwood and others (1995) indicated that for a withdrawal of 20 Mgal/d, water levels at the withdrawal sites would be as low as 5.7 ft above sea level. The estimated freshwater thickness (distance from the water table to the top of the transition zone) at the withdrawal sites would be as small as 154 ft. The numerical ground-water flow model developed by Underwood and others (1995) included 68.4 Mgal/d recharge from infiltration of rainfall. Results from the present study indicate that the 68.4 Mgal/d recharge estimate is probably high; this conclusion has important ground-water availability implications.

Because of uncertainty in the recharge, three numerical ground-water flow models of the Hawi area were developed for the present study. The three numerical ground-water flow models each incorporated a different recharge rate (from infiltration of rainfall, fog drip, and irrigation): (1) a low recharge of 19.9 Mgal/d, (2) an intermediate recharge of 37.5 Mgal/d, or (3) a high recharge of 55.4 Mgal/d. Ground-water availability for each of the three recharge rates is described below.

Results from withdrawal scenarios 1 to 4 using the low recharge estimate (19.9 Mgal/d from infiltration of rainfall, fog drip, and irrigation) indicate that (1) it may be possible to develop an additional 10 Mgal/d of fresh ground water from the Hawi area and maintain a freshwater-lens thickness of 160 ft near the withdrawal sites if appropriate well sites, depths, and withdrawal rates are used, and (2) it may be difficult to develop an addi-

tional 15 Mgal/d without causing saltwater to intrude the wells. High rates of withdrawal from closely spaced, deep wells will enhance the possibility for saltwater intrusion problems.

Results from withdrawal scenarios 5 to 8 using the intermediate recharge estimate (37.5 Mgal/d from infiltration of rainfall, fog drip, and irrigation) indicate that (1) it may be possible to develop an additional 15 Mgal/d of fresh ground water from the Hawi area and maintain a freshwater-lens thickness of 190 ft near the withdrawal sites if appropriate well sites, depths, and withdrawal rates are used, and (2) it may be difficult to develop an additional 20 Mgal/d and maintain a freshwater-lens thickness greater than 150 ft at all withdrawal sites.

Results from withdrawal scenarios 9 to 12 using the high recharge estimate (55.4 Mgal/d from infiltration of rainfall, fog drip, and irrigation) indicate that it may be possible to develop at least an additional 20 Mgal/d of fresh ground water from the Hawi area and maintain a freshwater-lens thickness of 200 ft near the withdrawal sites if appropriate well sites, depths, and withdrawal rates are used.

Other well-field configurations than the ones considered potentially could be used to develop more fresh ground water than indicated by the scenarios tested in this study.

Depth, spacing, and withdrawal rates of individual wells are important considerations in determining ground-water availability. Deep wells will increase the likelihood for saltwater intrusion. Concentrating too much withdrawal at too few sites also may increase the likelihood for saltwater intrusion. Development of ground-water resources farther inland may reduce the potential for saltwater intrusion problems because the freshwater lens is thicker. Regional models developed for the present study cannot predict whether local saltwater intrusion problems may occur at withdrawal sites (see "Model Limitations" section). Furthermore, the upper part of the transition zone may widen beneath withdrawal sites (Reilly and Goodman, 1987), thus increasing the potential for local saltwater intrusion.

Ground-water availability estimates for the Hawi area are highly dependent on the recharge estimate. Results of this study underscore the importance of collecting information to better constrain the recharge estimate so that better estimates of ground-water availability can be made.

MODEL LIMITATIONS

The numerical ground-water flow models developed in this study for the Hawi area have several limitations. One of the main limitations is the uncertainty in recharge. Because data are not available to better constrain the recharge estimate, it was necessary to develop three models using a range of recharge estimates. Results from this study indicate that it is possible to obtain reasonable agreement between measured and model-calculated water levels with three different recharge distributions by using appropriate hydraulic-conductivity and leakance distributions. Thus, without additional information to better constrain the recharge or hydraulic-characteristics distributions, it is not possible to develop a unique ground-water flow model. Clearly, improved recharge estimates are needed to reduce uncertainty in ground-water flow model predictions. Recharge estimates from a water-budget approach can be improved as data related to evapotranspiration, runoff, and fog drip become available. Independent methods of estimating recharge, such as salt balances or isotope studies, also can lead to reduced uncertainty in the recharge estimates.

In this study, model zones were created to represent high- and low-permeability zones within the Hawi area. It is possible that different distributions of hydraulic conductivity and leakance can be used in a model to produce acceptable matches between model-calculated and measured water levels. Although the zones that were created in this study are plausible, it is probable that other zonal geometries could produce similar results. The number of model zones was minimized because of the limited data. A refined model can be developed and a better representation of the flow system can be obtained as more data become available to constrain the model.

There are an insufficient number of monitoring wells at high altitudes to define the spatial distribution of water levels in the inland, southeastern part of the study area. Thus, the distributions of model-calculated water levels and freshwater-saltwater interface altitudes, although informative, are unverified in places.

The model-calculated water-level decline at a model node used to represent a withdrawal well may underestimate the water-level decline in an actual well because the model-calculated water-level decline represents an average decline for the area around the model node (see figs. 24-26) as opposed to the maximum

decline that exists at the withdrawal well. Saltwater intrusion at a withdrawal well may be a problem even if the average altitude of the model-calculated freshwater-saltwater interface is below the bottom of the simulated well.

Because the ground-water flow model contains only a single layer, vertical hydraulic-head gradients cannot be simulated. Thus, model-calculated water-level declines caused by additional withdrawals may be underestimated near partially penetrating wells. On the other hand, because a single-layer numerical model cannot account for vertical flow, the numerical model may overestimate the rise in the position of the freshwater-saltwater interface caused by withdrawal from partially penetrating wells, especially for highly anisotropic aquifers in which the vertical hydraulic conductivity is several orders of magnitude less than the horizontal hydraulic conductivity.

The AQUIFEM-SALT code assumes a sharp interface between freshwater and saltwater and cannot be used to predict changes in salinity, either at the regional or local scale. The model simulates the location of the freshwater-saltwater interface but cannot be used to simulate local upconing in the vicinity of pumped wells. Furthermore, the AQUIFEM-SALT code uses the Ghyben-Herzberg relation that tends to underestimate freshwater-lens thickness in the coastal discharge zone and overestimate freshwater-lens thickness in the mountainous interior area.

Because the models were not calibrated for transient conditions, they cannot be used to predict time-varying water levels. Thus, following a change in withdrawal or recharge rates, the amount of time for water-level changes to occur cannot be predicted using the models developed for this study. The models are, nevertheless, useful tools for predicting the possible regional hydrologic effects of additional withdrawals in the Hawi area for steady-state conditions.

SUMMARY AND CONCLUSIONS

The Hawi study area is located on the windward (northeastern) side of the crest of the Kohala Mountains. The Kohala Mountains are formed by the Kohala Volcano, the oldest and northernmost of five volcanoes forming the island of Hawaii. The study area covers about 55 square miles and is bounded on the southwest by the crest of the Kohala Mountains, on the east by the

eastern drainage divide of Pololu Stream, and on the north by the coast. Mean annual rainfall in the Hawi area ranges from less than 40 in. near the coast at Upolu Point to between 120 and 160 in. inland, near the headwater of Pololu Stream.

Younger Hawi Volcanics and older Pololu Volcanics underlie the Hawi study area. The permeability of the volcanic rocks is spatially variable. The hydraulic conductivity of the Pololu Volcanics that form the main aquifer is generally hundreds to thousands of feet per day.

Fresh ground water in the study area is found in two main forms: (1) as a freshwater-lens system in the dike-free lava flows, and (2) as a dike-impounded system where overall permeability is reduced because of the presence of dikes. Perched water also exists near the contact between Pololu Volcanics and Hawi Volcanics. Measured water levels from wells drilled into the freshwater lens range from a few feet above sea level to 11 ft above sea level. Measured water levels indicate that there is a general northerly movement of ground water in the freshwater lens.

In the Hawi area, ground water is withdrawn from the freshwater-lens and perched ground-water systems. Although annual average withdrawal from the freshwater-lens system exceeded 14 Mgal/d (including both freshwater and brackish water) in the past when sugarcane was grown in the area, current withdrawal from the freshwater-lens system is less than 1 Mgal/d.

Average annual recharge in the Hawi area was estimated to be 37.5 Mgal/d with a daily water budget that accounts for evapotranspiration before recharge. Because of uncertainty in the factors controlling the water budget in the Hawi area, low and high recharge estimates of 19.9 and 55.4 Mgal/d, respectively, were computed from the quantified uncertainty. The recharge estimates from this study are lower than the previously estimated recharge of 68.4 Mgal/d from a monthly water budget that accounts for recharge before evapotranspiration. Recharge estimates from a water-budget approach can be improved as data related to evapotranspiration, runoff, and fog drip become available. Independent methods of estimating recharge also can lead to reduced uncertainty in the recharge values.

Three numerical ground-water flow models, corresponding to the three different estimated recharge distributions, were developed for the Hawi area to simulate ground-water levels and discharges for the 1990's.

The models account for spatially varying hydraulic characteristics of the geologic materials, recharge, and ground-water withdrawals. Hydraulic characteristics were estimated by comparing measured and model-calculated water levels. With the low recharge estimate (19.9 Mgal/d), the hydraulic-characteristic values tested that produced the lowest average-absolute error between measured and model-calculated water levels were a hydraulic conductivity of 1,500 ft/d and a leakance of 0.1 ft/d/ft for the northwestern part of the study area, and a hydraulic conductivity of 300 ft/d and a leakance of 0.005 ft/d/ft for the southeastern part. With the intermediate recharge estimate (37.5 Mgal/d), the hydraulic-characteristic values tested that produced the lowest average-absolute error between measured and model-calculated water levels were a hydraulic conductivity of 2,250 ft/d and a leakance of 0.05 ft/d/ft for the northwestern part of the study area, and a hydraulic conductivity of 500 ft/d and a leakance of 0.01 ft/d/ft for the southeastern part. With the high recharge estimate (55.4 Mgal/d), the hydraulic-characteristic values tested that produced the lowest average-absolute error between measured and model-calculated water levels were a hydraulic conductivity of 3,000 ft/d and a leakance of 0.05 ft/d/ft for the northwestern part of the study area, and a hydraulic conductivity of 700 ft/d and a leakance of 0.02 ft/d/ft for the southeastern part.

The three numerical ground-water flow models developed for this study were used to simulate the response of the freshwater-lens system to withdrawals at rates in excess of the average 1990's withdrawal rates. Each of two withdrawal rates (above average 1990's withdrawal rates) and two distributions of withdrawal sites were tested in each of the three models.

Results from numerical simulations indicate that (1) for the low recharge estimate (19.9 Mgal/d from infiltration of rainfall, fog drip, and irrigation) it may be possible to develop an additional 10 Mgal/d of fresh ground water from the Hawi area and maintain a freshwater-lens thickness of 160 ft near the withdrawal sites, (2) for the intermediate recharge estimate (37.5 Mgal/d from infiltration of rainfall, fog drip, and irrigation) it may be possible to develop an additional 15 Mgal/d of fresh ground water from the Hawi area and maintain a freshwater-lens thickness of 190 ft near the withdrawal sites, and (3) for the high recharge estimate (55.4 Mgal/d from infiltration of rainfall, fog drip, and irrigation) it may be possible to develop at least an additional 20 Mgal/d of fresh ground water from the Hawi

area and maintain a freshwater-lens thickness of 200 ft near the withdrawal sites. Other well-field configurations than the ones considered potentially could be used to develop more fresh ground water than indicated by the scenarios tested in this study. Depth, spacing, and withdrawal rates of individual wells are important considerations in determining ground-water availability. Deep wells will increase the likelihood for saltwater intrusion. Concentrating too much withdrawal at too few sites also may increase the likelihood for saltwater intrusion. Development farther inland may reduce the potential for saltwater intrusion problems because the freshwater lens is thicker. Regional models developed for this study cannot predict whether local saltwater intrusion problems may occur at individual withdrawal sites.

Ground-water availability estimates for the Hawaii area are highly dependent on the recharge estimate. Results of this study underscore the importance of collecting information to better constrain the recharge estimate so that better estimates of ground-water availability can be made.

REFERENCES CITED

- Allen, R.G., Pereira, L.S., Raes, Dirk, and Smith, Martin, 1998, Crop evapotranspiration: guidelines for computing crop water requirements: Food and Agriculture Organization of the United Nations, FAO Irrigation and Drainage Paper 56, 300 p.
- Bear, Jacob, 1979, *Hydraulics of groundwater*: McGraw-Hill Publishing Co., New York, 569 p.
- Bruijnzeel, L.A., and Proctor, J., 1993, Hydrology and biogeochemistry of tropical montane cloud forests: what do we really know?, in Hamilton, L.S., Juvik, J.O., and Scatena, F.N., eds., *Tropical Montane Cloud Forests, Proceedings of an International Symposium at San Juan, Puerto Rico, May 31 to June 5, 1993*, p. 25–46.
- Bruijnzeel, L.A., and Veneklaas, E.J., 1998, Climatic conditions and tropical montane forest productivity: the fog has not lifted yet: *Ecology*, v. 79, no. 1, p. 3–9.
- Dalrymple, G.B., 1971, Potassium-argon ages from the Pololu volcanic series, Kohala Volcano, Hawaii: *Geological Society of America Bulletin*, v. 82, no. 7, p. 1,997–1,999.
- Davis, D.A., and Yamanaga, George, 1963, Preliminary report on the water resources of Kohala Mountain and Mauna Kea, Hawaii: State of Hawaii, Department of Land and Natural Resources, Division of Water and Land Development, Circular C14, 44 p.
- Domenico, P.A., and Schwartz, F.W., 1990, *Physical and chemical hydrogeology*: New York, John Wiley & Sons, Inc., 824 p.
- Doorenbos, J., and Pruitt, W.O., 1977, Guidelines for predicting crop water requirements: Food and Agriculture Organization of the United Nations, FAO Irrigation and Drainage Paper 24, revised 1977, 144 p.
- Dykes, A.P., 1997, Rainfall interception from a lowland tropical rainforest in Brunei: *Journal of Hydrology*, v. 200, nos. 1-4, p. 260-279.
- Ekern, P.C., 1964, Direct interception of cloud water on Lanaihale, Hawaii: *Soil Science Society of America Proceedings*, v. 28, no. 3, p. 419–421.
- Ekern, P.C., 1966, Evapotranspiration of bermudagrass sod, *Cynodon dactylon* L. Pers., in Hawaii: *Agronomy Journal*, v. 58, no. 4, p. 387–390.
- Ekern, P.C., 1983, Measured evaporation in high rainfall areas, leeward Koolau Range, Oahu, Hawaii: University of Hawaii Water Resources Research Center Technical Report no. 156, 60 p.
- Ekern, P.C., and Chang, J.-H., 1985, Pan evaporation: State of Hawaii, 1894-1983: State of Hawaii, Department of Land and Natural Resources, Division of Water and Land Development, Report R74, 172 p.
- Giambelluca, T.W., 1983, Water balance of the Pearl Harbor-Honolulu basin, Hawai'i, 1946–1975: University of Hawaii Water Resources Research Center Technical Report no. 151, 151 p.
- Giambelluca, T.W., Nullet, M.A., and Schroeder, T.A., 1986, Rainfall atlas of Hawai'i: State of Hawaii, Department of Land and Natural Resources, Division of Water and Land Development, Report R76, 267 p.
- Giambelluca, T.G., Loague, Keith, Green, R.E., and Nullet, M.A., 1996, Uncertainty in recharge estimation: impact on groundwater vulnerability assessments for the Pearl Harbor Basin, O'ahu, Hawai'i, U.S.A.: *Journal of Contaminant Hydrology*, v. 23, p. 85–112.
- Hydrosphere, 1996, Climate data, NCDC Summary of the day—West 2, v. 7.3, computer compact disc.
- Jacobi, J.D., 1989, Vegetation maps of the upland plant communities on the islands of Hawai'i, Maui, Moloka'i, and Lana'i: Honolulu, Hawaii, University of Hawaii, Department of Botany Technical Report no. 68, 25 p.
- Jones, C.A., 1980, A review of evapotranspiration studies in irrigated sugarcane in Hawaii: *Hawaii Planters' Record*, v. 59, no. 9. p. 195–214.
- Juvik, J.O., and Ekern, P.C., 1978, A climatology of mountain fog on Mauna Loa, Hawaii island: University of Hawaii Water Resources Research Center Technical Report no. 118, 63 p.
- Juvik, J.O., and Nullet, Dennis, 1995, Relationships between rainfall, cloud-water interception, and canopy throughfall in a Hawaiian montane forest, chap. 11 of Hamilton,

- L.S., Juvik, J.O., and Scatena, F.N., eds., Tropical Montane Cloud Forests: New York, Springer-Verlag, p. 165–182.
- Miller, M.E., 1987, Hydrogeologic characteristics of central Oahu subsoil and saprolite: Implications for solute transport: Honolulu, Hawaii, University of Hawaii, M.S. thesis, 231 p.
- Moore, J.G., Clague, D.A., Holcomb, R.T., Lipman, P.W., Normark, W.R., and Torresan, M.E., 1989, Prodigious submarine landslides on the Hawaiian ridge: *Journal of Geophysical Research*, v. 94, no. B12, p. 17,465–17,484.
- Oki, D.S., 1997, Geohydrology and numerical simulation of the ground-water flow system of Molokai, Hawaii: U.S. Geological Survey Water-Resources Investigations Report 97-4176, 62 p.
- Penman, H.L., 1956, Evaporation: an introductory survey: *Netherlands Journal of Agricultural Science*, v. 4, p. 9–29.
- Presley, T.K., 1999, The geohydrologic setting of Pololu Stream, island of Hawaii, Hawaii: U.S. Geological Survey Water-Resources Investigations Report 99-4009, 22 p.
- Priestley, C.H.B., and Taylor, R.J., 1972, On the assessment of surface heat flux and evaporation using large-scale parameters: *Monthly Weather Review*, v. 100, no. 2, p. 81–92.
- Reilly, T.E., and Goodman, A.S., 1987, Analysis of saltwater upconing beneath a pumping well: *Journal of Hydrology*, v. 89, nos. 3/4, p. 169–204.
- Sato, H.H., Ikeda, Warren, Paeth, Robert, Smythe, Richard, and Takehiro, Minoru, Jr., 1973, Soil survey of island of Hawaii, State of Hawaii: U.S. Department of Agriculture, Soil Conservation Service, 115 p. plus 195 map sheets.
- Schellekens, Jaap, Scatena, F.N., Bruijnzeel, L.A., and Wickel, A.J., 1999, Modelling rainfall interception by a lowland tropical rain forest in northeastern Puerto Rico: *Journal of Hydrology*, v. 225, p. 168–184.
- Schellekens, Jaap, Bruijnzeel, L.A., Scatena, F.N., Bink, N.J., and Holwerda, F., 2000, Evaporation from a tropical rain forest, Luquillo experimental forest, eastern Puerto Rico: *Water Resources Research*, v. 36, no. 8, p. 2,183–2,196.
- Scott, G.A.J., 1975, Relationships between vegetation cover and soil avalanching in Hawaii: *Proceedings of the Association of American Geographers*, v. 7, p. 208–212.
- Shade, P.J., 1995, Water budget for the Kohala area, island of Hawaii: U.S. Geological Survey Water-Resources Investigations Report 95-4114, 19 p.
- Shade, P.J., 1999, Water budget of east Maui, Hawaii: U.S. Geological Survey Water-Resources Investigations Report 98-4159, 36 p.
- Shuttleworth, W.J., and Calder, I.R., 1979, Has the Priestley-Taylor equation any relevance to forest evapotranspiration?: *Journal of Applied Meteorology*, v. 18, no. 5, p. 639–646.
- Srikanthan, Ratnasingham, and McMahon, T.A., 1982, Stochastic generation of monthly streamflows: *Journal of the Hydraulics Division, Proceedings of the American Society of Civil Engineers*, v. 108, no. HY3, p. 419–441.
- State of Hawaii, 1991, Hawaii County Water Use and Development Plan, Hawaii Water Plan: State of Hawaii, Commission on Water Resource Management, Review Draft, February 1992.
- Stearns, H.T., 1940, Supplement to geology and ground-water resources of the island of Oahu, Hawaii: Territory of Hawaii, Hawaii Division of Hydrography Bulletin 5, 164 p.
- Stearns, H.T., and Macdonald, G.A., 1946, Geology and ground-water resources of the island of Hawaii: Territory of Hawaii, Hawaii Division of Hydrography Bulletin 9, 363 p.
- Thorntwaite, C.W., 1948, An approach toward a rational classification of climate: *The Geographical Review*, v. 38, no. 1, p. 55–94.
- Thorntwaite, C.W., and Mather, J.R., 1955, The water balance: *Publications in Climatology*, v. 8, no. 1, p. 1–104.
- Underwood, M.R., Meyer, William, and Souza, W.R., 1995, Ground-water availability from the Hawi aquifer in the Kohala area, Hawaii: U.S. Geological Survey Water-Resources Investigations Report 95-4113, 57 p.
- U.S. Geological Survey, 1977, Surface water supply of the United States, 1966-70: U.S. Geological Survey Water-Supply Paper 2137, 750 p.
- Voss, C.I., 1984, AQUIFEM-SALT: A finite-element model for aquifers containing a seawater interface: U.S. Geological Survey Water-Resources Investigations Report 84-4263, 37 p.
- Wilcox, Carol, 1996, Sugar water: Honolulu, Hawaii, University of Hawaii Press, 191 p.
- Waterloo, M.J., Bruijnzeel, L.A., Vugts, H.F., and Rawaqa, T.T., 1999, Evaporation from *Pinus caribaea* plantations on former grassland soils under maritime tropical conditions: *Water Resources Research*, v. 35, no. 7, p. 2,133–2,144.
- Wentworth, C.K., 1939, The specific gravity of sea water and the Ghyben-Herzberg ratio at Honolulu: *University of Hawaii Bulletin*, v. 18, no. 8, 24 p.
- Wolfe, E.W., and Morris, Jean, 1996, Geologic map of the island of Hawaii: U.S. Geological Survey Miscellaneous Investigations Series Map I-2524-A, 1:100,000 scale.